Pairing, Quartetting and Clustering within a covariant approach

Raphaël-David Lasseri

September 12 – 2018, IPN, Orsay

Institut de Physique Nucléaire, Université Paris-Saclay

I Introduction

II Formalisms and methods

III Nuclear clustering

IV Superfluidities

Introduction

Introduction

Motivations

Introduction

Interacting fermions of 4 different species:

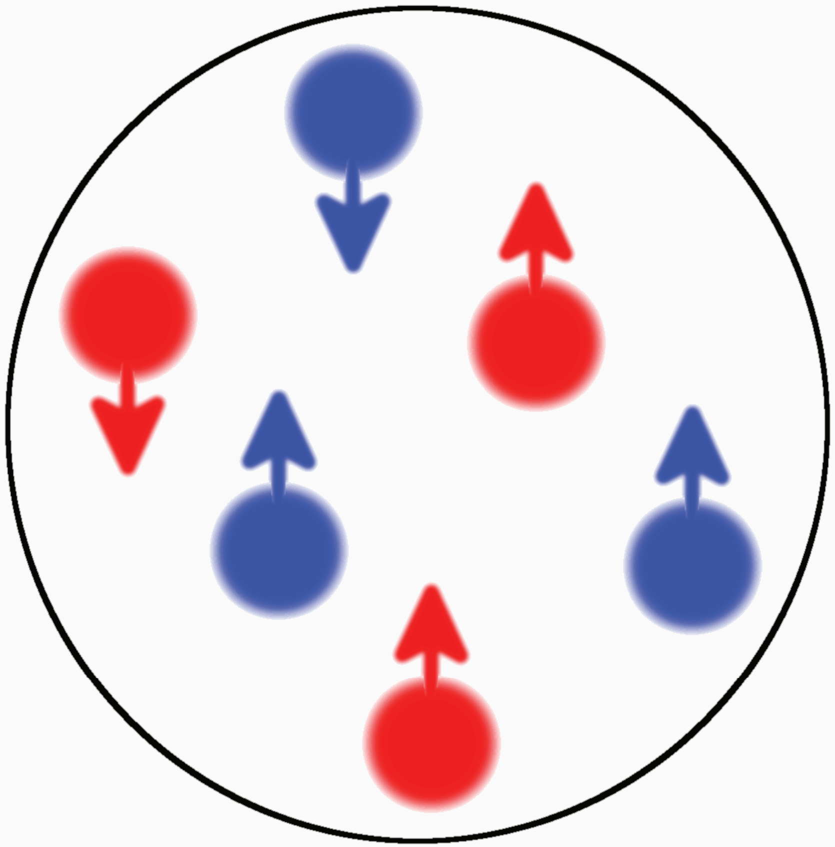

How are they distributed ?

Formal Motivations

Most general *pairing* hamiltonian

$$H^{pp} = -\int d^3r[g^{T=1} \sum_{\nu=\pm1,0} P^\dagger_\nu(r)P_\nu(r) + g^{T=0} \sum_{\mu=\pm1,0} Q^\dagger_\mu(r)Q_\mu(r)]$$

Operators being:

- $P^\dagger_\nu$ spin-singlet isovector pair creator
- $Q^\dagger_\mu$ spin-triplet isoscalar pair creator

Consequences and questions

In presence of an attractive interaction:

- Form pairs
- Form quartets

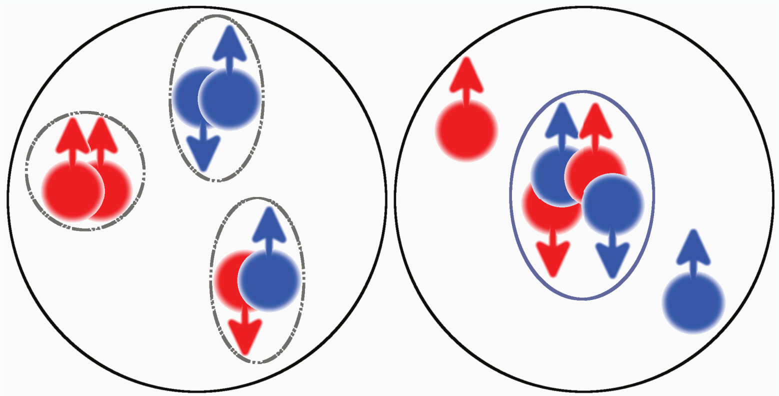

Consequences and questions

In presence of an attractive interaction:

- Form pairs
- Form quartets

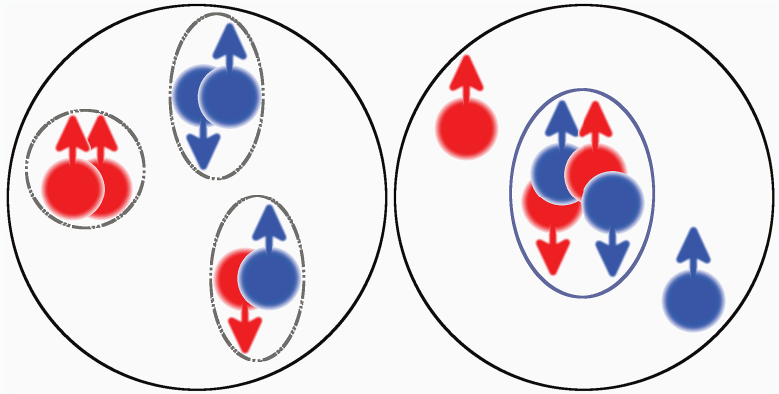

Consequences and questions

In presence of an attractive interaction:

- Form pairs
  - ◇ Pairs spatial extension
  - ◇ Possible phases
- Form quartets

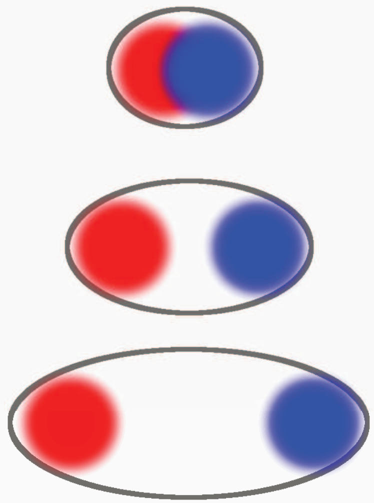

Consequences and questions

In presence of an attractive interaction:

- Form pairs
  - ◇ Pairs spatial extension
  - ◇ Possible phases
- Form quartets

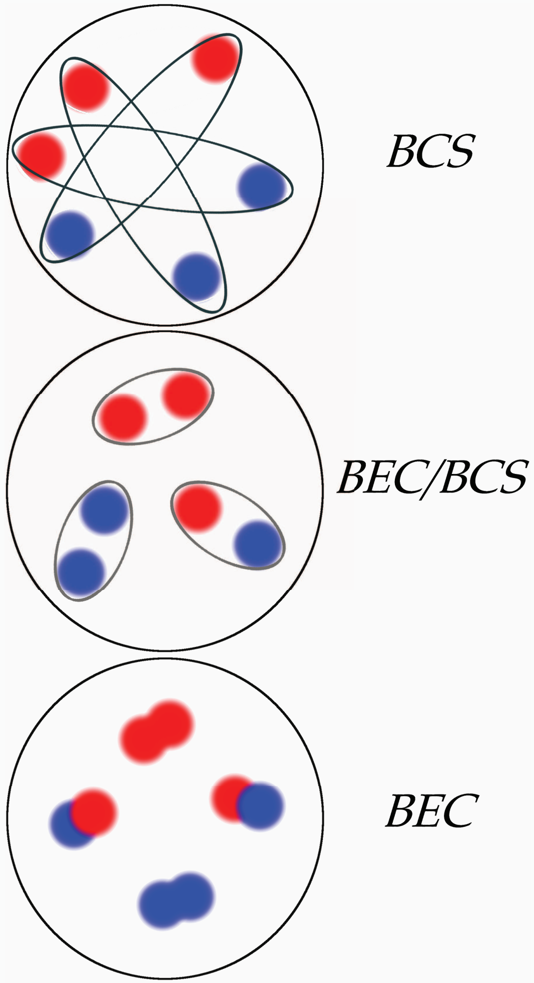

Consequences and questions

In presence of an attractive interaction:

- Form pairs
- Form quartets
  - ◇ Quartets spatial extension
  - ◇ Link between quartet and α-clustering

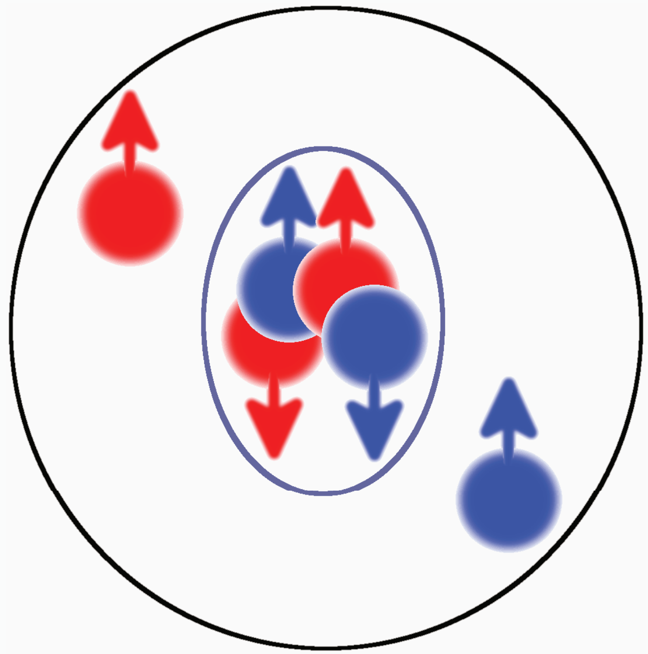

Consequences and questions

In presence of an attractive interaction:

- Form pairs
- Form quartets
  - ◇ Quartets spatial extension
  - ◇ Link between quartet and α-clustering

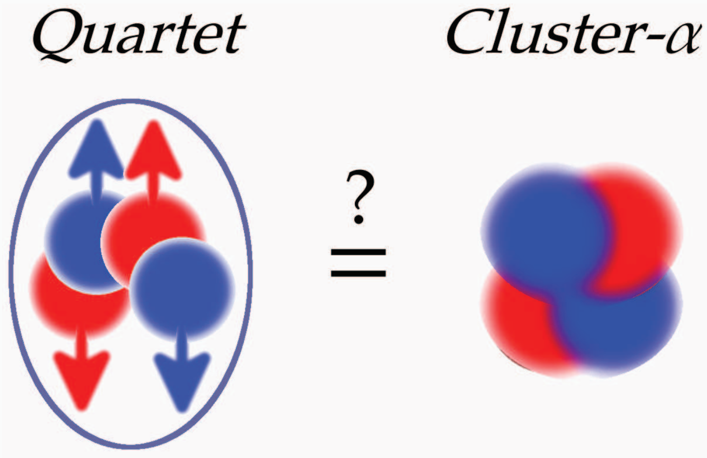

Elements of formalism

Elements of formalism

EDF Techniques

EDF range

1. Universality of the description
2. Precision in known regions
3. Increases of phenomenological level

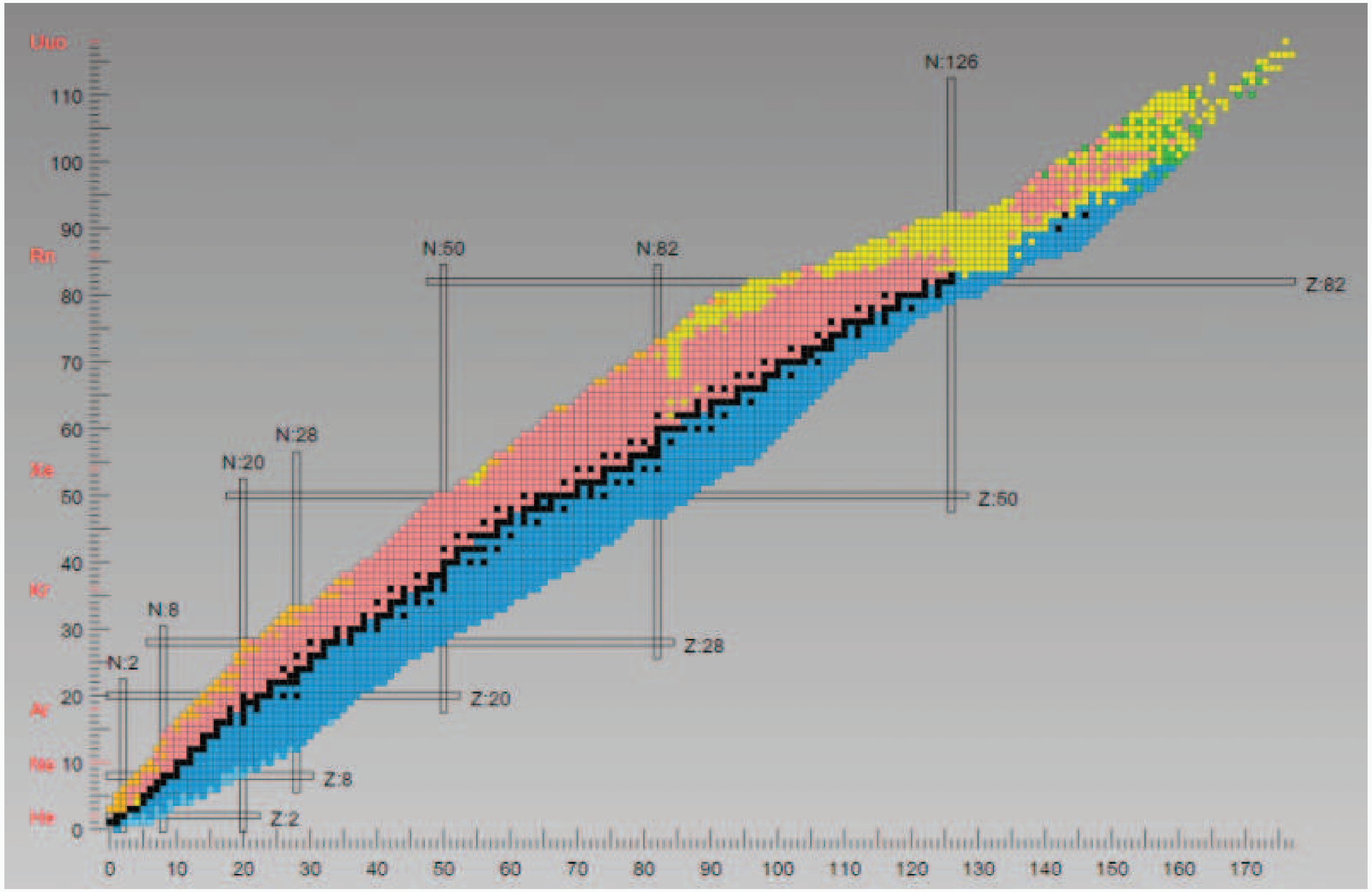

Importance of the covariance

- No kinematic interest $\left\langle \frac{v_{\text{Nucleons}}}{c} \right\rangle \simeq 0.25$
- No more analytical connection with QCD

Importance of the covariance

- No kinematic interest $\left\langle \frac{v_{\text{Nucleons}}}{c} \right\rangle \simeq 0.25$
- No more analytical connection with QCD

◇ Conserve QCD **scales**:

$S \simeq -400\text{MeV}$ and $V \simeq 350\text{MeV}$

- Account the non-relativistic regime $(V + S) \simeq 50\text{MeV}$
- Spin-orbit natural emergence $(V - S) \simeq 750\text{MeV}$

⋆ *Posteriori*: Promote clusters formation

Relativistic Energy Density Functional (R-EDF)

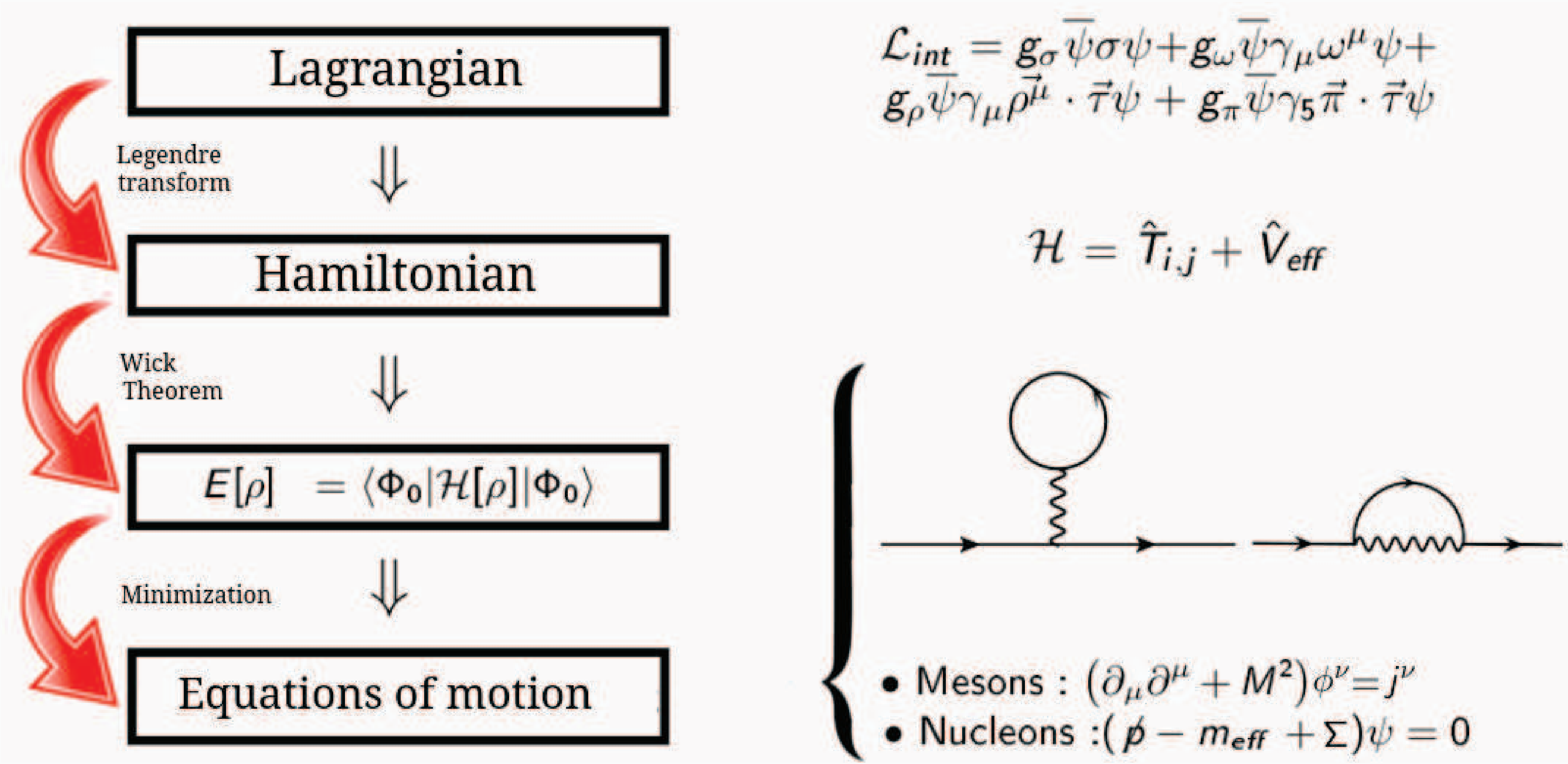

RMF equations

Minimisation of the relativistic functional

$$\delta\left[\mathcal{E}^{RMF}-\sum_{kl}\Lambda_{kl}(\rho^2-\rho)_{kl}\right]=0$$

RMF equations:

$$[h[\rho],\rho]=0$$

$$(-\Delta+m_m^2)\phi_m=\pm Tr(\Gamma_m\rho)$$

With:

$$h[\rho]=\frac{\delta\mathcal{E}^{RMF}}{\delta\rho}$$

RMF equations:

$$[h[\rho], \rho] = 0$$

$$(-\Delta + m_m^2)\phi_m = \pm Tr(\Gamma_m \rho)$$

With:

$$h[\rho] = \frac{\delta \mathcal{E}^{RMF}}{\delta \rho}$$

Self-consistent resolution

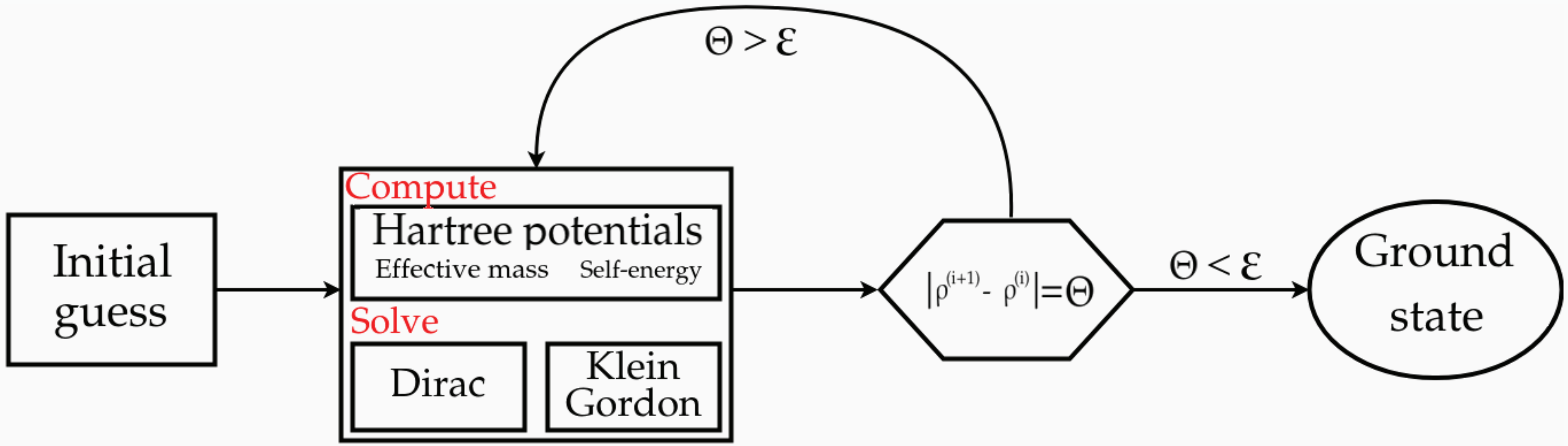

Elements of formalism

Collective correlations

Collective correlations – Principles

Taking correlations into account by:

- *P*-*H* configurations mixing
- Symmetry breaking

Particle-hole excitation of states with differents angular momentum

- Control of the incorporated correlations
- Factorial scaling

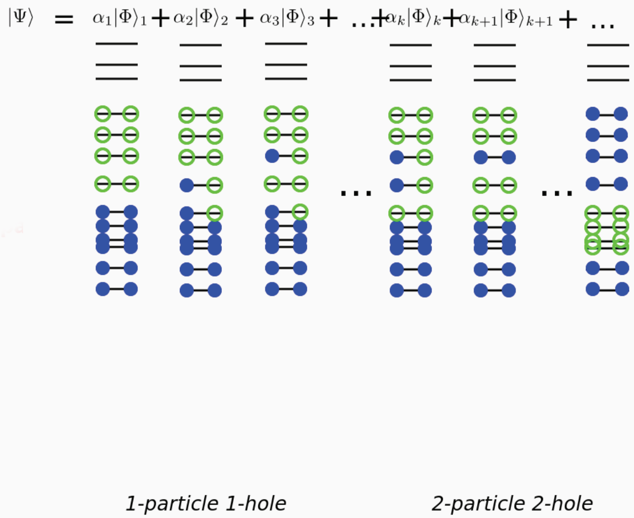

Collective correlations – Principles

Taking correlations into account by:

- P-H configurations mixing
- Symmetry breaking

Breaking of $O(3)$ and $U(1)$

- Capture collective behavior
- Numerically achievable

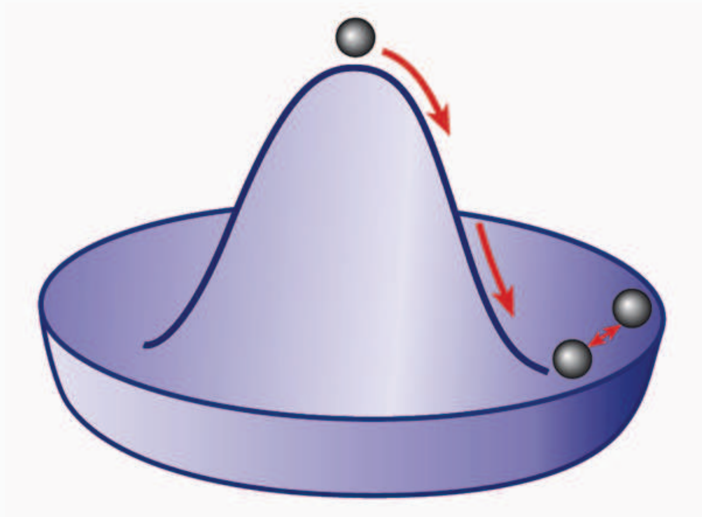

Pairing treatment – Bogolioubov

$$\beta_i = \sum_j U^*_{ji} b_j + V^*_{ji} b^\dagger_j$$

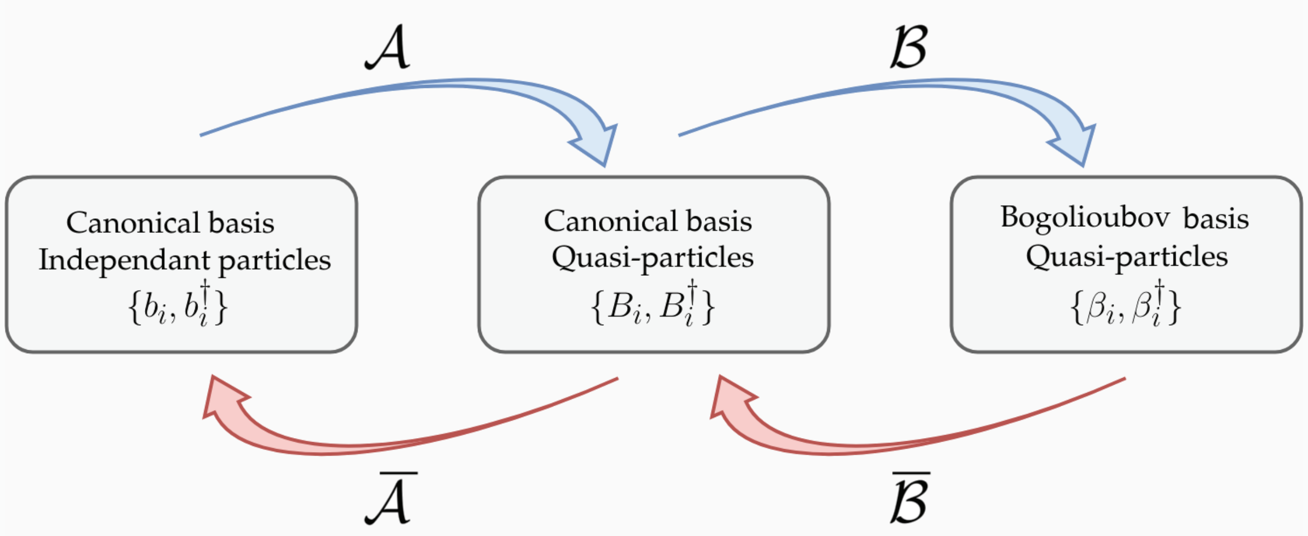

$$|\Phi_0\rangle = \prod_{i>0} \beta_i |0\rangle \qquad \hat{N} |\Phi_0\rangle \neq N |\Phi_0\rangle$$

1-body density:

$$\rho_{ij} = \frac{\langle \Phi_0 | b_j^\dagger b_i | \Phi_0 \rangle}{\langle \Phi_0 | \Phi_0 \rangle}$$

Pairing tensor:

$$\kappa_{ij} = \frac{\langle \Phi_0 | b_j b_i | \Phi_0 \rangle}{\langle \Phi_0 | \Phi_0 \rangle}$$

Pairing treatment – Bogolioubov

Relativistic **H**artree **B**ogolioubov (RHB)

Generalized density

$$\mathcal{R} = \begin{pmatrix} \rho & \kappa \\ -\kappa^* & 1-\rho^* \end{pmatrix}$$

$$\mathcal{E}^{\mathrm{RHB}} \equiv \mathcal{E}^{\mathrm{RHB}}[\mathcal{R}] = \mathcal{E}^{\mathrm{RHB}}[\rho, \kappa]$$

$$\delta \left[\mathcal{E}^{\mathrm{RHB}}[\mathcal{R}] - \mu N - Tr\{\Lambda(\mathcal{R}^2 - \mathcal{R})\} \right] = 0$$

Sound modification:

$$[\mathcal{H}, \mathcal{R}] = 0$$

•$|\kappa| = 0$ Classical phase

•$|\kappa| \neq 0$ Superfluid phase

Practical realisation – HO expansion

Basis of Harmonic Oscillator eigenstates

$$V_{OH}(r,z) = \frac{1}{2}M\left(\omega_r^2 r^2 + \omega_z z^2\right) \text{ or } V_{OH}(x,y,z) = \frac{1}{2}M\left(\omega_x^2 x^2 + \omega_z^2 z^2 + \omega_z^2 z^2\right)$$

Pros	Cons
Simple operator expressions	Artificial stability
Numerically reachable	Corollary: Poor *drip-lines* description

Parameters

- Shell number
- $\hbar\omega$

Reach a "true" minimum

$\hbar\omega$ Impact

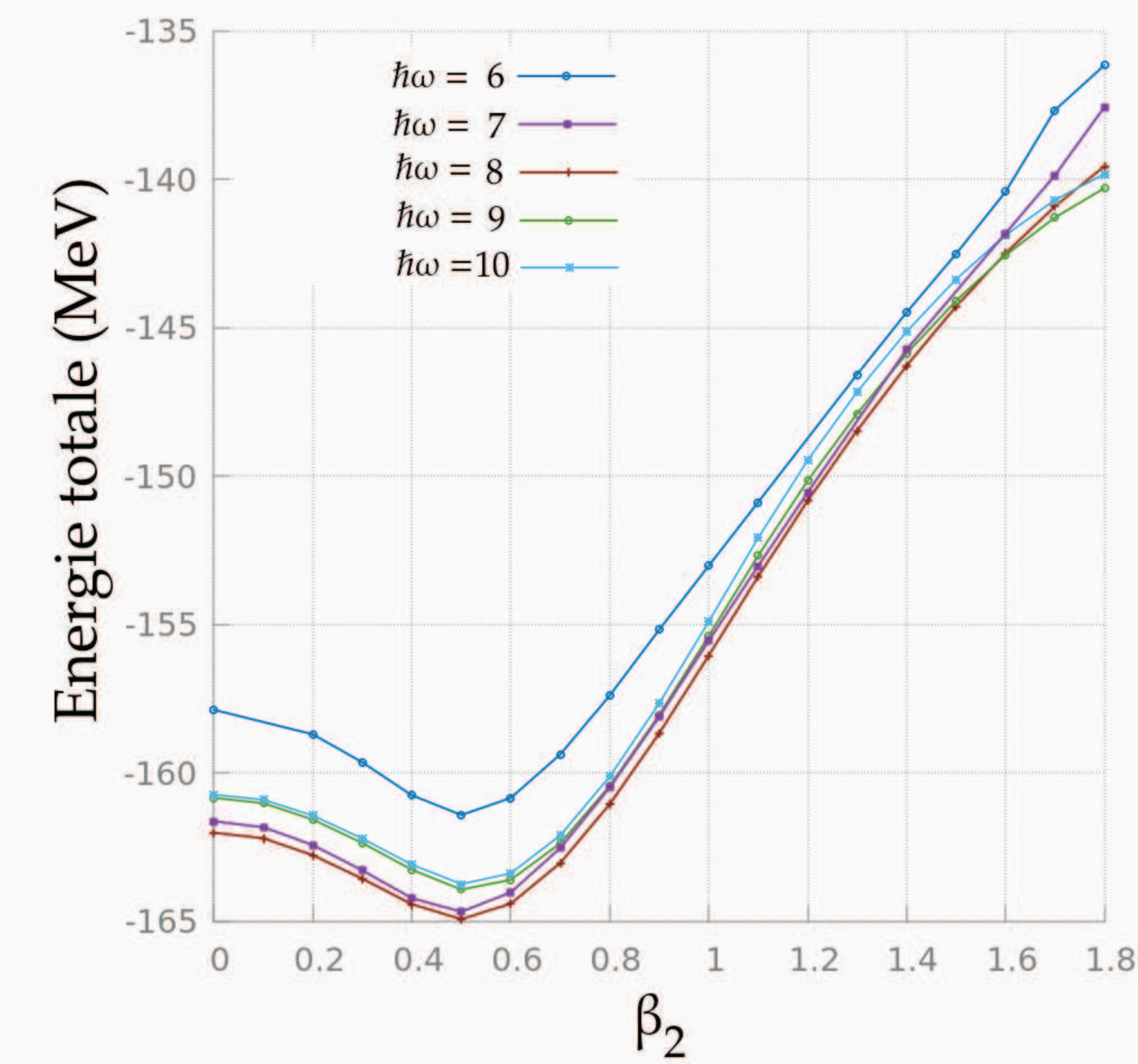

Shell number impact

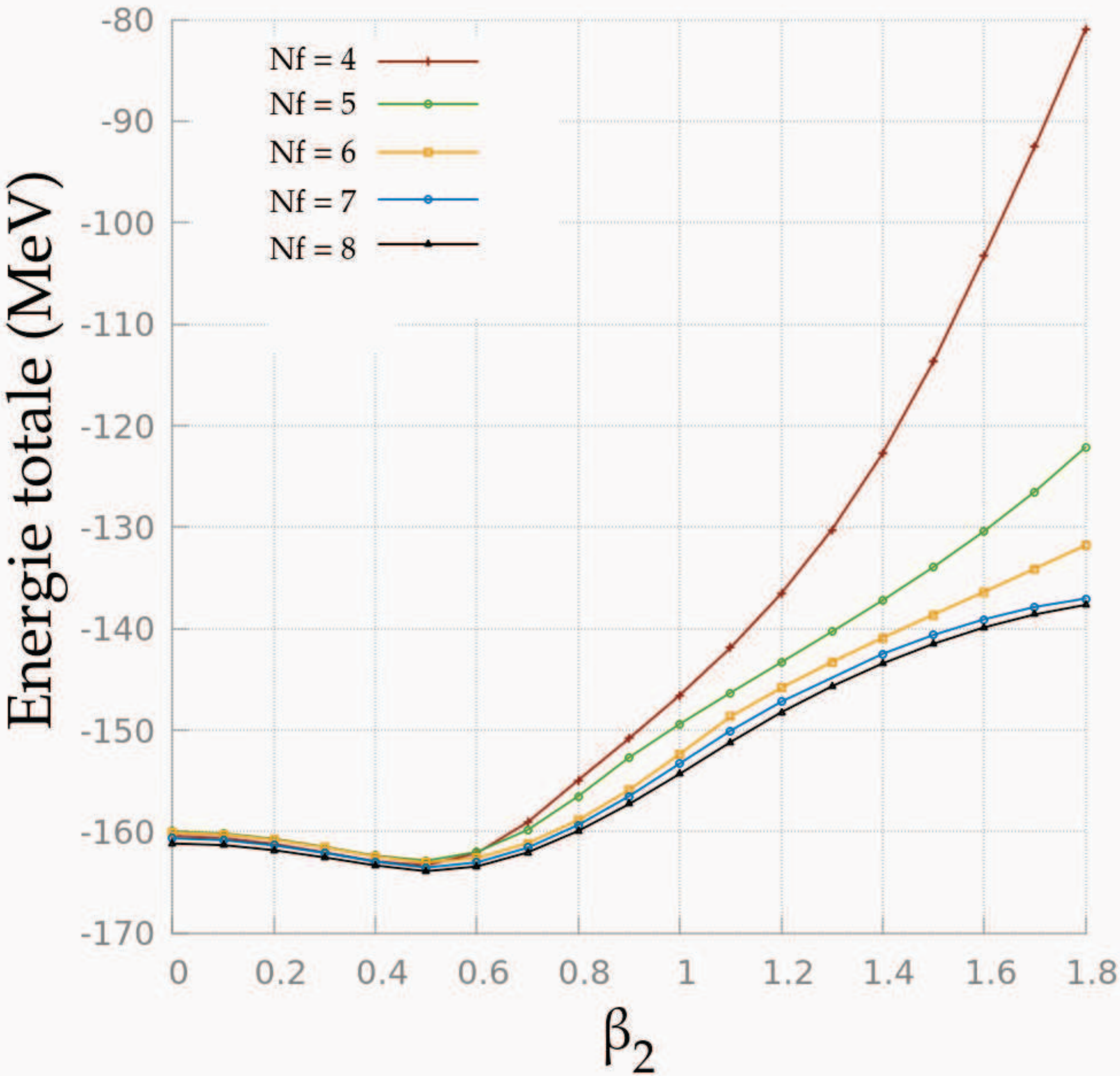

Spherical	Axial	Octupolar
R	β_2	β_3
	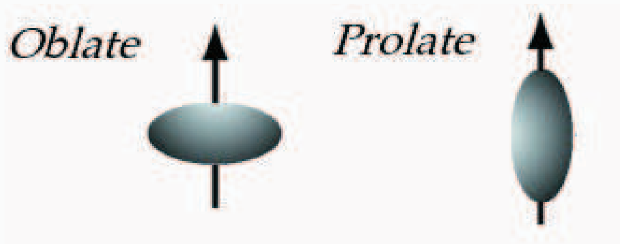	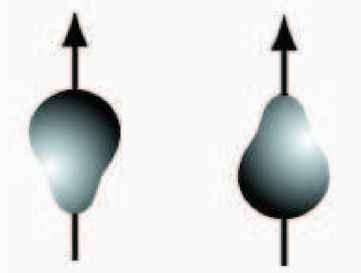

Classification des déformations – DD-ME2

Spherical	Axial	Octupolar
R	β_2	β_3

^{210}Pb

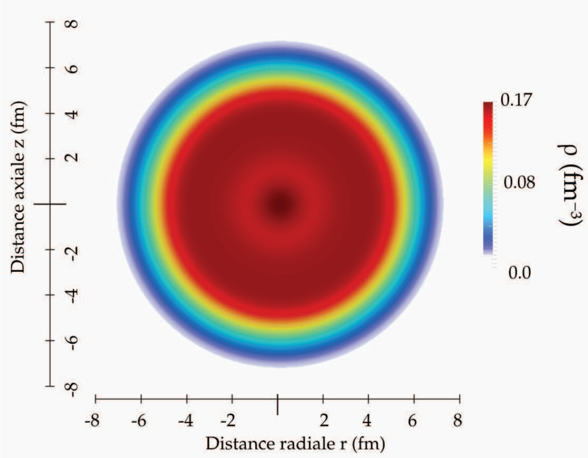

$E_{\text{Exp}} = -1645.5$ MeV

$E_{\text{RMF}} = -1648.1$ MeV

^{234}U

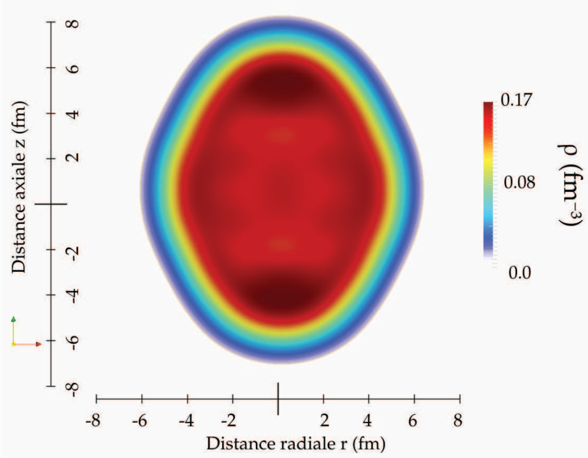

$E_{\text{Exp}} = -1778.0$ MeV

$E_{\text{RMF}} = -1775.6$ MeV

^{224}Ra

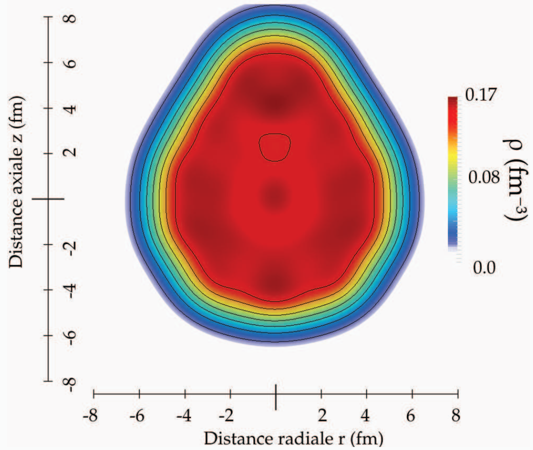

$E_{\text{Exp}} = -1720.3$ MeV

$E_{\text{RMF}} = -1726.8$ MeV

Triaxiality and beyond – DD-ME2

Triaxial configuration, with parity breaking: ^{44}Ca

$\bullet \beta_2 = 0.2$ $\bullet \beta_3 = 0.3$

$\bullet \gamma = 30$ $\bullet \beta_{32} = 0.1$

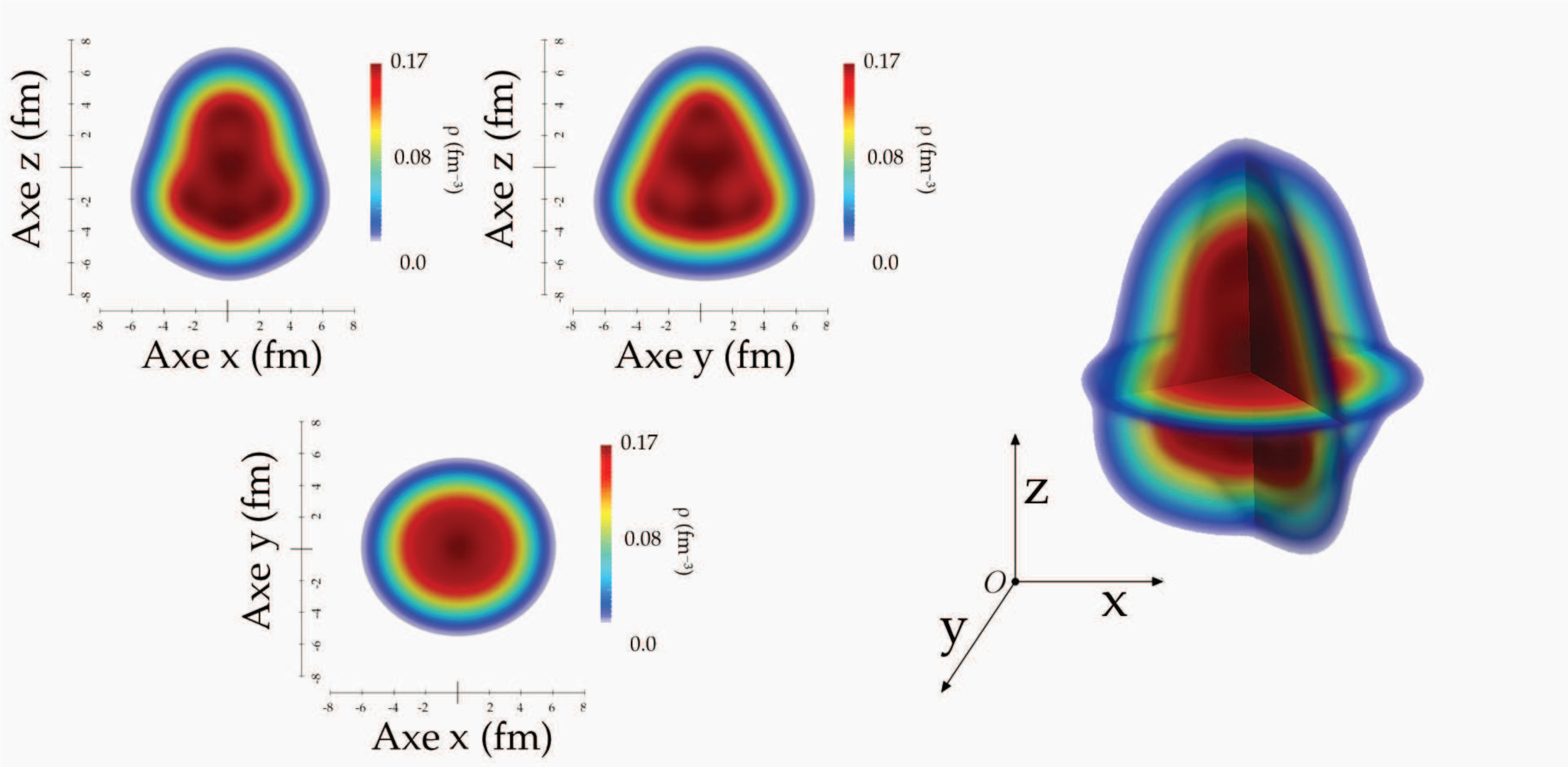

RMF under multiple constraints

Adding several constraints at functional level

$$\mathcal{E}'(\rho) = \langle \Phi_0 | H | \Phi_0 \rangle - \sum_{\lambda\mu} \overbrace{\Lambda_{\lambda\mu}}^{\text{Contrainte}} \left(\langle \Phi_0 | Q_{\lambda\mu} | \Phi_0 \rangle - \underbrace{q_{\lambda\mu}}_{\text{Valeur voulue}} \right)$$

How to set the $\Lambda_{\lambda\mu}$?

- One or two constraints: Empirically
- Beyond: Complex problem...

Solution: bio-mimetism !

Genetical algorithms – Presentation

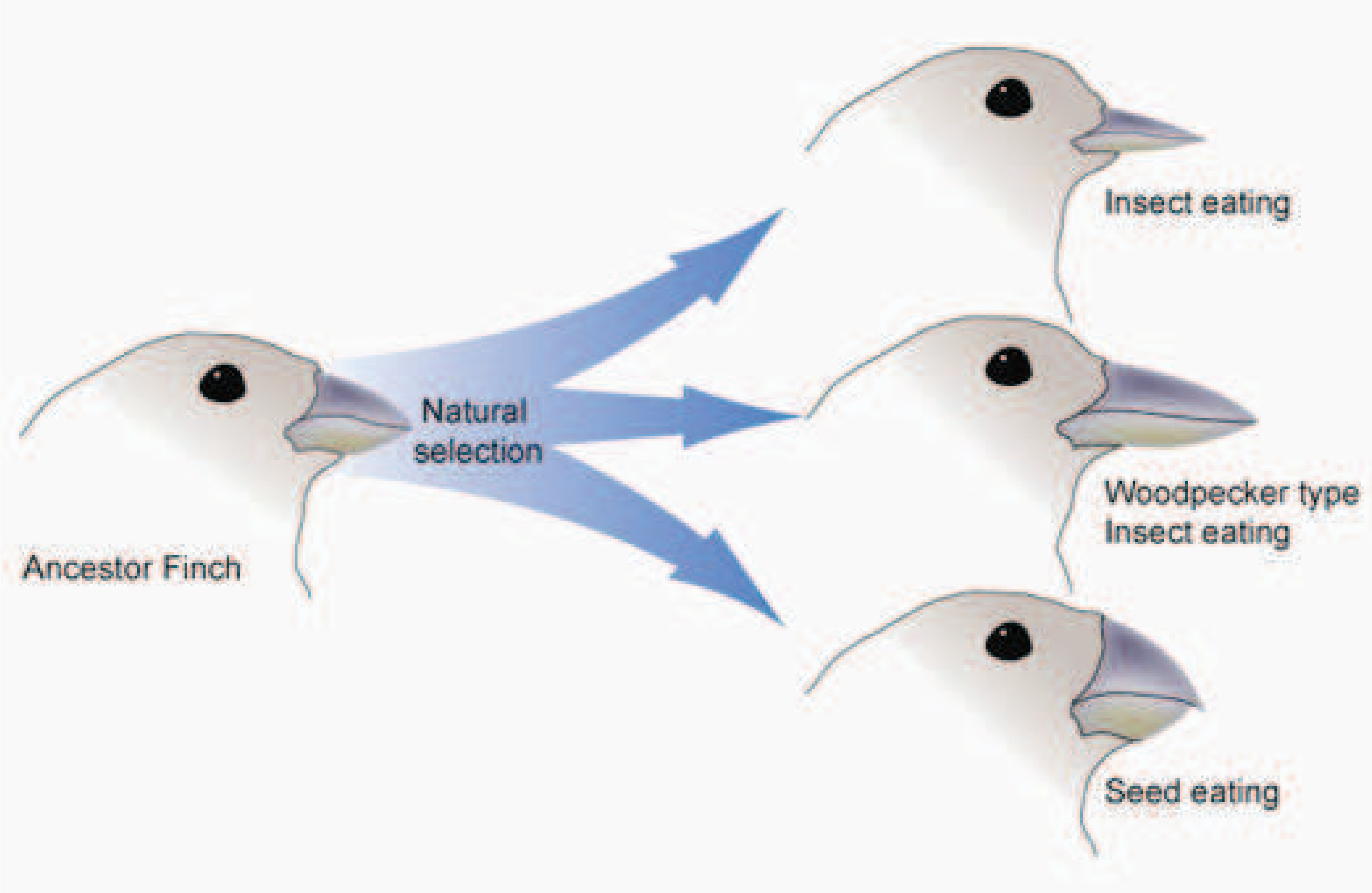

Genetical algorithms – Presentation

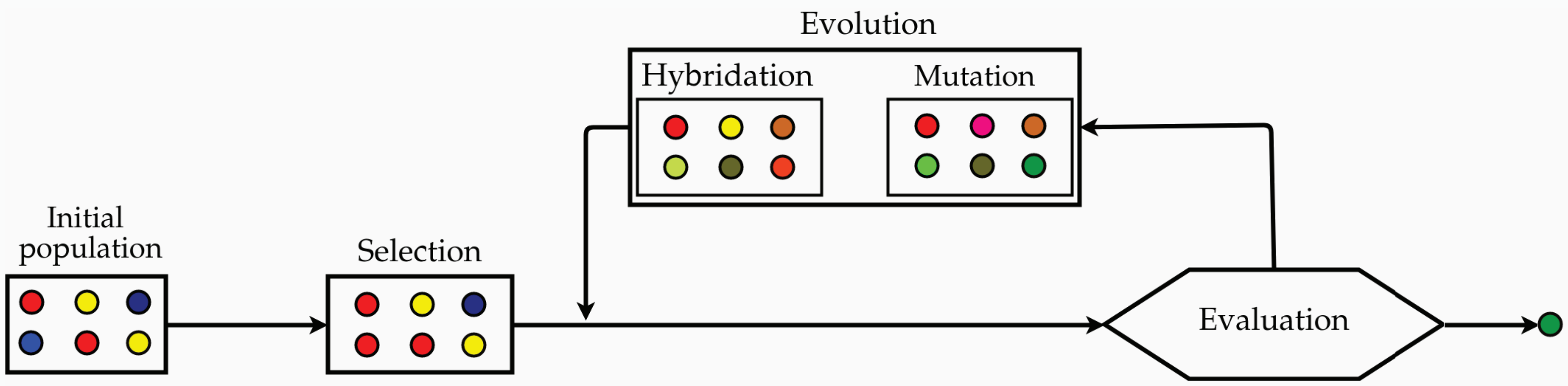

Minimisation of a 1D function:

Gradient descent (bad):

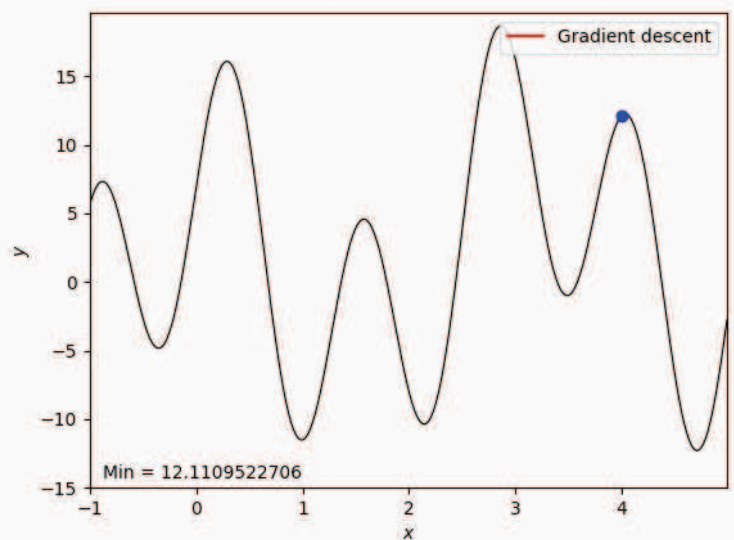

Genetic:

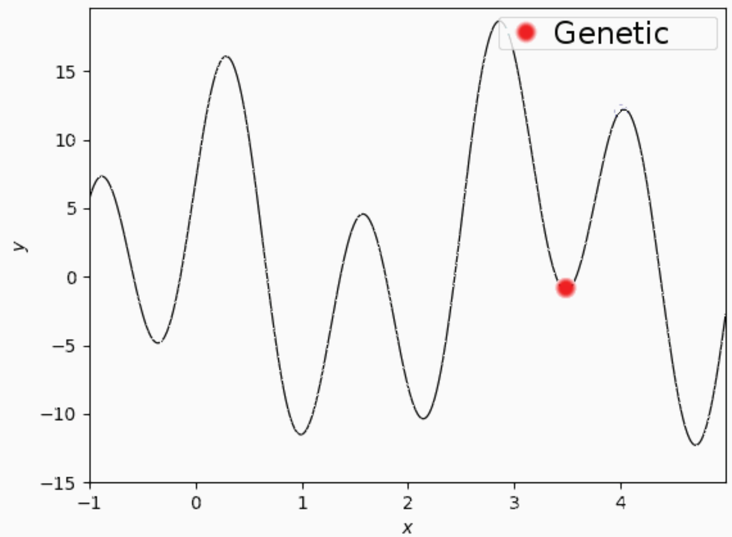

Genetical algorithms – Applications

$$\text{Individual: } I^{(i)} = \begin{pmatrix} c^{(i)}_{\text{Radius}} \\ c^{(i)}_{Q_{20}} \\ c^{(i)}_{Q_{30}} \\ c^{(i)}_{Q_{32}} \\ c^{(i)}_{\gamma} \end{pmatrix}, \quad \text{Population: } P = \{I^{(0)}, .., I^{(i)}, .., I^{(n)}\}$$

1. Selection (tournament): $\mathcal{F}(I^{(a)}, I^{(b)}) = min \begin{pmatrix} |{E'_n}^{(a)} - {E'_{n-1}}^{(a)}| \\ |{E'_n}^{(b)} - {E'_{n-1}}^{(b)}| \end{pmatrix}$
2. Evolution: $I^{(i)} = \begin{pmatrix} c^{(i)}_{\text{Radius}} \\ c^{(i)}_{Q_{20}} \\ c^{(i)}_{Q_{30}} \\ c^{(i)}_{Q_{32}} \\ c^{(i)}_{\gamma} \end{pmatrix} \xrightarrow[\text{mutations}]{\text{Random}} \tilde{I}^{(i)} = \begin{pmatrix} c^{(i)}_{\text{Rayon}} \\ c^{(i)}_{Q_{20}} \\ c^{(i)}_{Q_{30}} \\ c^{(i)}_{Q_{32}} \\ c^{(i)}_{\gamma} \end{pmatrix} \cdot \begin{pmatrix} 0.231 \\ 0.091 \\ 0.834 \\ 0.621 \\ 0.005 \end{pmatrix}$
3. Evaluation: $\forall I \quad |E'^{(n)} - E'^{(n-1)}|$

Genetical algorithms – Applications

$$\text{Individual: } I^{(i)} = \begin{pmatrix} c^{(i)}_{\text{Radius}} \\ c^{(i)}_{Q_{20}} \\ c^{(i)}_{Q_{30}} \\ c^{(i)}_{Q_{32}} \\ c^{(i)}_{\gamma} \end{pmatrix}, \quad \text{Population: } P = \{I^{(0)}, .., I^{(i)}, .., I^{(n)}\}$$

1. Selection (tournament): $\mathcal{F}(I^{(a)}, I^{(b)}) = min \begin{pmatrix} |{E'_n}^{(a)} - {E'_{n-1}}^{(a)}| \\ |{E'_n}^{(b)} - {E'_{n-1}}^{(b)}| \end{pmatrix}$
2. Evolution: $I^{(i)} = \begin{pmatrix} c^{(i)}_{\text{Radius}} \\ c^{(i)}_{Q_{20}} \\ c^{(i)}_{Q_{30}} \\ c^{(i)}_{Q_{32}} \\ c^{(i)}_{\gamma} \end{pmatrix} \xrightarrow[\text{mutations}]{\text{Random}} \tilde{I}^{(i)} = \begin{pmatrix} c^{(i)}_{\text{Rayon}} \\ c^{(i)}_{Q_{20}} \\ c^{(i)}_{Q_{30}} \\ c^{(i)}_{Q_{32}} \\ c^{(i)}_{\gamma} \end{pmatrix} \cdot \begin{pmatrix} 0.231 \\ 0.091 \\ 0.834 \\ 0.621 \\ 0.005 \end{pmatrix}$
3. Evaluation: $\forall I \quad |E'^{(n)} - E'^{(n-1)}|$

Genetical algorithms – Applications

$$\text{Individual: } I^{(i)} = \begin{pmatrix} c^{(i)}_{\text{Radius}} \\ c^{(i)}_{Q_{20}} \\ c^{(i)}_{Q_{30}} \\ c^{(i)}_{Q_{32}} \\ c^{(i)}_{\gamma} \end{pmatrix}, \quad \text{Population: } P = \{I^{(0)}, .., I^{(i)}, .., I^{(n)}\}$$

1. Selection (tournament): $\mathcal{F}(I^{(a)}, I^{(b)}) = min \begin{pmatrix} |{E'_n}^{(a)} - {E'_{n-1}}^{(a)}| \\ |{E'_n}^{(b)} - {E'_{n-1}}^{(b)}| \end{pmatrix}$
2. Evolution: $I^{(i)} = \begin{pmatrix} c^{(i)}_{\text{Radius}} \\ c^{(i)}_{Q_{20}} \\ c^{(i)}_{Q_{30}} \\ c^{(i)}_{Q_{32}} \\ c^{(i)}_{\gamma} \end{pmatrix} \xrightarrow[\text{mutations}]{\text{Random}} \tilde{I}^{(i)} = \begin{pmatrix} c^{(i)}_{\text{Rayon}} \\ c^{(i)}_{Q_{20}} \\ c^{(i)}_{Q_{30}} \\ c^{(i)}_{Q_{32}} \\ c^{(i)}_{\gamma} \end{pmatrix} \cdot \begin{pmatrix} 0.231 \\ 0.091 \\ 0.834 \\ 0.621 \\ 0.005 \end{pmatrix}$
3. Evaluation: $\forall I \quad |E'^{(n)} - E'^{(n-1)}|$

Set of dynamical constraints

Genetical algorithms – Results

Important numerical progress[1]

Nucleus and constraints	Iterations (classical)	Iterations (genetical)
^{16}O $\{R = 4\text{fm}, \beta_2 = 0.3, \beta_3 = 0.1\}$	1281	1513
^{16}O $\{R = 4\text{fm}, \beta_2 = 0.3, \beta_3 = 0.1, \gamma = 0\}$	1281	421
^{16}O $\{R = 4\text{fm}, \beta_2 = 0.3, \beta_3 = 0.1, \gamma = 0, \beta_{32} = 0.3\}$	1542	530
^{120}Sn $\{R = 4\text{fm}, \beta_2 = 0.3, \beta_3 = 0.1\}$	938	1119
^{120}Sn $\{R = 4\text{fm}, \beta_2 = 0.3, \beta_3 = 0.1, \gamma = 0\}$	2362	576
^{120}Sn $\{R = 4\text{fm}, \beta_2 = 0.3, \beta_3 = 0.1, \gamma = 0, \beta_{32} = 0.3\}$	2729	613

Futures: a new kind of HFB solver.

[1] R.D. Lasseri *in preparation* (2018)

Nuclear clustering

Nuclear clustering

What is a cluster ?

Clusters

Experimental clues

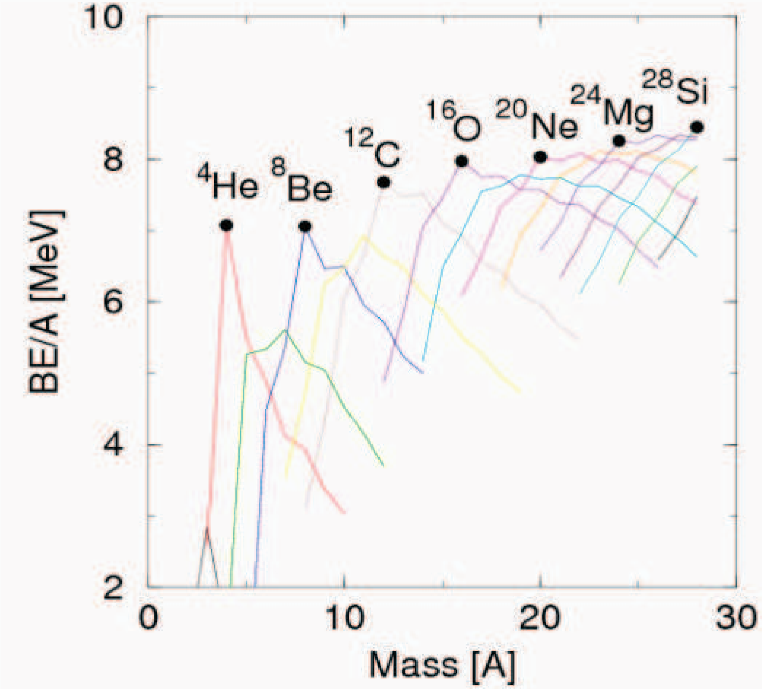

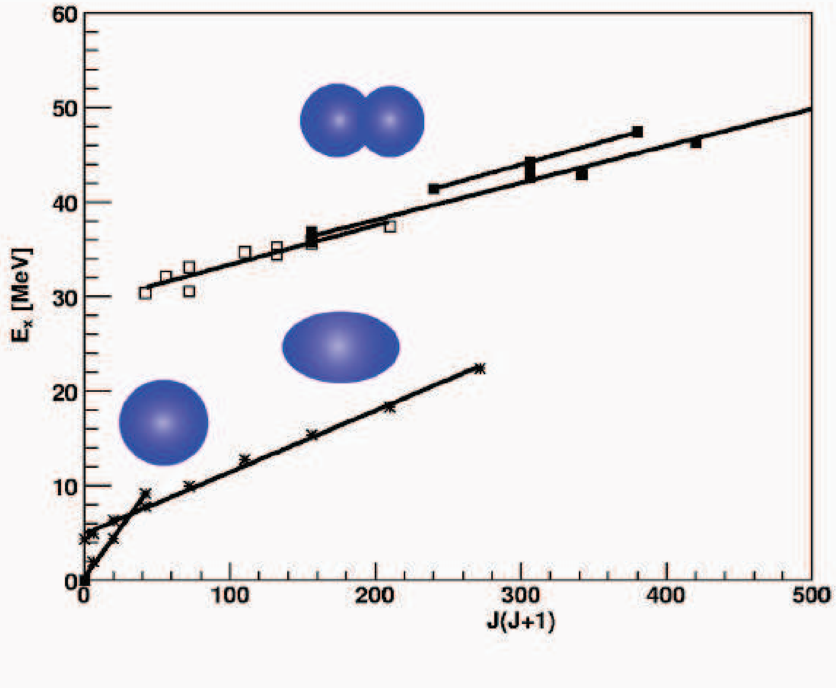

Outline:

1. Emergence
2. Localisation
3. Phase transition

Nuclear clustering

Clusters emergence

Clusterised configuration of Carbon 12

RHB exploration of $\{\beta_2, \beta_3, \beta_{32}, \gamma\}$

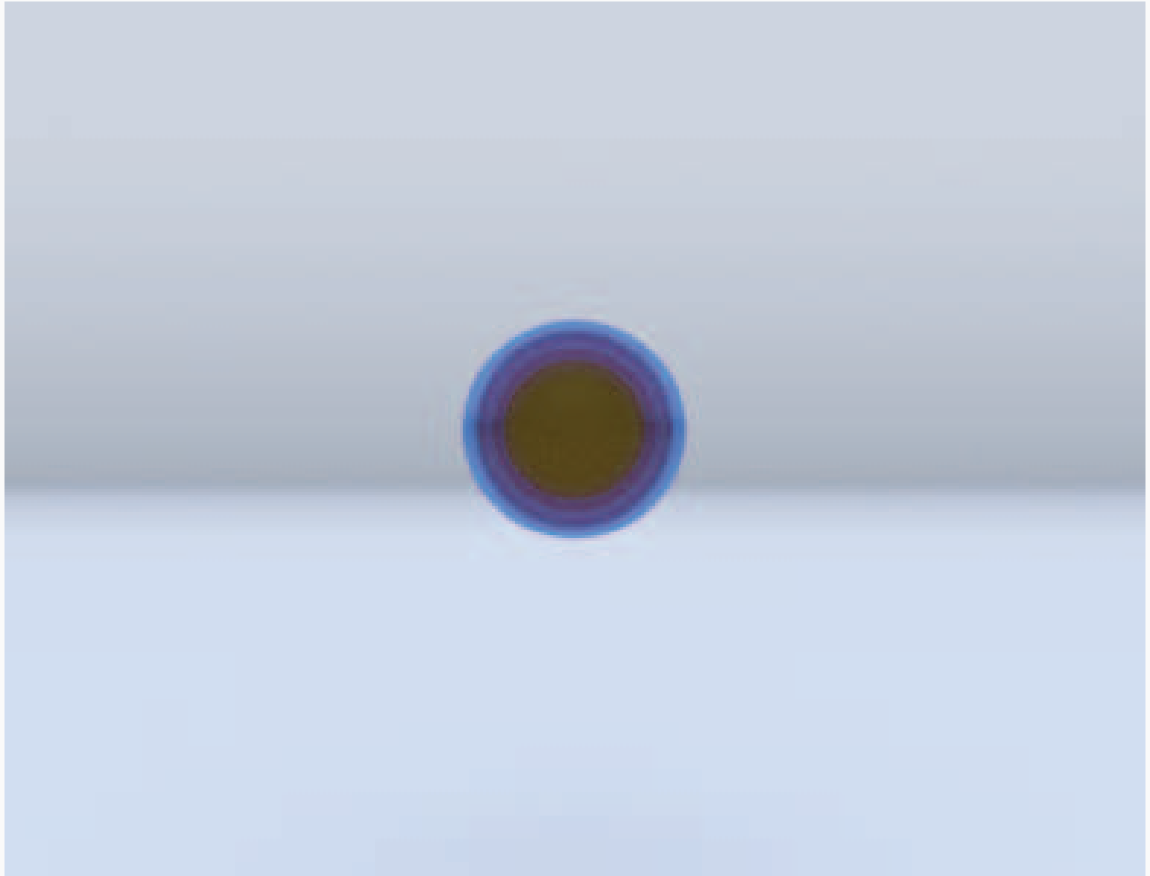

Natural emergence of localised sub-structures[2]

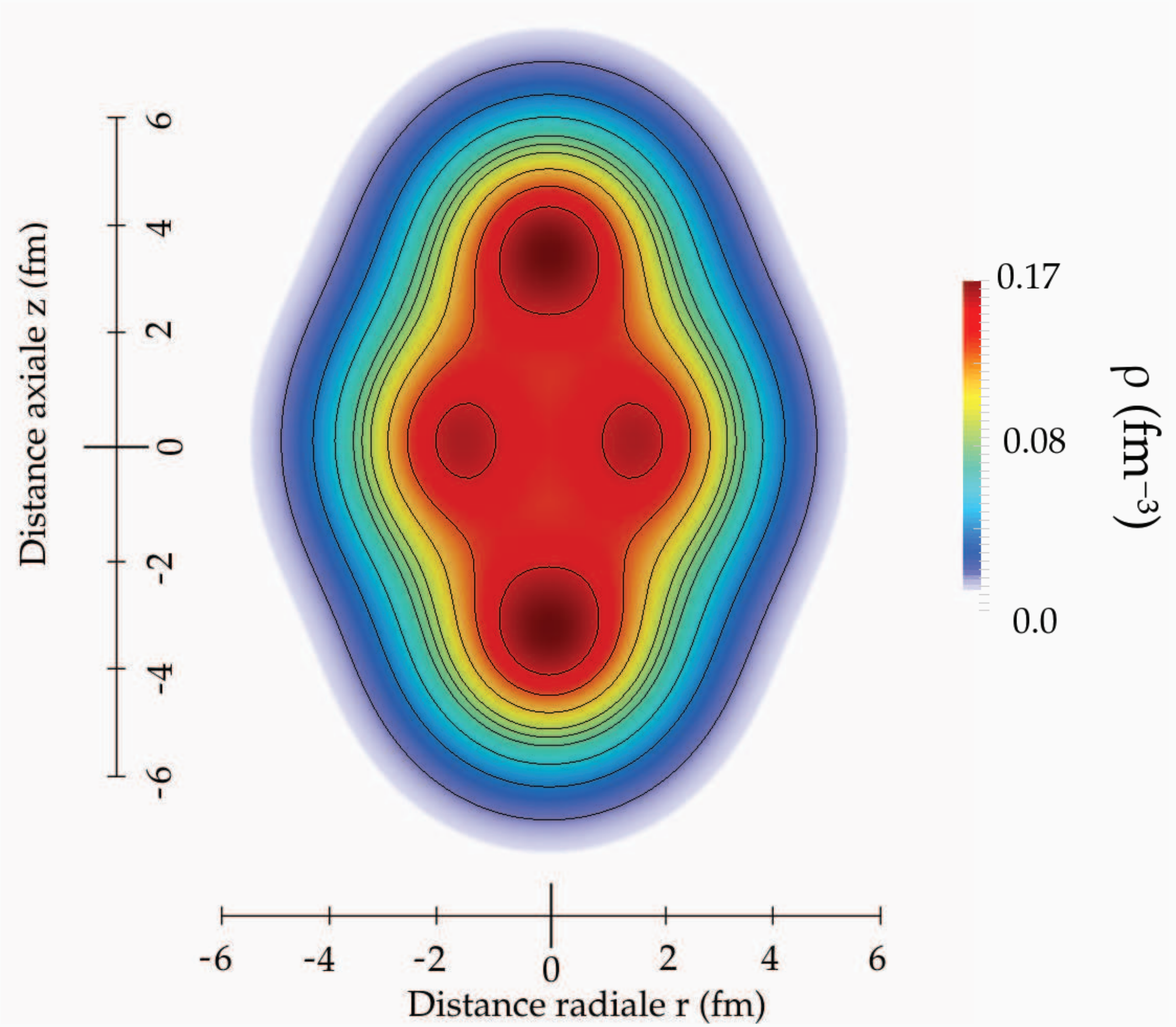

[2] Ebran, Khan, Niksic, Vretenar, Nature, 487 :341 EP –, Jul 2012

Neon 20 – Relativistic specificity

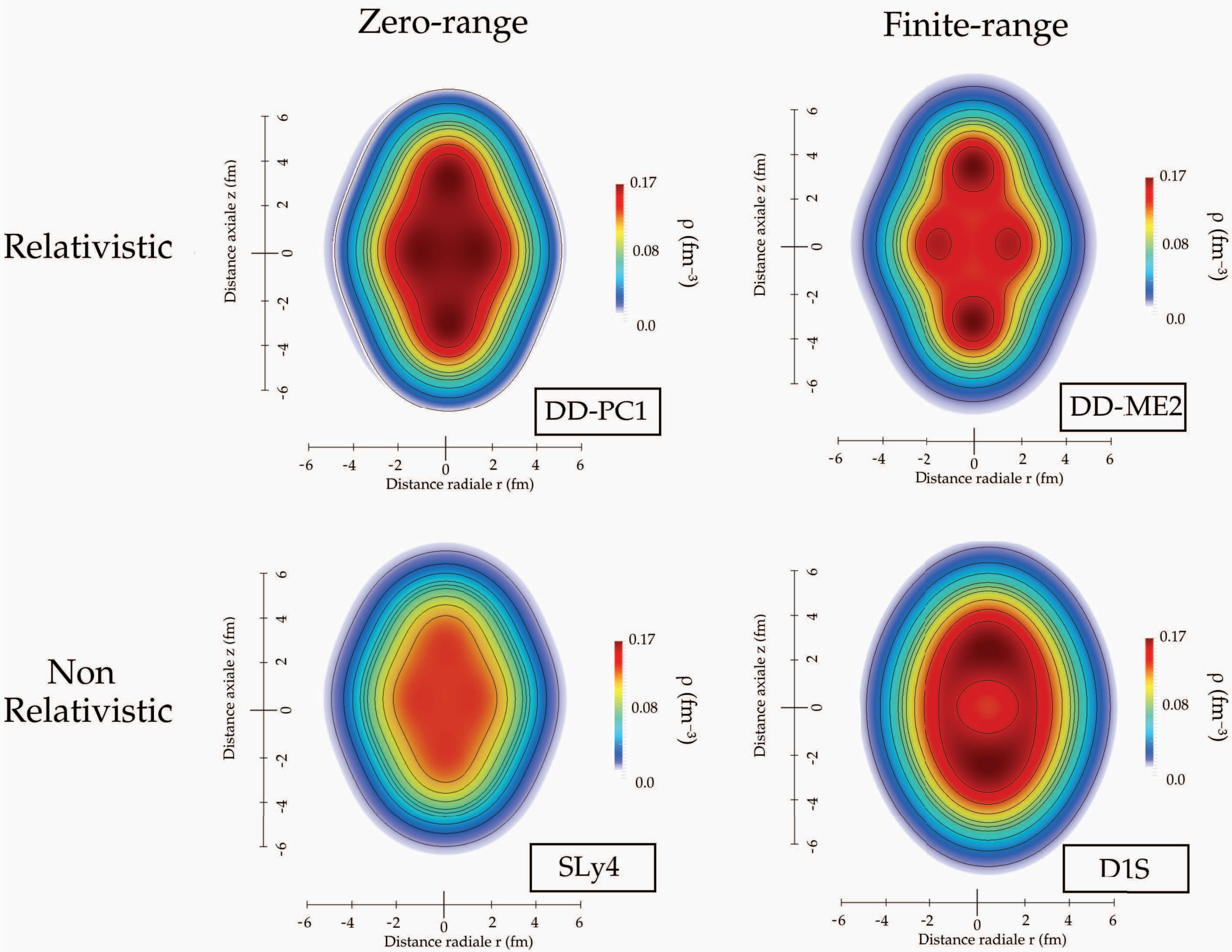

Localisation measure

$$C_{\tau\sigma}(\mathbf{r}) = \left[1 + \left(\frac{\tau_{\tau\sigma}\rho_{\tau\sigma} - \frac{1}{4}[\nabla\rho_{\tau\sigma}]^2}{\rho_{\tau\sigma}\tau_{\tau\sigma}^{\mathrm{TF}}} \right)^2 \right]^{-1}$$

$$\text{Two regimes: } C_{\tau\sigma} = \begin{cases} 0.5 & \text{Delocalised} \\ 1.0 & \text{Totally localised} \end{cases}$$

Localisation measure

$$C_{\tau\sigma}(\mathbf{r}) = \left[1 + \left(\frac{\tau_{\tau\sigma}\rho_{\tau\sigma} - \frac{1}{4}[\nabla\rho_{\tau\sigma}]^2}{\rho_{\tau\sigma}\tau_{\tau\sigma}^{\mathrm{TF}}}\right)^2\right]^{-1}$$

Two regimes: $C_{\tau\sigma} = \begin{cases} 0.5 & \text{Delocalised} \\ 1.0 & \text{Totally localised} \end{cases}$

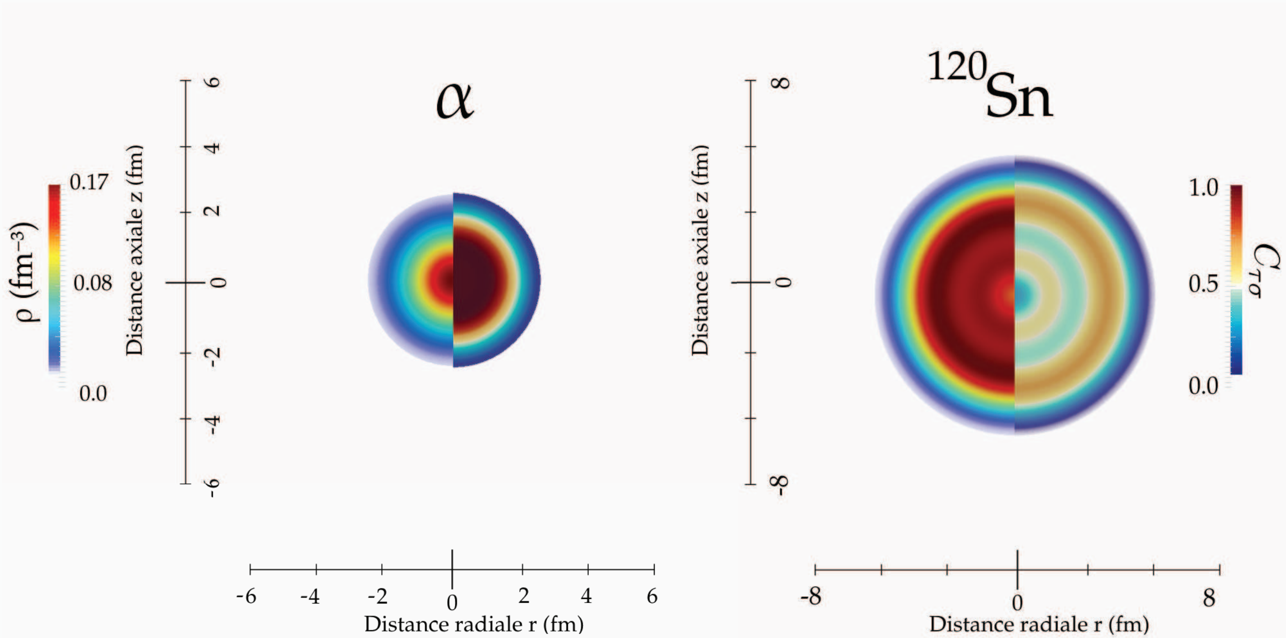

Emergence of two well-localised clusters

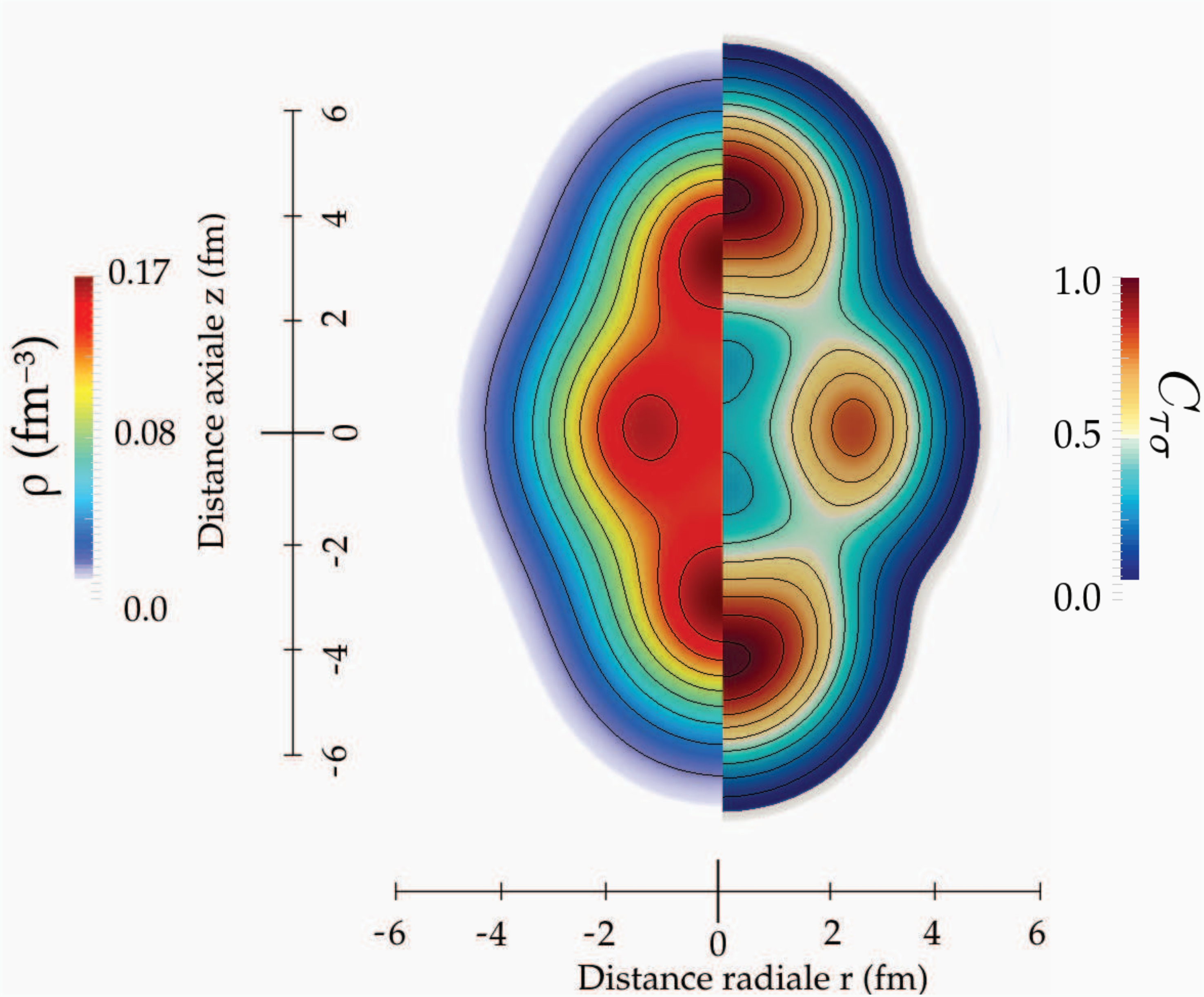

Nuclear clustering

Localisation

Spatial dispersion

Possibles phases

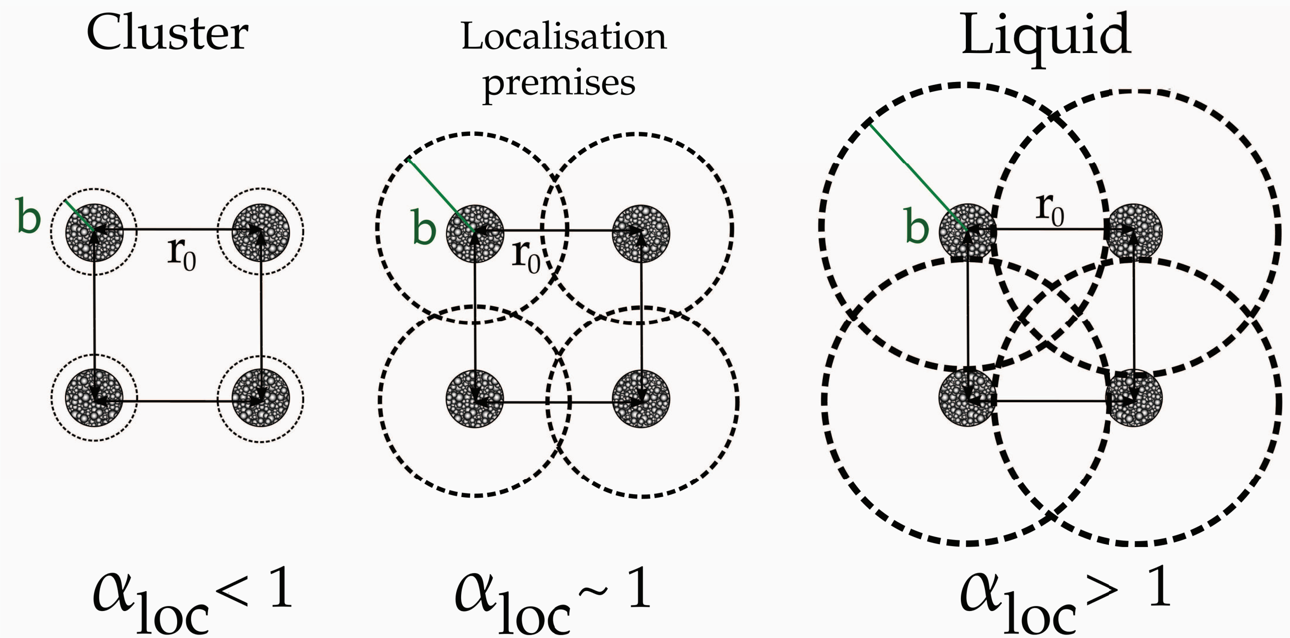

Ingredients

- Nucleonic wavefunction spatial-extension
- Dispersion of the system

Generalised localisation parameter

$$\alpha_{\mathrm{loc}} \equiv f\left(\frac{b}{r_0}\right) \propto f\left(\frac{A}{m \cdot R}\right)$$

Spatial dispersion – Microscopic results

Nuclei where cluster formation is boosted[3]

Microscopic computation of valence-state dispersion

$$\alpha_{\text{loc}} \equiv f\left(\frac{A}{m \cdot R}\right)$$

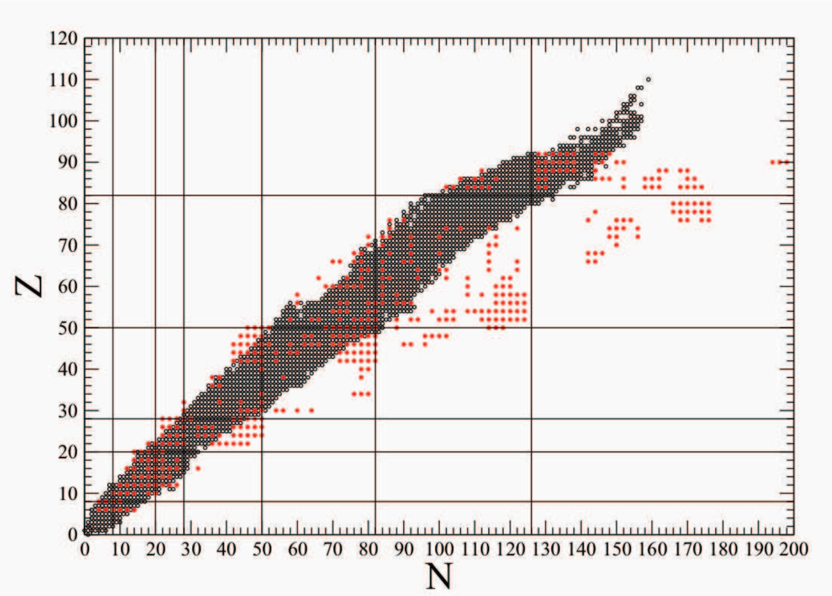

[3] Ebran, Khan, **Lasseri**, Vretenar, PRC 97, 061301(R), Rapid Communication (2018) (2018)

Nuclei where cluster formation is boosted

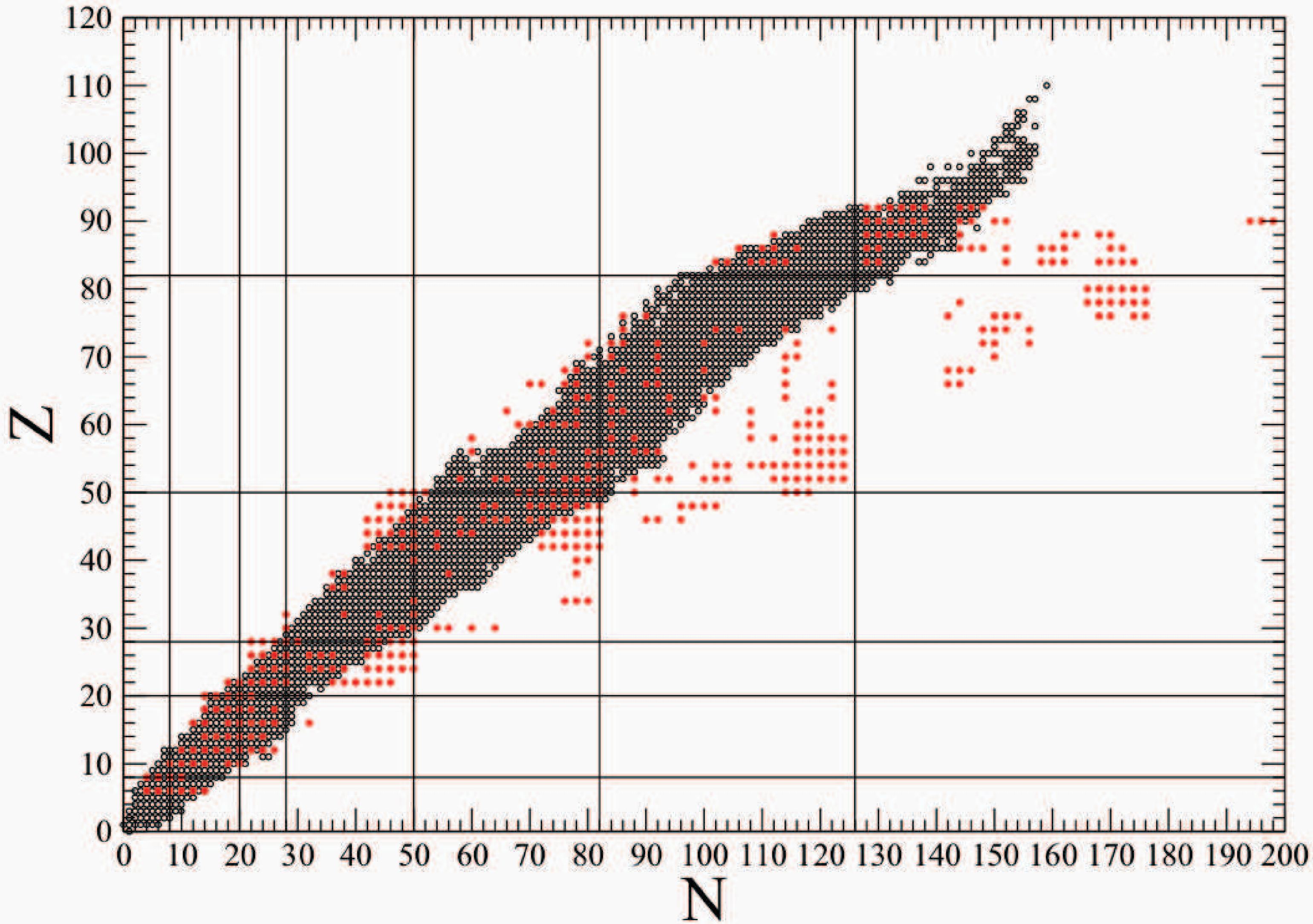

Nuclear "Phases" – Calcium 40

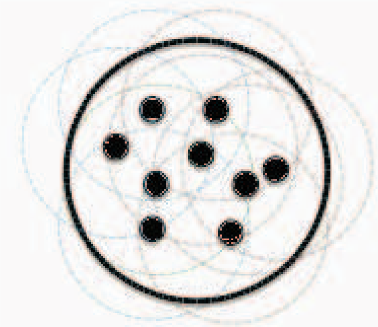

$$\underbrace{\text{Liquid}}_{\alpha_{loc} > 1}$$

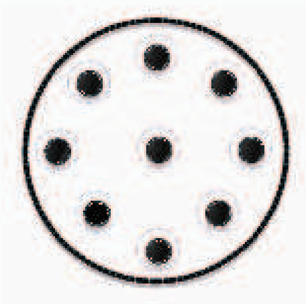

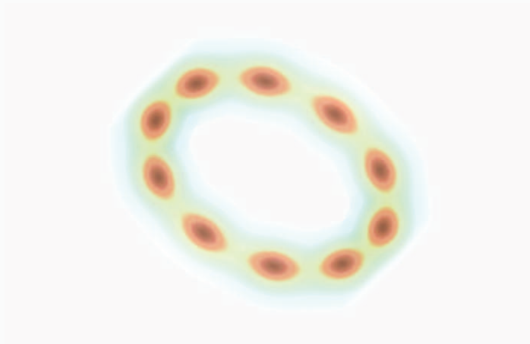

$$\underbrace{\text{Cluster}}_{\alpha_{loc} \leq 1}$$

Nuclear clustering

Phase transition

Description

How to shift from one phase to the other ?

^{16}O: From a sphere to a tetrahedron – Principle

Transition from a continuous symmetry to a discrete one [3]

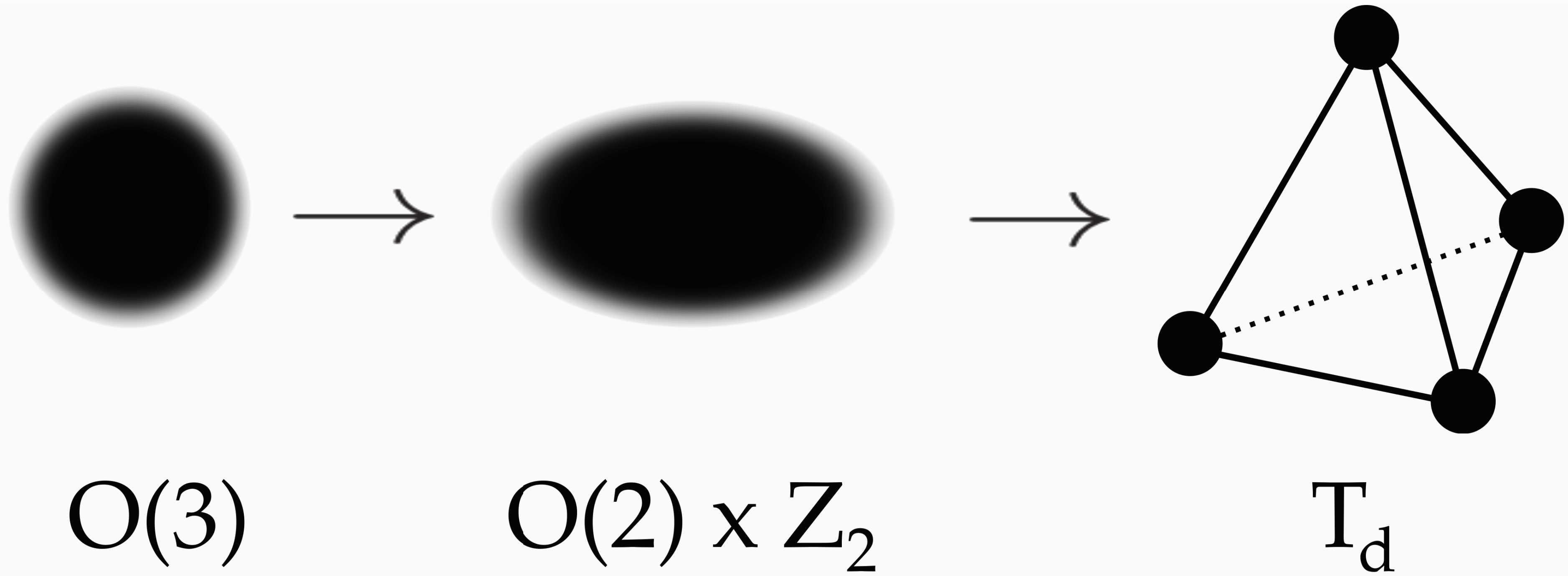

[3] R.D Lasseri et al, in preparation (2018)

^{16}O: From a sphere to a tetrahedron – Results

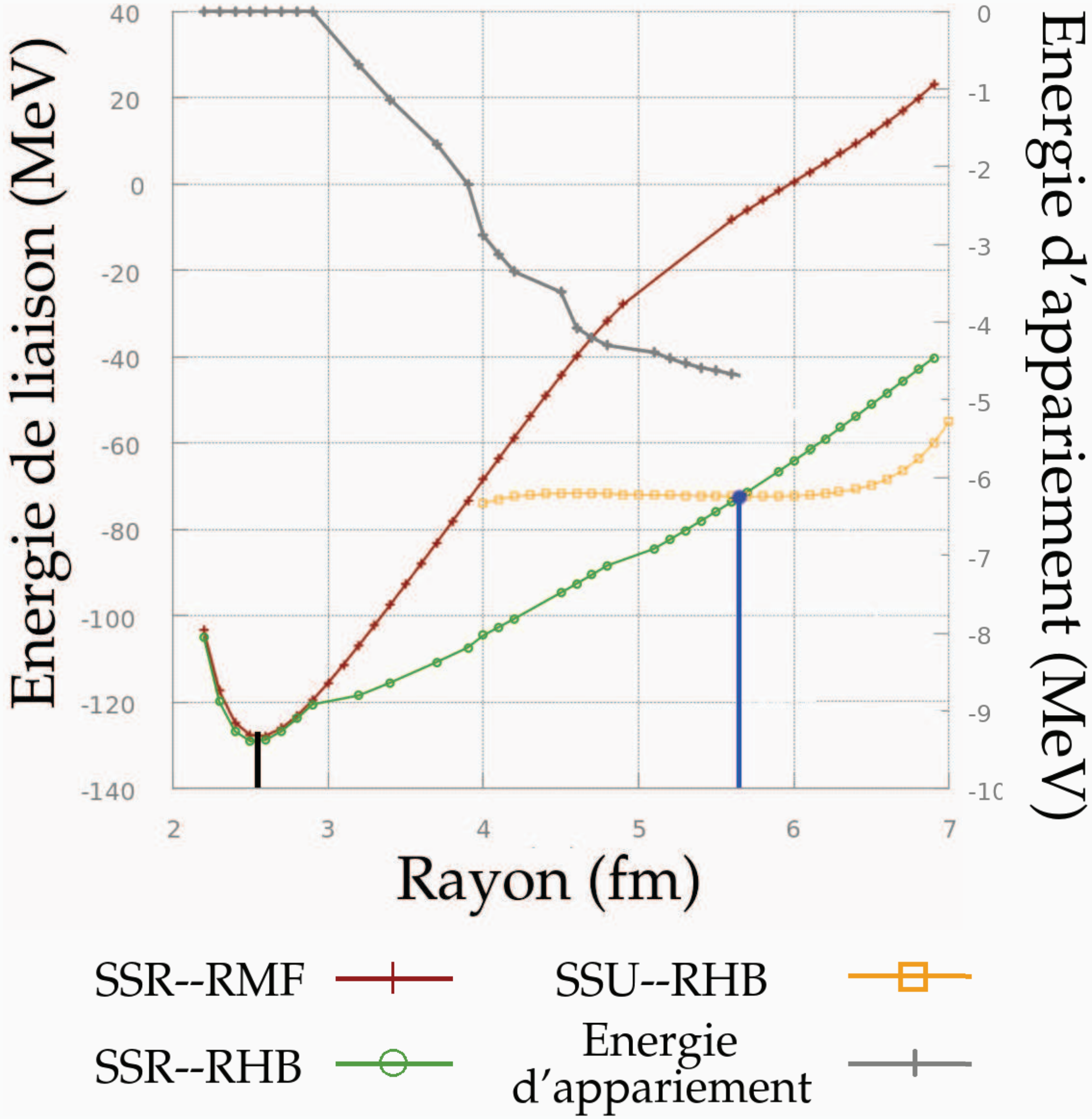

$$\alpha_{loc} \equiv f\left(\frac{A}{m \cdot R}\right)$$

^{16}O: From a sphere to a tetrahedron – Results

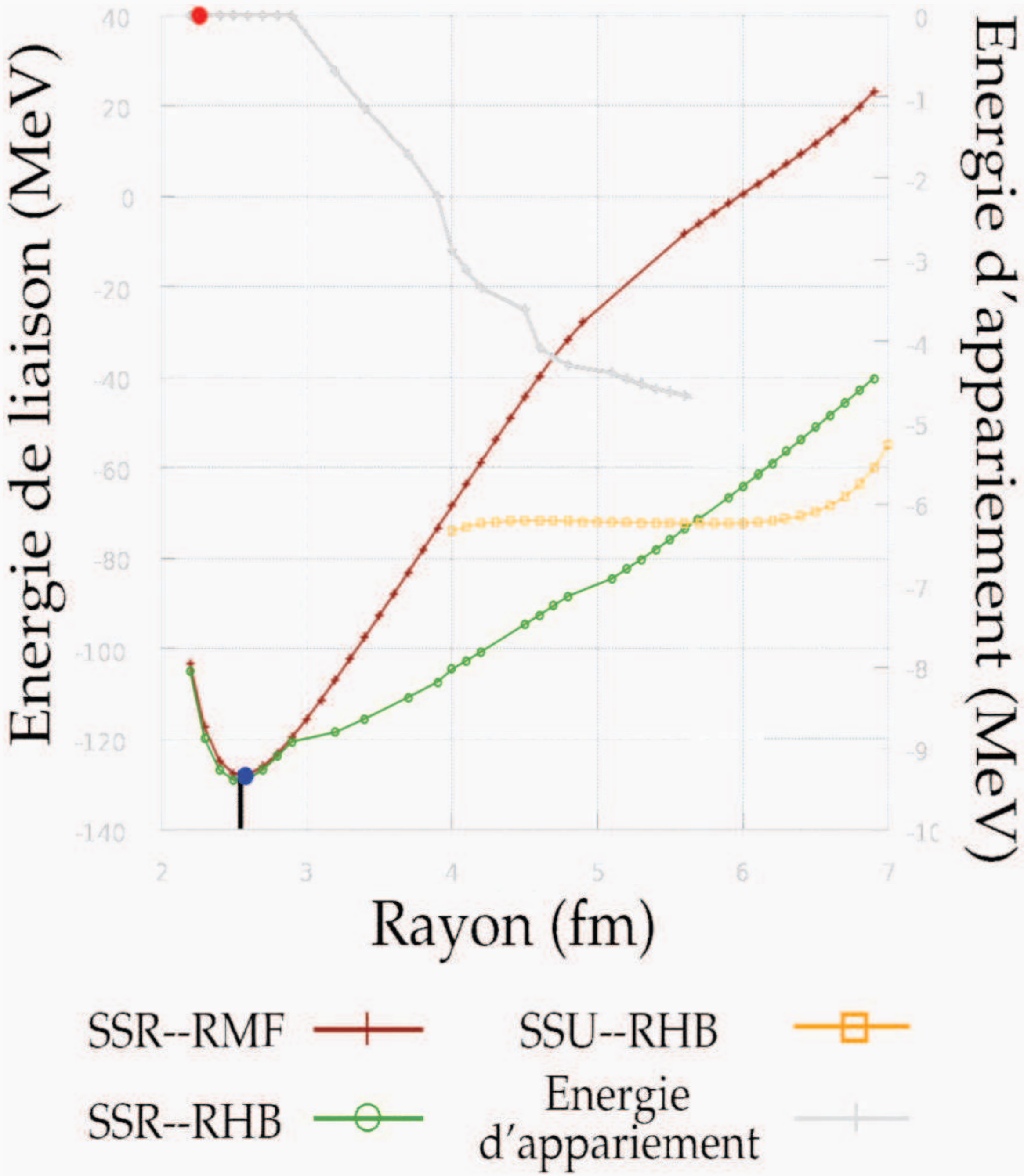

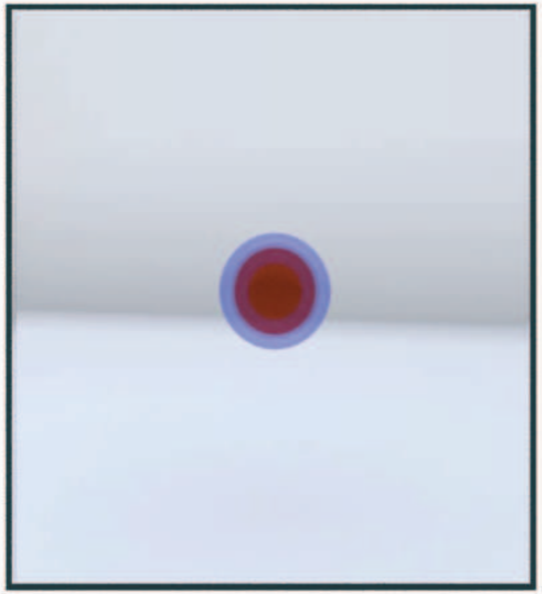

^{16}O: From a sphere to a tetrahedron – Caracterisation

Mott transition[4]

- Transition to a localised system
- $\dfrac{\rho_{\text{GS}}}{\rho_{\text{Tetra}}} = \left(\dfrac{2.7}{5.8}\right)^3 = 0.1$

Superfluid transition

- Pairing collapse $|\kappa| = 0$
- Emergence of 4-body structure

[4] Röpke, Schmidt, Münchow, Schulz, Nuclear Physics A (1983)

Superfluidities

Superfluidities

Pairing

Pairing – Illustration

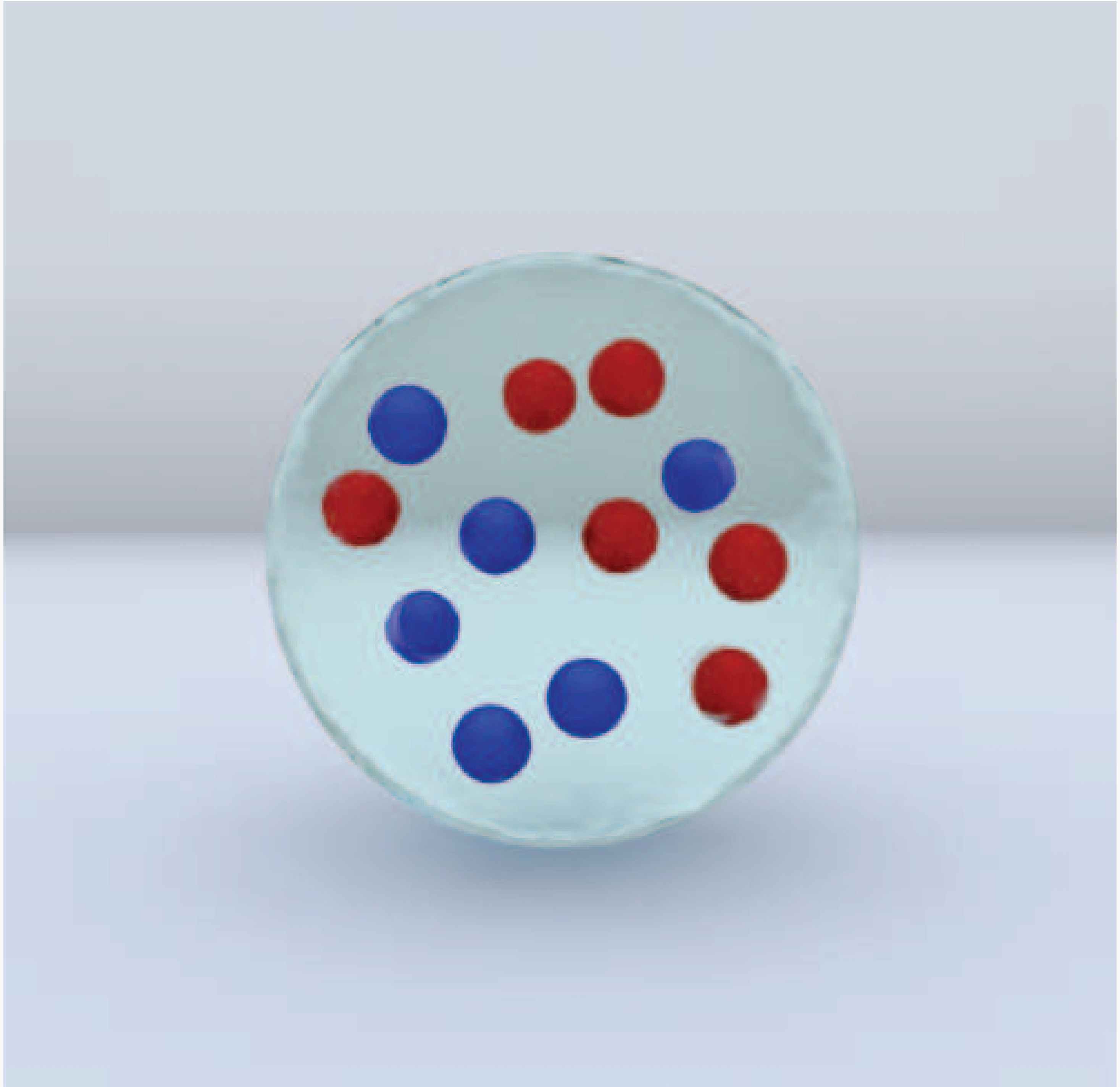

Impact on the structure

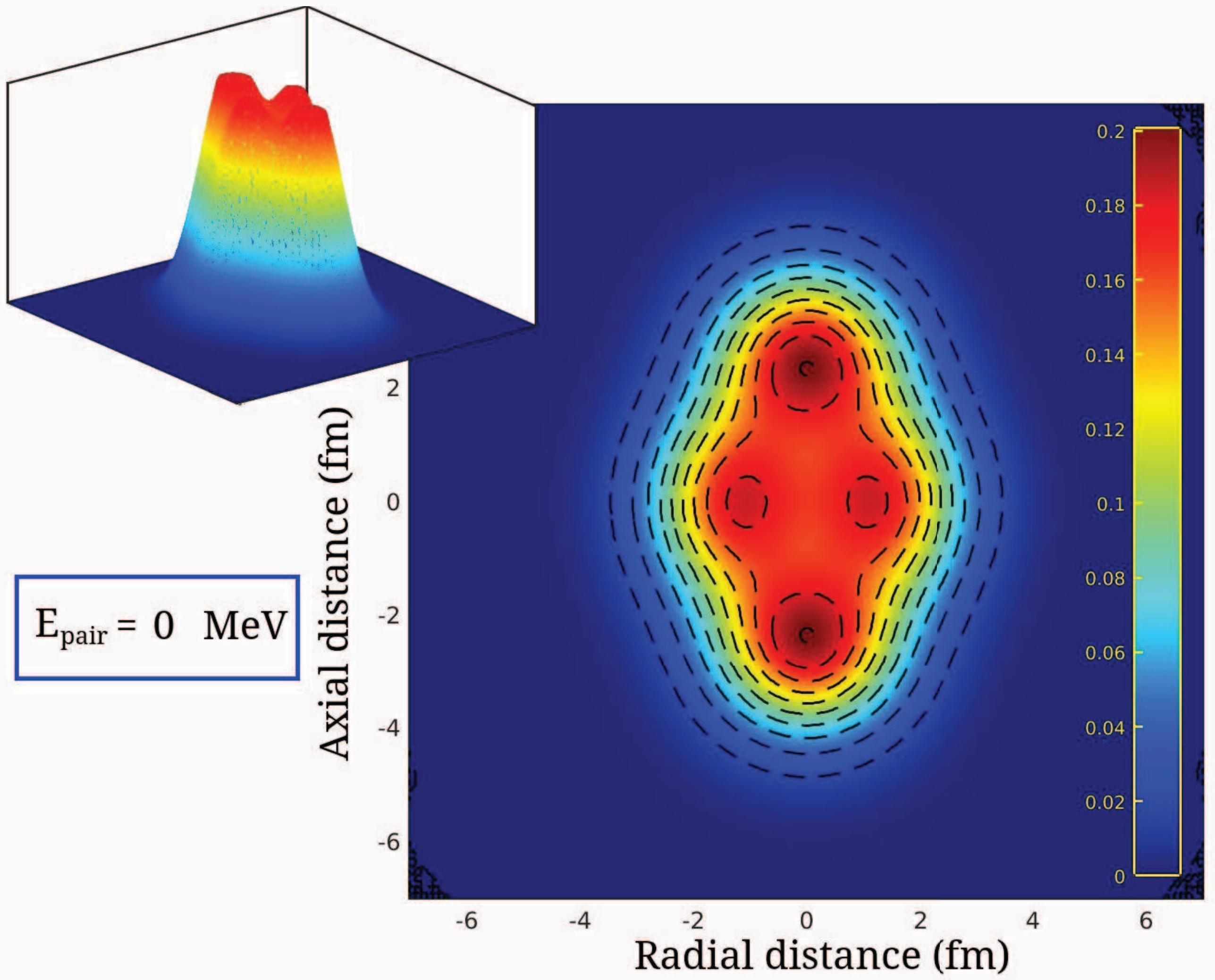

Density of ^{20}Ne

Impact on the structure

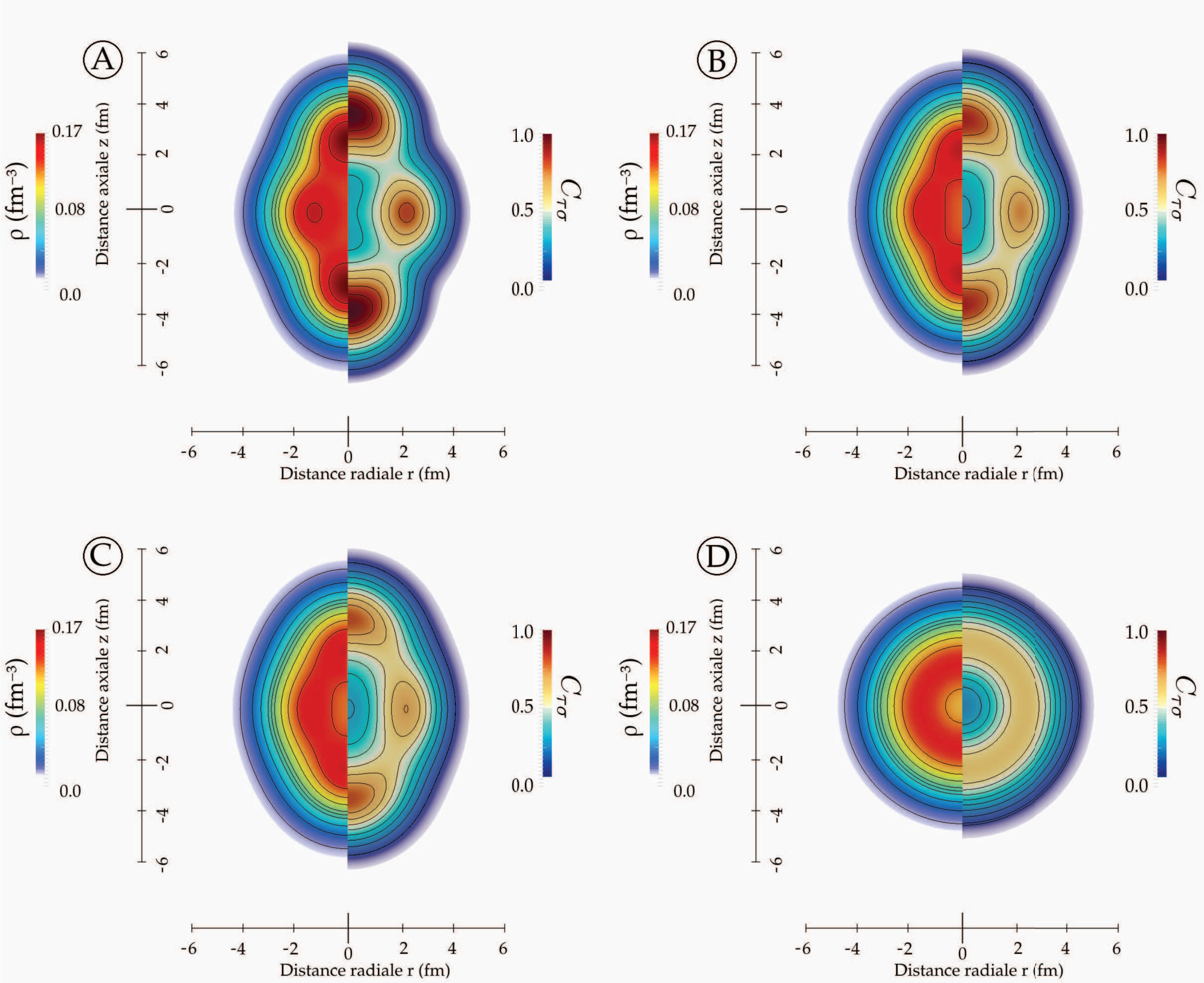

Competition between pairing and localisation

Superfluidities

Structure of a pair

Pairing tensor – Definitions

Joint probability

$$\Gamma_2(1,2) = \langle\Psi|\psi^\dagger(1)\psi^\dagger(2)\psi(2)\psi(1)|\Psi\rangle \tag{1}$$

Within RHB framework

$$\Gamma_2(1,2) = \underbrace{\rho^{(1)}(1)\rho^{(1)}(2)}_{\text{Mean-field}} + \overbrace{|\kappa(1,2)|^2}^{\text{Correlations}} \tag{2}$$

Central object:

$$\kappa(1,2) = \sum_k u_k v_k f_k(1) f_{\bar{k}}(2)$$

$$\kappa(\mathbf{r}_2, \mathbf{r}_2)$$

- 2-Body operator
- Capture 2-body correlations

Pairing tensor – Diagonal part

$$\kappa(\mathbf{r}_1 = \mathbf{r}_2)$$

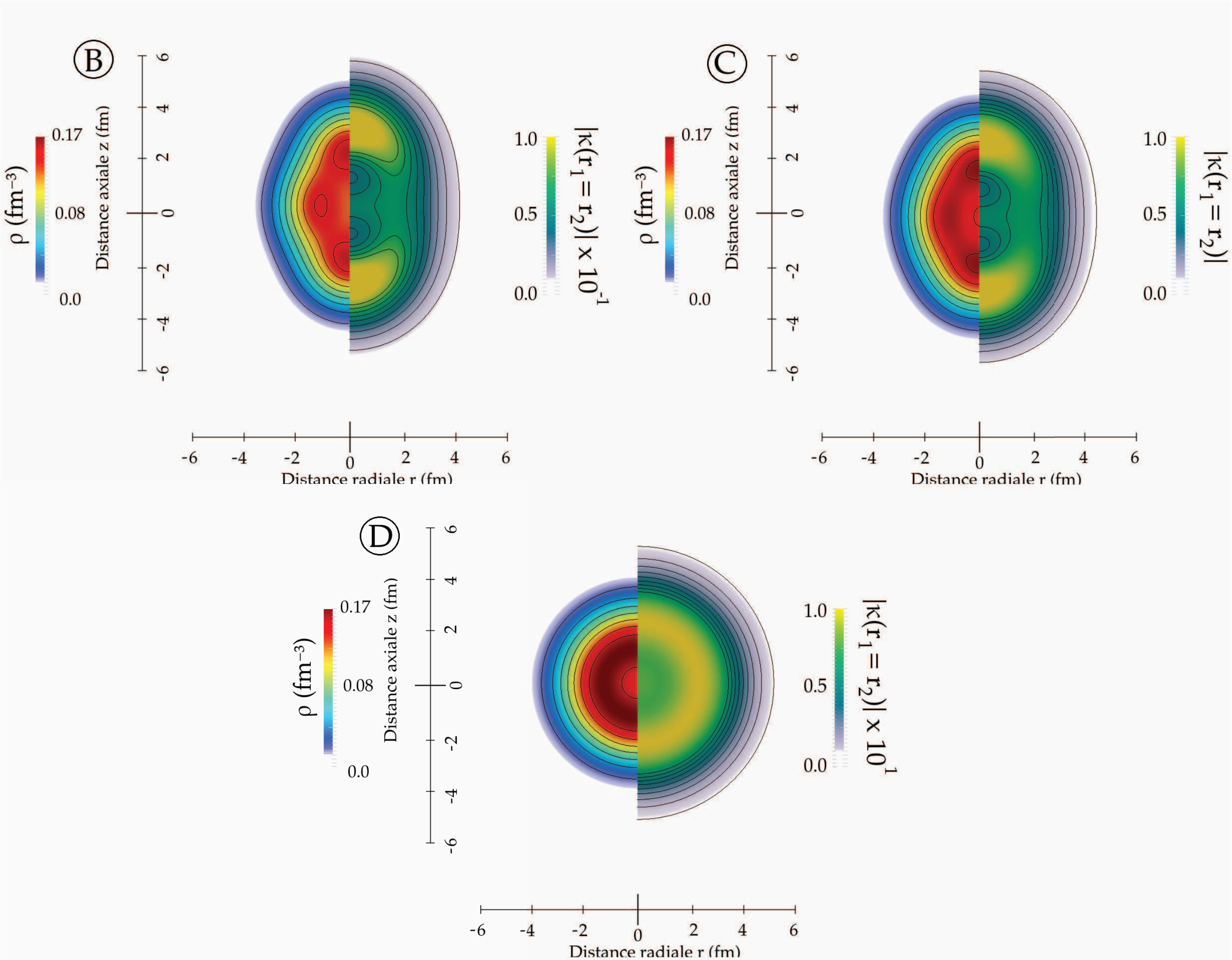

Pairing tensor – Non-local part

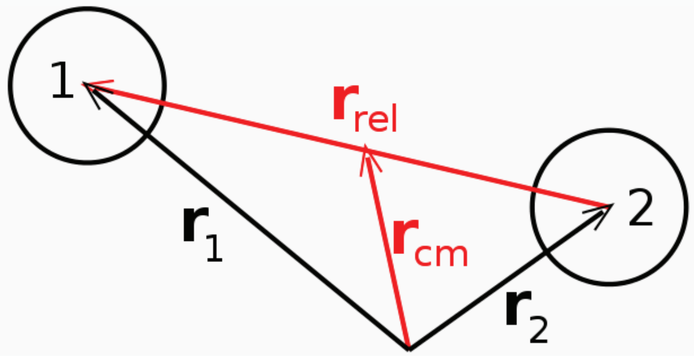

$$\{\mathbf{r}_1, \mathbf{r}_2\} \quad \underbrace{\longleftrightarrow}_{\text{Talmi-Moshinsky}} \quad \{\mathbf{r}, \mathbf{R}\}$$

$$\Phi_{\mathbf{n}_a}(\mathbf{r}_1)\Phi_{\mathbf{n}_b}(\mathbf{r}_2) = \sum_{\mathbf{n}_c} \mathcal{M}_{\mathbf{n}_a,\mathbf{n}_b}^{\mathbf{n}_c,\mathbf{n}_a+\mathbf{n}_b-\mathbf{n}_c} \Phi_{\mathbf{n}_c}(\mathbf{R})\Phi_{\mathbf{n}_a+\mathbf{n}_b-\mathbf{n}_c}(\mathbf{r})$$

- Numerically intensive
- Transformation defined on $\mathbb{R}^+$

Talmi transformations

For two 1D oscillators

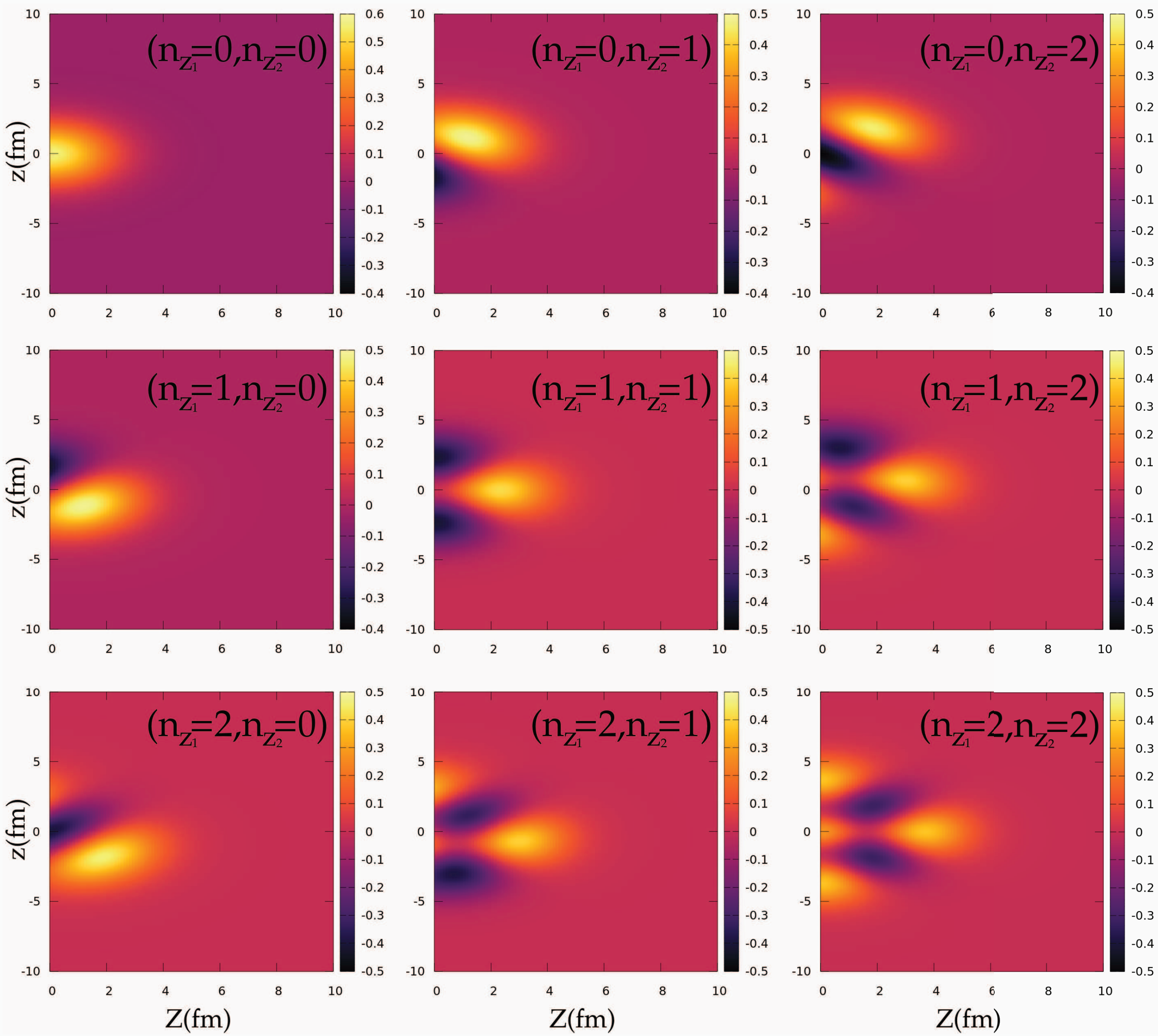

Talmi transformations

However defined only over $L^2(\mathbb{R}^+$

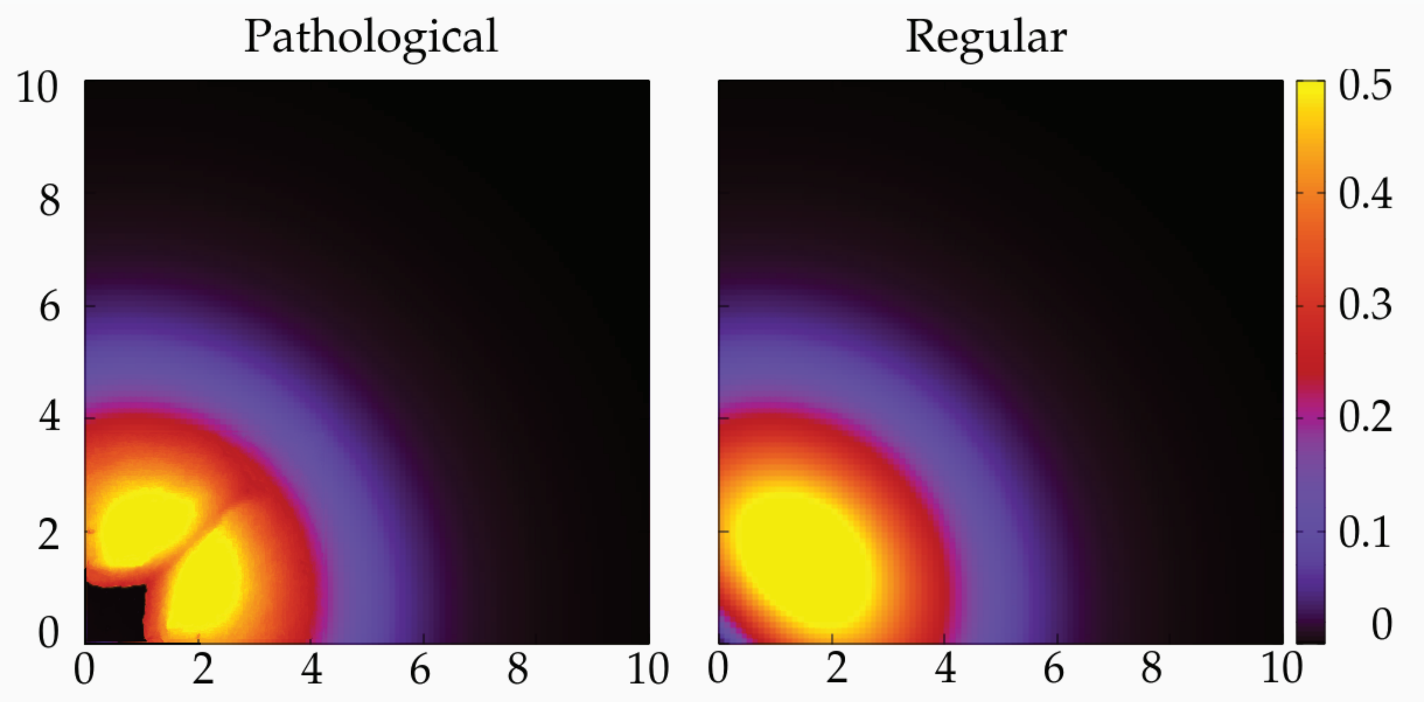

Artefacts symmetry might appear

Pairing tensor – Non-local part (2)

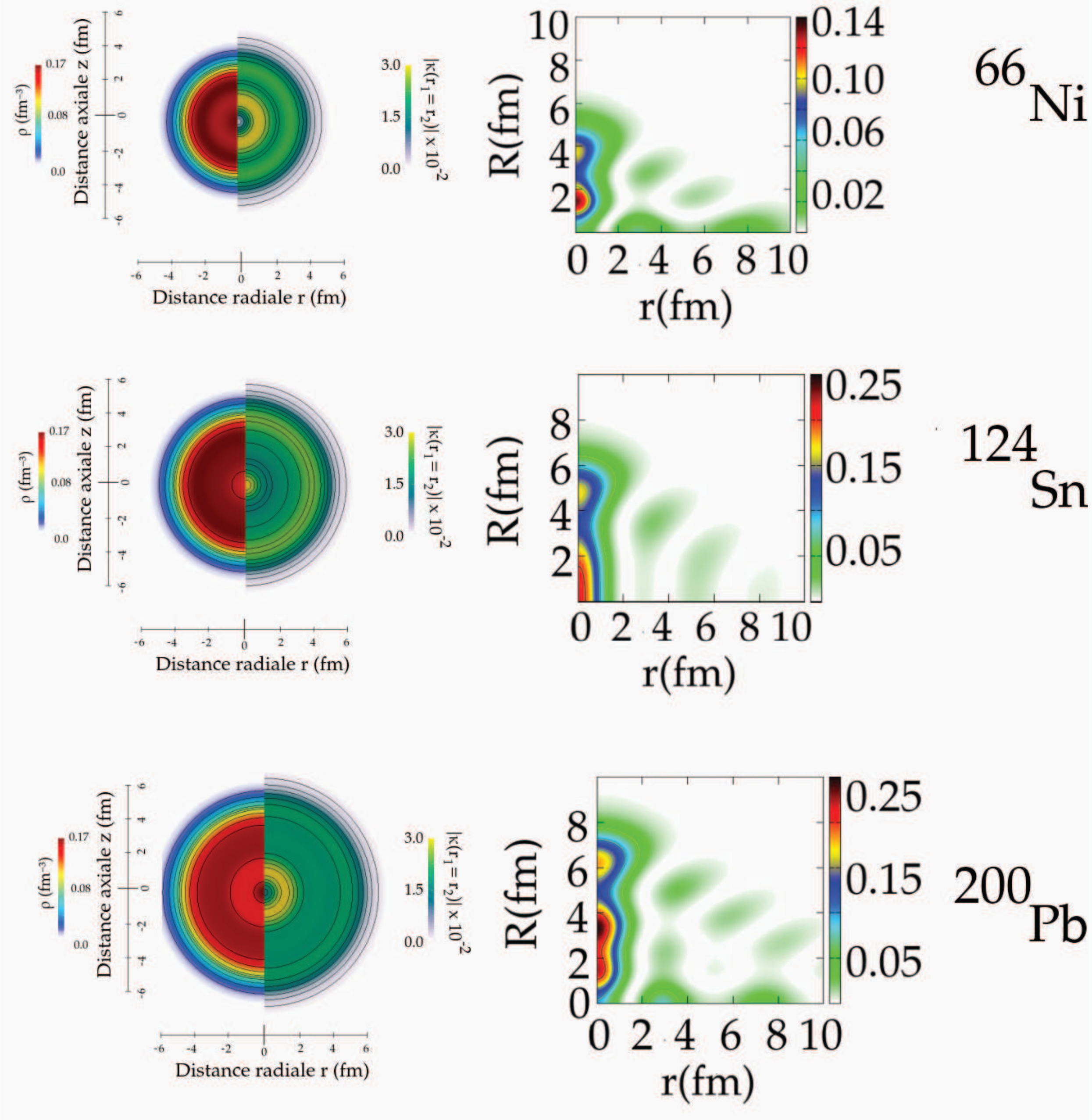

Pairing tensor – Coherence length

$$\xi(\mathbf{R}) = \left(\frac{\int \mathbf{r}^2 |\kappa(\mathbf{R},\mathbf{r})|^2 d\mathbf{r}}{\int |\kappa(\mathbf{R},\mathbf{r})|^2 d\mathbf{r}} \right)^2$$

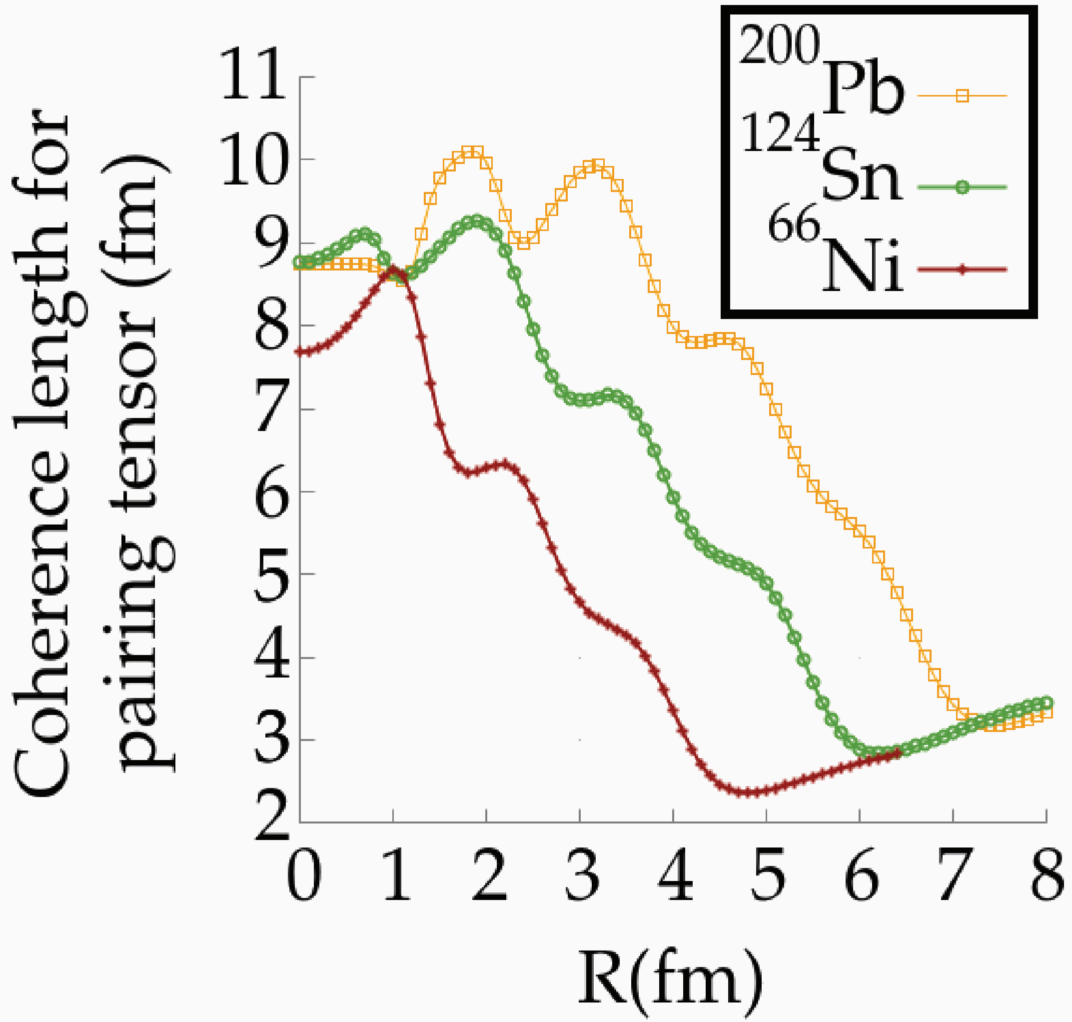

Pairing tensor – Coherence length

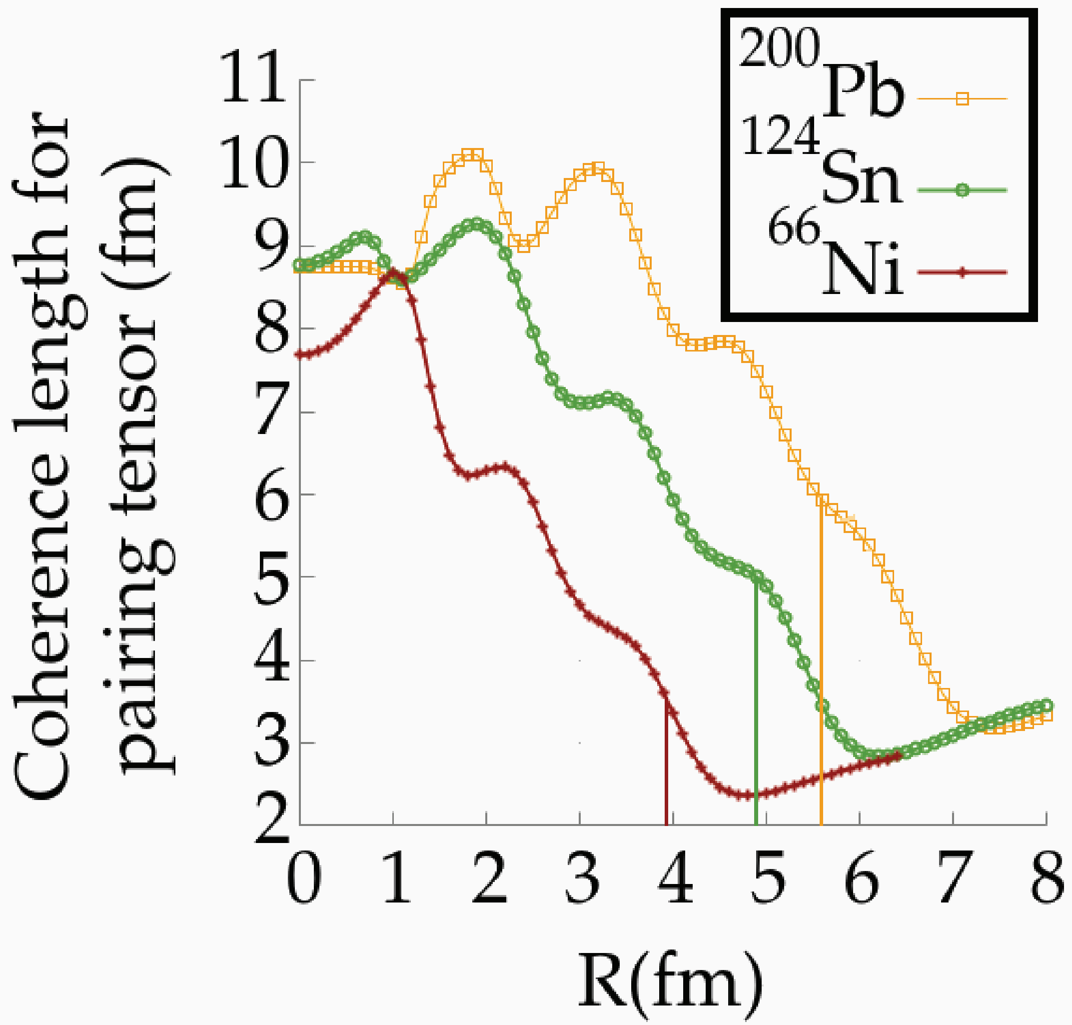

Need to restore particle number conservation

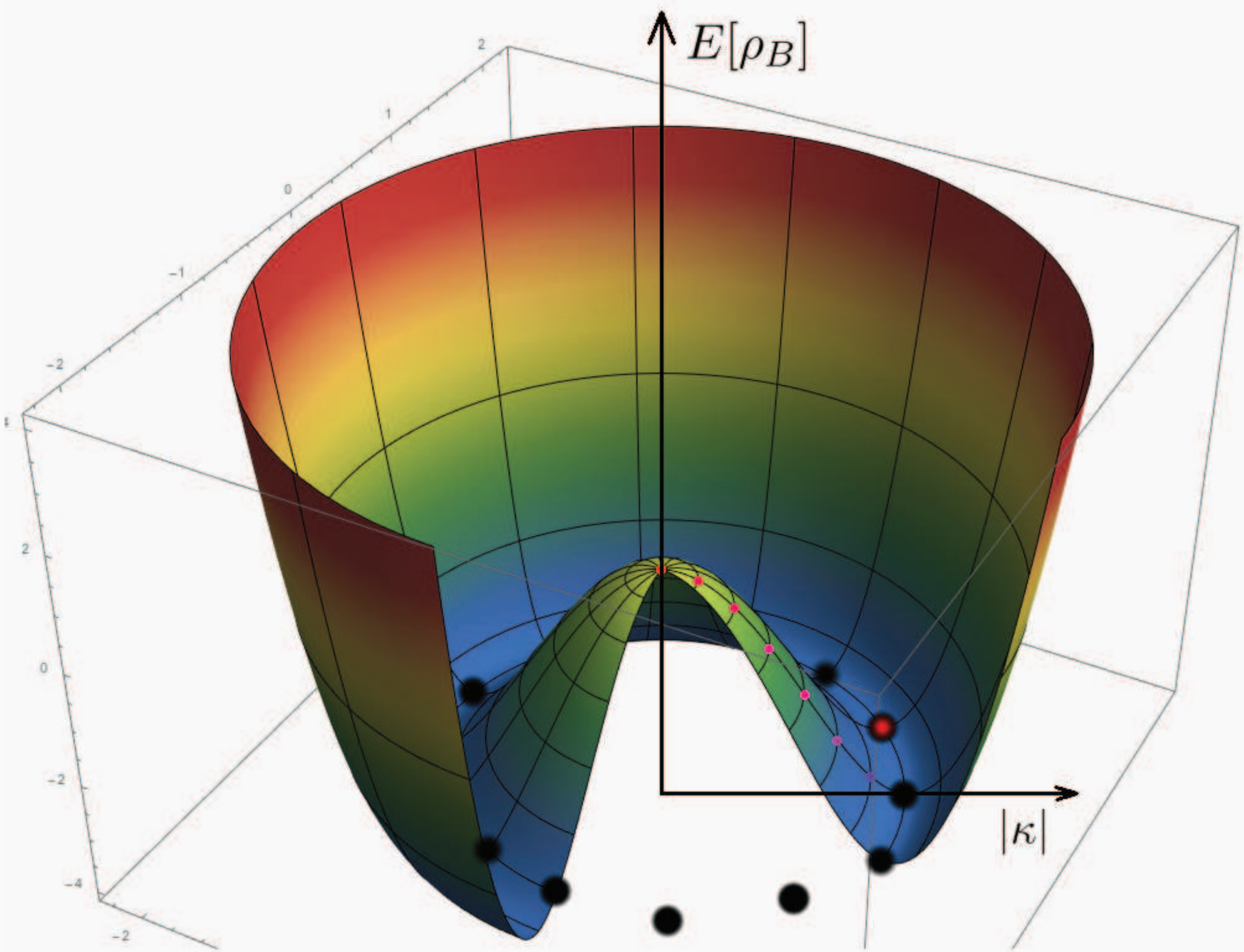

Symmetry restoration – Principle

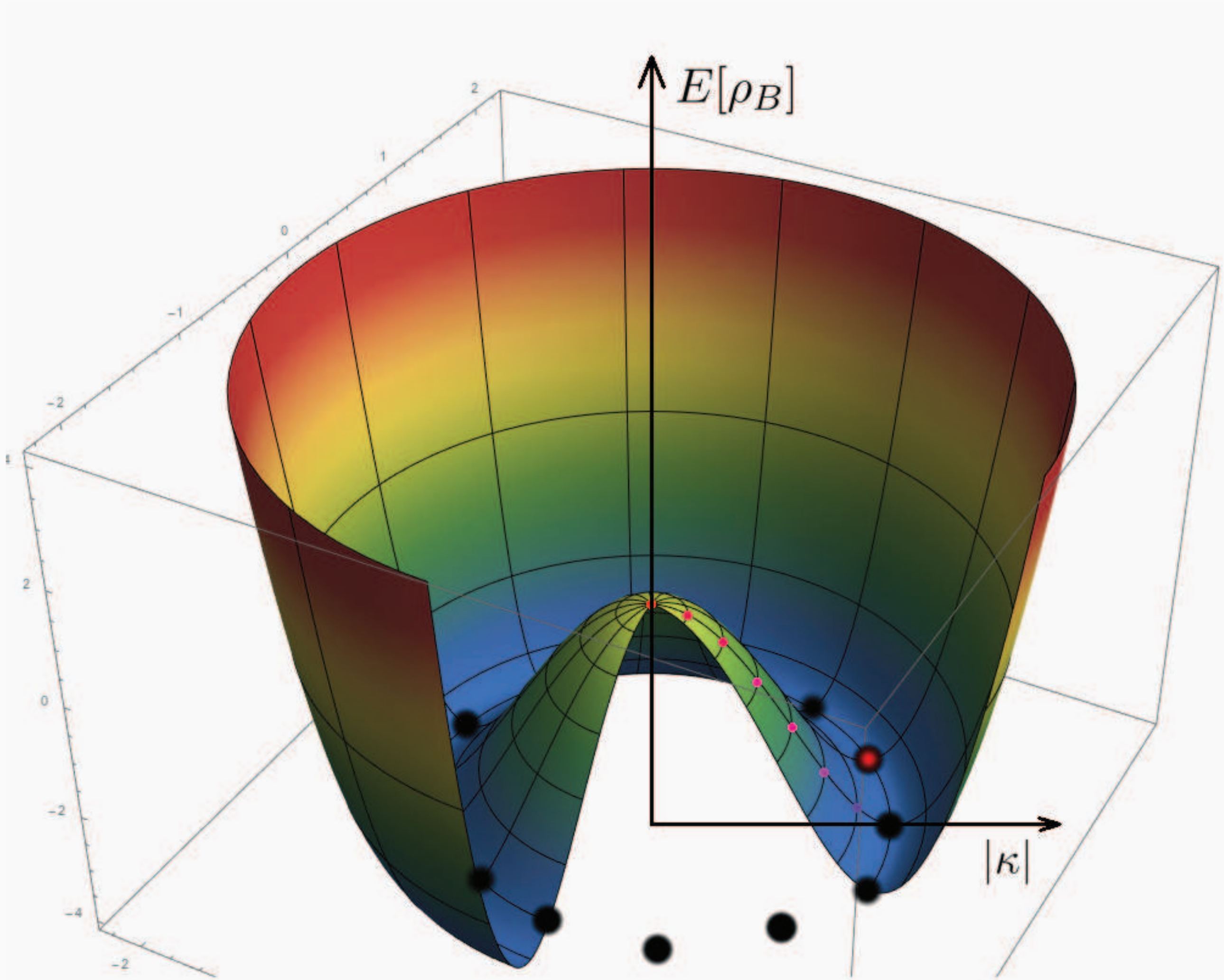

$$|\Phi^N\rangle = \frac{1}{2\pi}\int_0^{2\pi} d\theta \left(e^{i\theta(\hat{N}-N)} \prod_{i>0} \left(u_i + v_i a_i^\dagger a_{\bar{i}}^\dagger \right) |0\rangle \right)$$

Symmetry restoration – Formalism

A N particles state:

$$|\Phi^N\rangle = \frac{1}{N!}\left(\sum_i x_i a_i^\dagger a_{\bar{i}}^\dagger\right)^N |0\rangle = \frac{\left(\Gamma^\dagger\right)^N}{N!}|0\rangle$$

Correlated pairs operators

$$\Gamma^\dagger = \sum_i x_i a_i^\dagger a_{\bar{i}}^\dagger$$

Recurrence relations

$$|\Phi^N\rangle = |\Phi^N(i)\rangle + x_i\sqrt{N}P_i^\dagger\,|\Phi^{N-1}(i)\rangle$$

Left to minimize

$$E_{\text{Pair}} = \frac{\langle\Phi^N|H_{\text{Pair}}|\Phi^N\rangle}{\langle\Phi^N|\Phi^N\rangle}$$

Symmetry restoration – Impact

Non-local part of the pairing tensor[5]

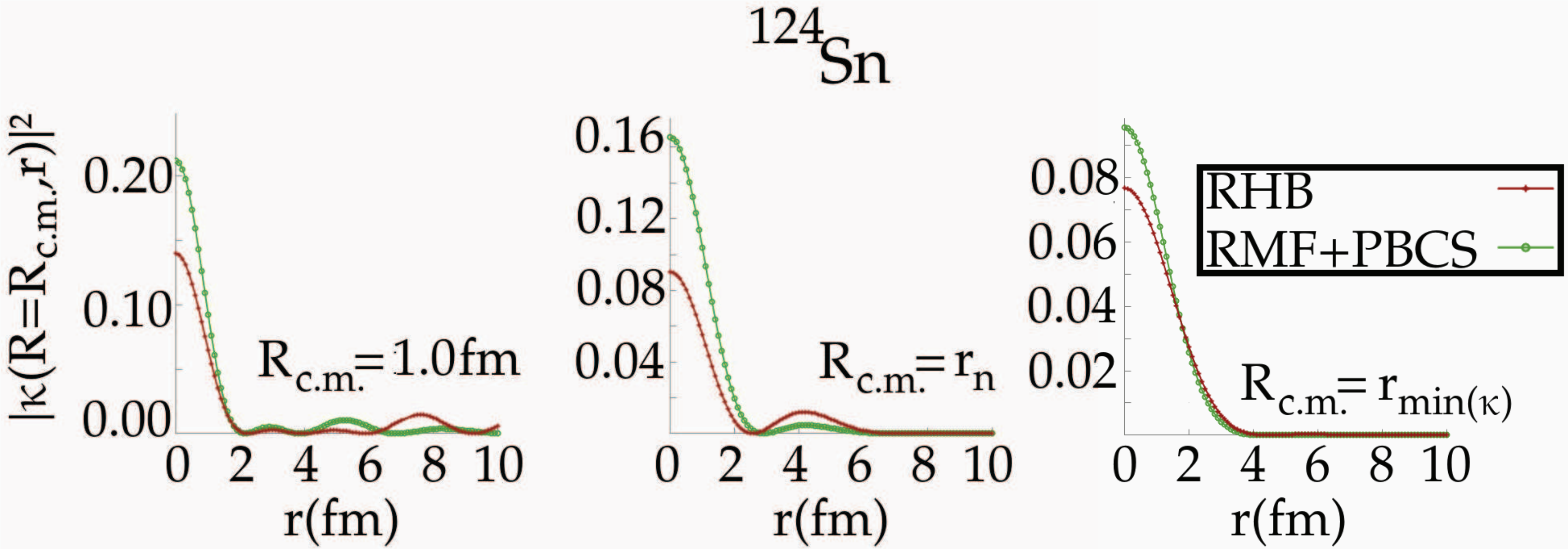

[5]Lasseri,Ebran,Khan,Sandulescu PRC 98, 014310 (2018) (2018)

Correlations strenght

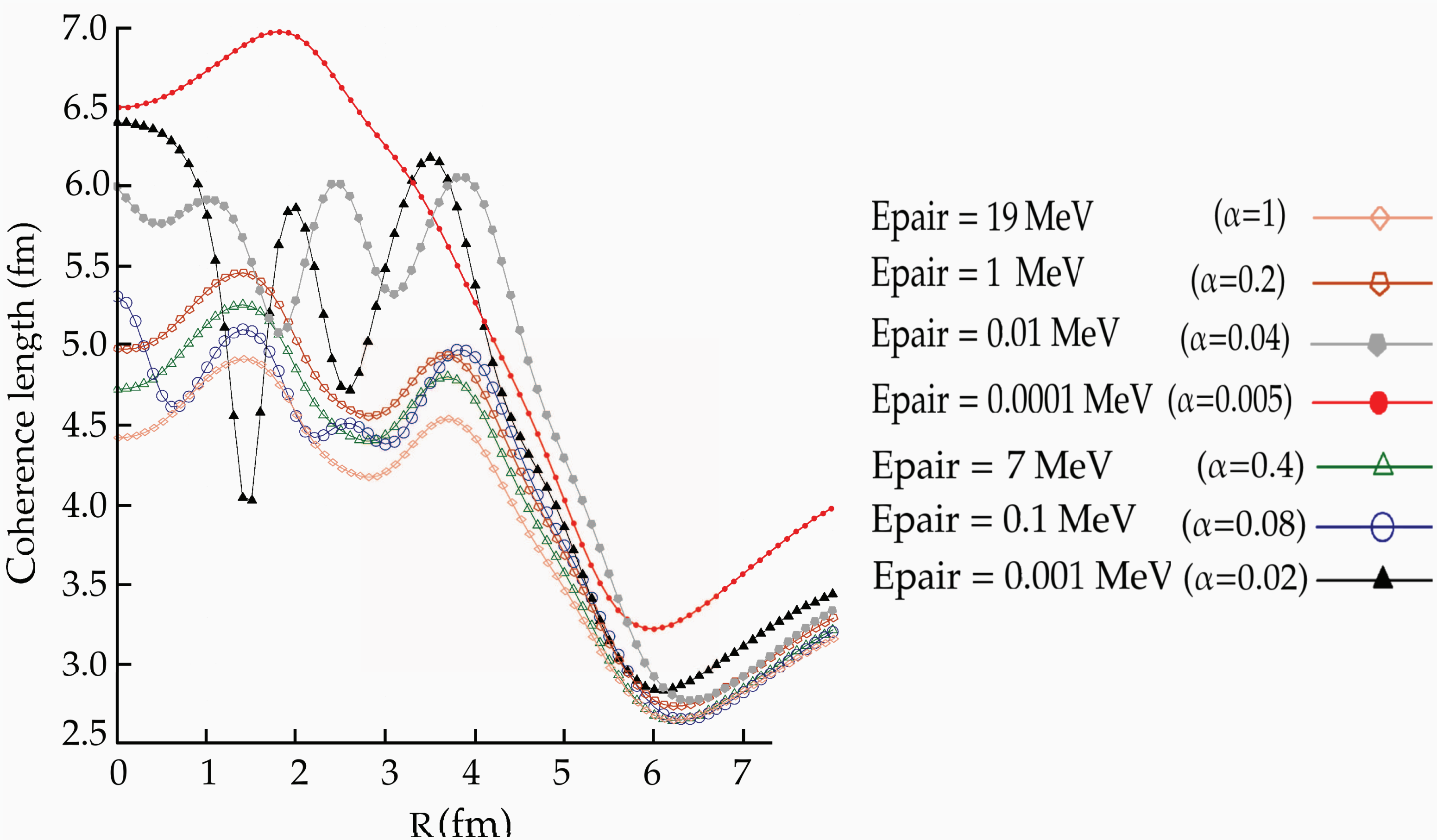

Correlations strenght

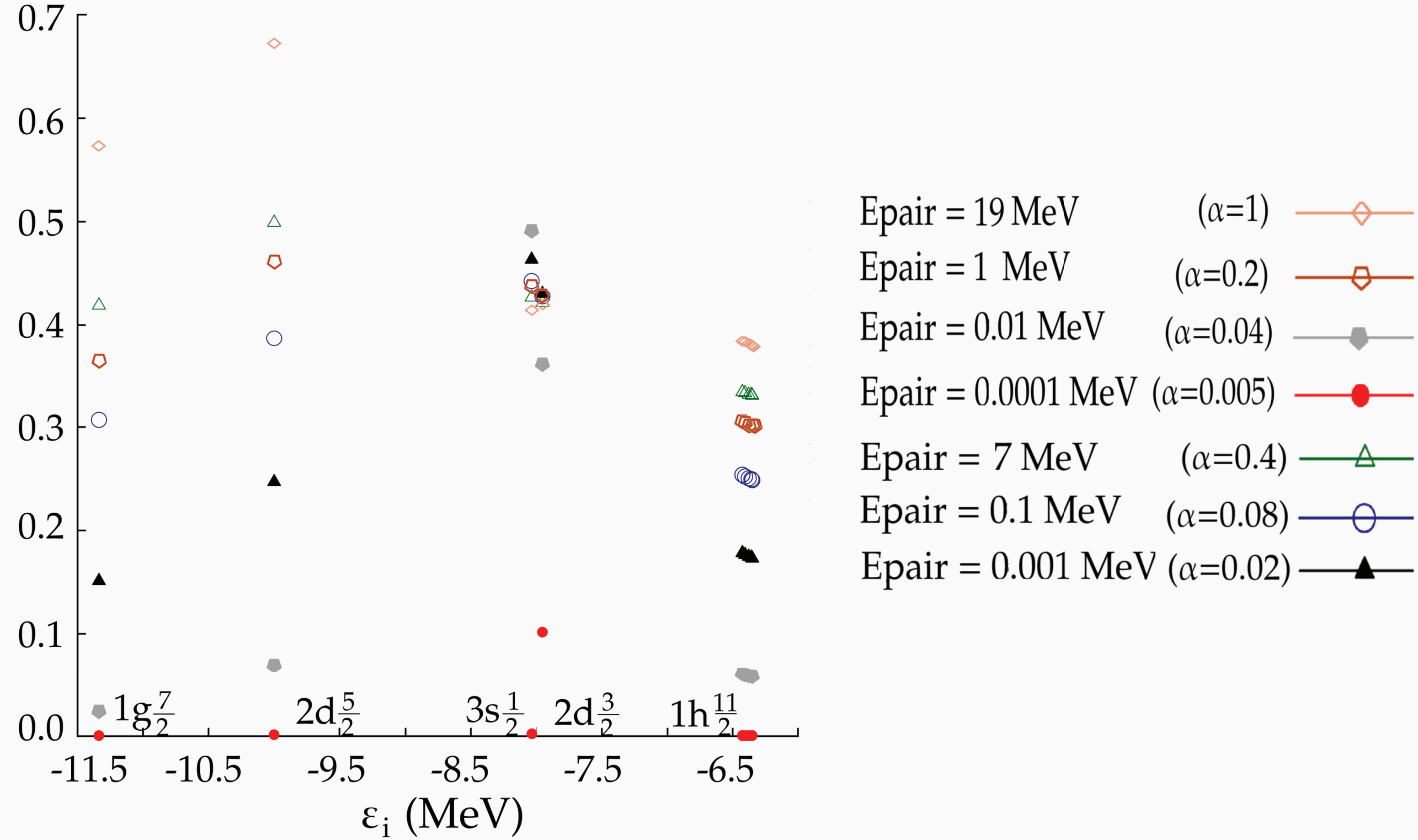

Correlations strenght

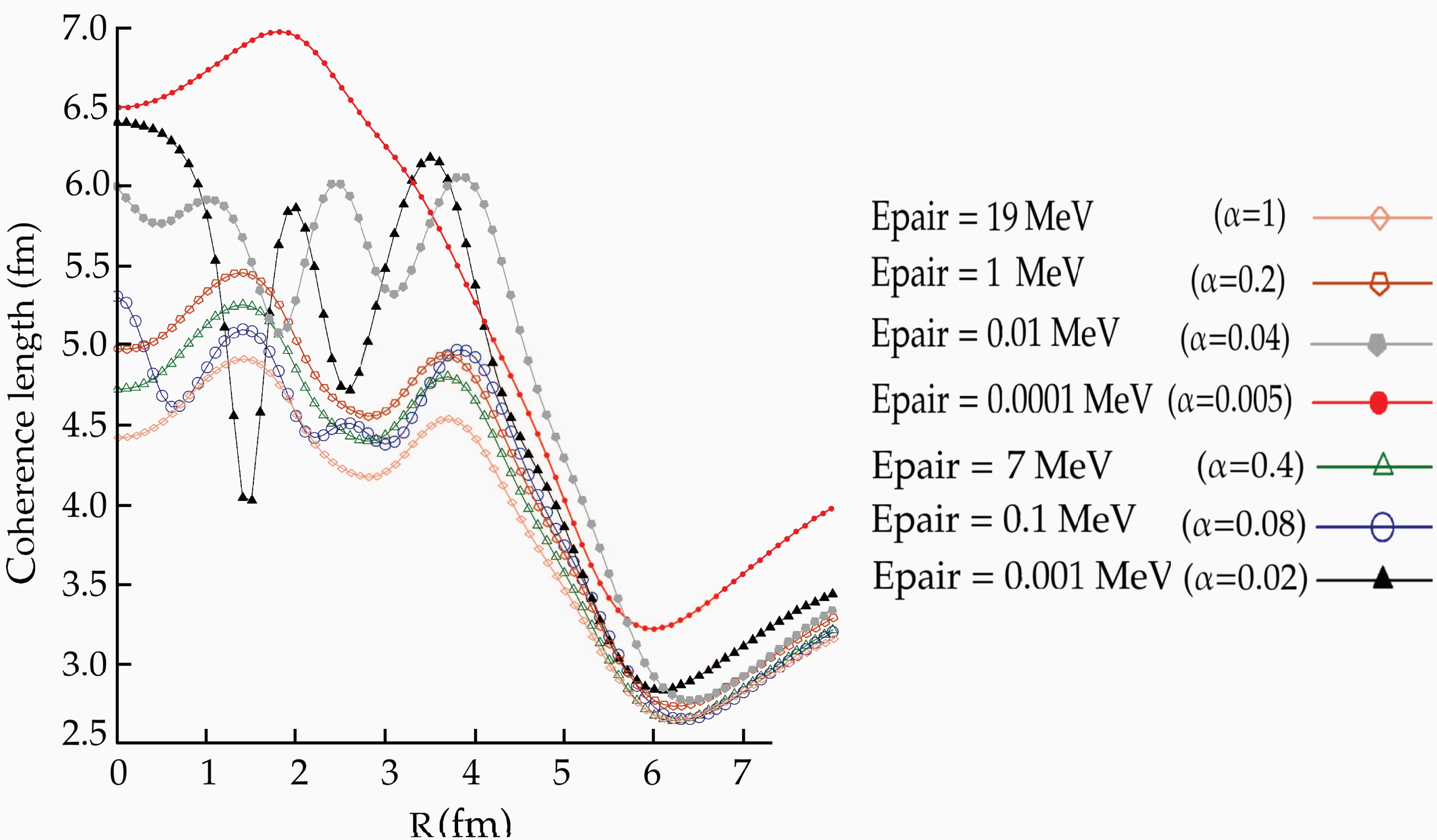

BEC or BCS ? – Definitions

One shall study Cooper-pair properties

$$\phi_C(\mathbf{r}_1, \mathbf{r}_2) = \sum_k y_k f_k(r_1) f_{\bar{k}}(r_2)$$

Which in RHB formalism becomes:

$$\phi_C(\mathbf{r}_1, \mathbf{r}_2) = \sum_k \frac{u_k}{v_k} f_k(r_1) f_{\bar{k}}(r_2)$$

Thus as for κ one can define:

$$\xi_C(\mathbf{R}) = \left(\frac{\int \mathbf{r}^2 |\phi_C(\mathbf{R}, \mathbf{r})|^2 d\mathbf{r}}{\int |\phi_C(\mathbf{R}, \mathbf{r})|^2 d\mathbf{r}} \right)^2$$

BEC or BCS ? – Conclusions (^{66}Ni)

- Internucleonic mean distance d_n
- Averaged "size" of a Cooper pair ξ

$$\chi = \frac{\xi_C}{d_n} = \begin{cases} > 1 & \text{BCS} \\ < 1 & \text{BEC} \end{cases}$$

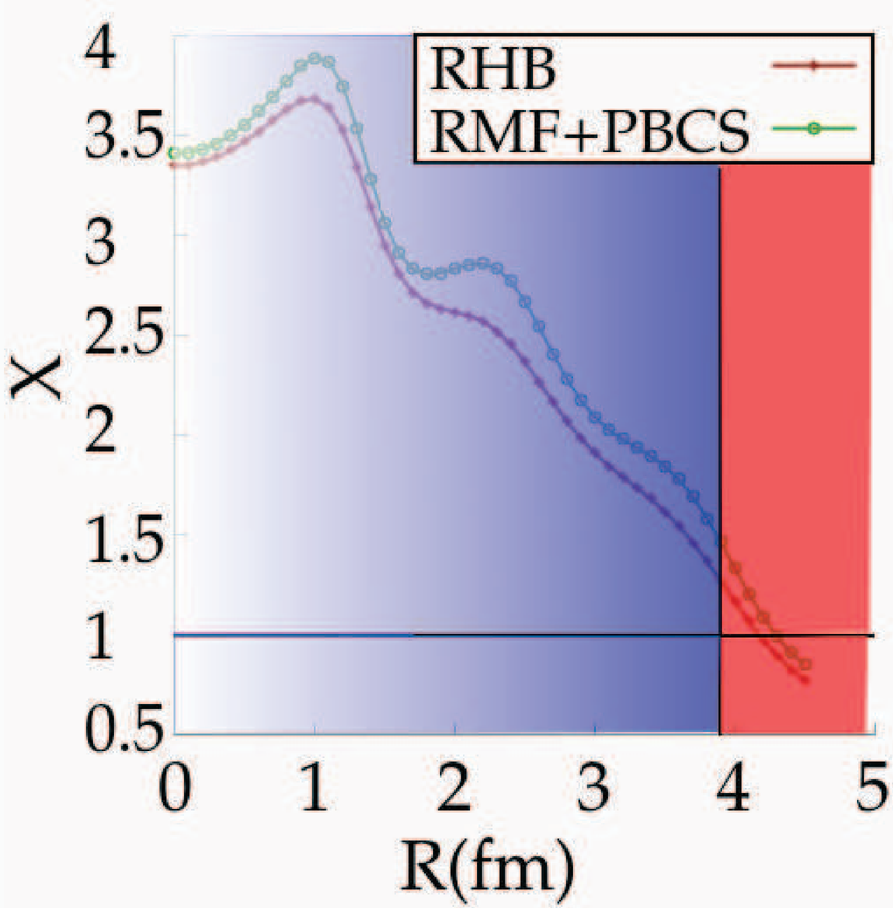

BEC or BCS ? – Conclusions (^{66}Ni)

- Internucleonic mean distance d_n
- Averaged "size" of a Cooper pair ξ

$$\chi = \frac{\xi_C}{d_n} = \begin{cases} > 1 & \text{BCS} \\ < 1 & \text{BEC} \end{cases}$$

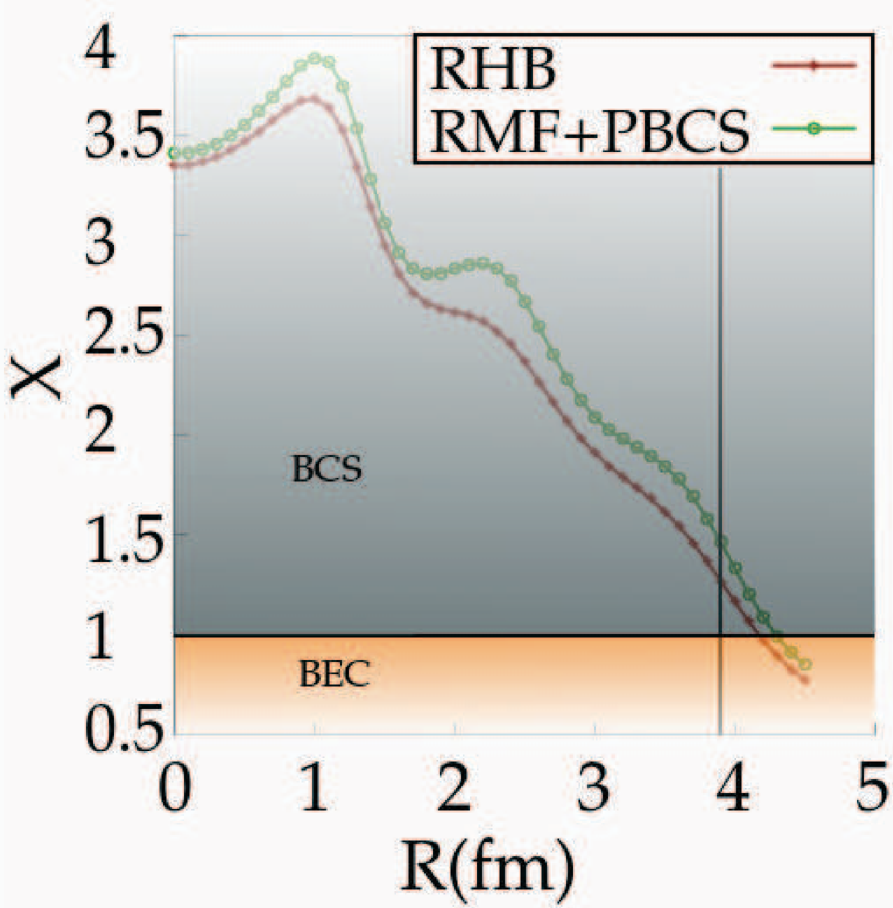

Superfluidities

4-Body correlations

Quartet – Illustration

Superfluidities

Quartet Condensation Model (QCM)

Quartteting – QCM Formalism

Study of quarttet correlations impact

Motivations:

◇ Generalisation ◇ α-clusters

Model:

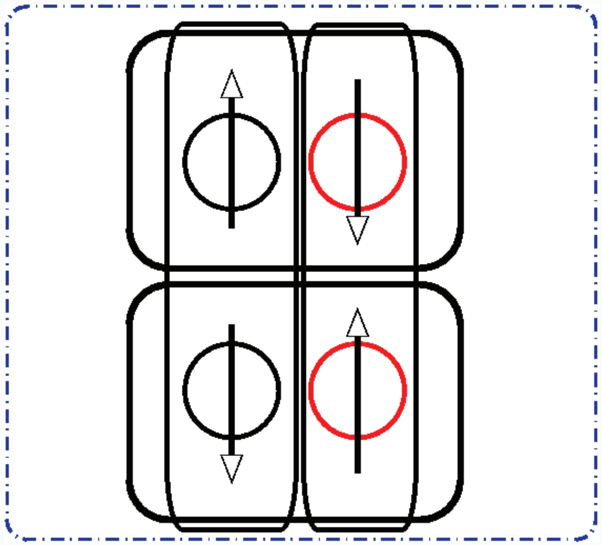

Quartet $\equiv$ A **pair** of nucleonic pairs $\{nn, pp, np\}$

Hypotheses

- Isospin symmetry
- Isovector outweight isoscalar

Quartteting – QCM Formalism

Study of quarttet correlations impact

Motivations:

◇ Generalisation ◇ α-clusters

Modele:

$$|\Phi_q\rangle = \mathcal{Q}\,|0\rangle = \left(2\Gamma_1^\dagger\Gamma_{-1}^\dagger - \Gamma_0^{\dagger\,2}\right)^{n_q}|0\rangle$$

With:

- $\Gamma_\tau^\dagger = \sum_i x_i P_{i\tau}^\dagger$
- $P_{i,\tau}^\dagger$ pair creation operators.
- n_q quartets number.

Quartetting – Implementation

- Finite-range realistic *pp* interaction
- Numerical valence/core separation

Quartet term inclusion

$$\mathcal{E}[\rho] = \underbrace{\langle \Phi_{core} | \mathcal{H} | \Phi_{core} \rangle}_{\text{RMF}} + \underbrace{\langle \Phi_q | \mathcal{H}' | \Phi_q \rangle}_{\text{Quartet term}}$$

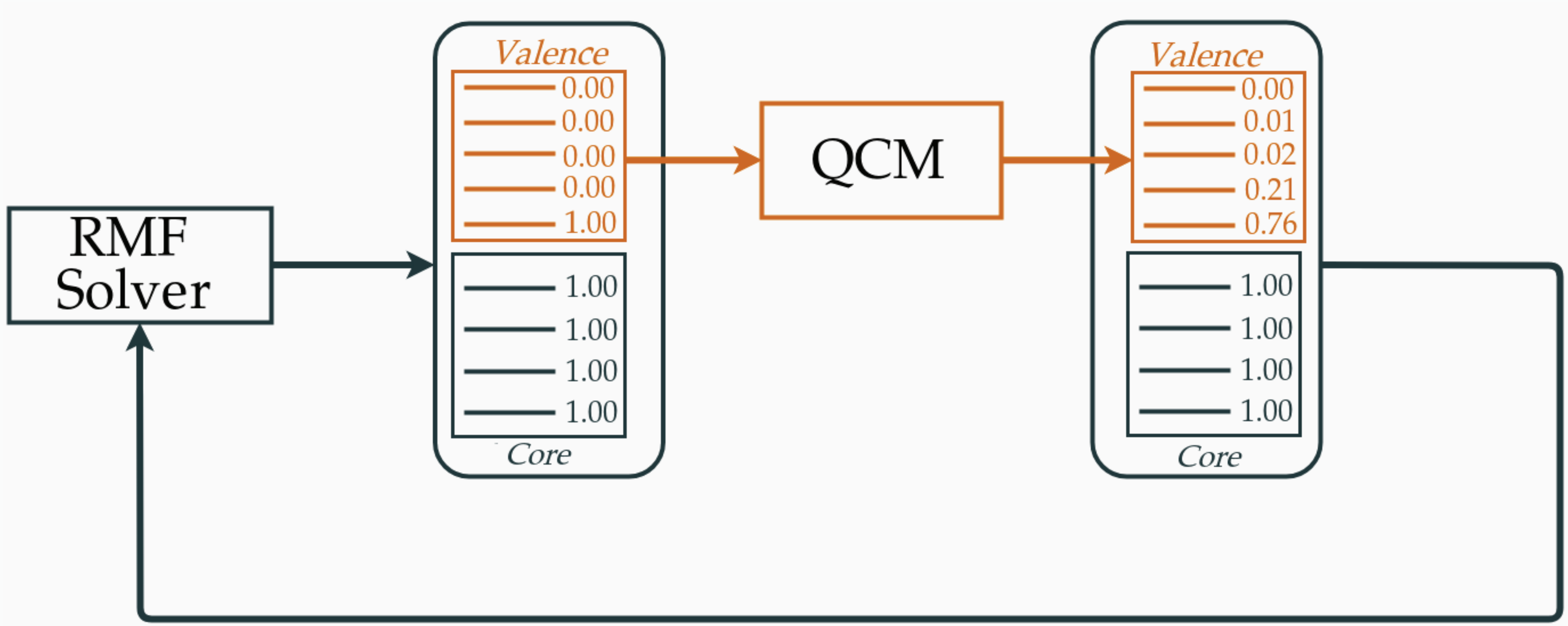

Neon 20 structure

At density level (PES[6]):

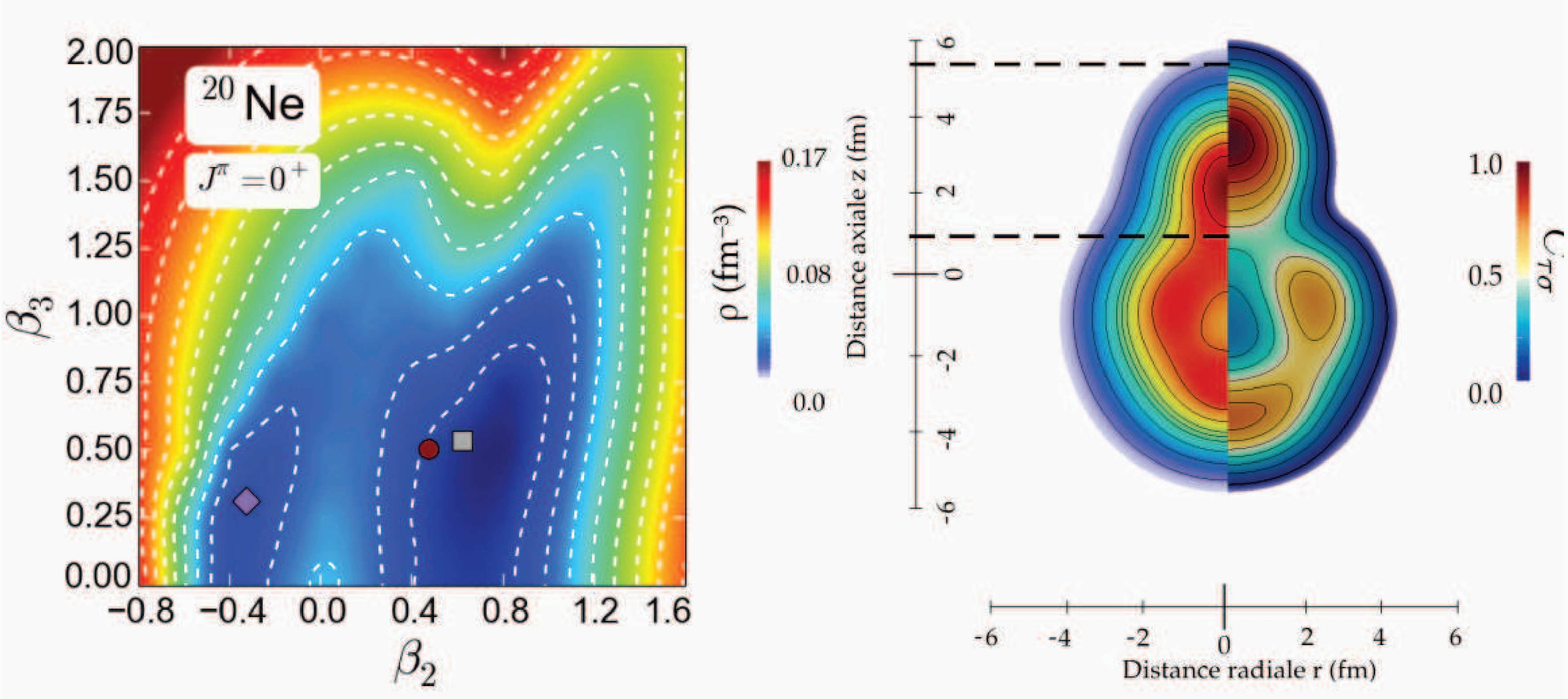

^{20}Ne: ^{16}O $+ \alpha$

[6] Marevic, Ebran, Khan et al Phys. Rev. C 97, 024334 (2018)

Neon 20 structure

At single-particle energy level:

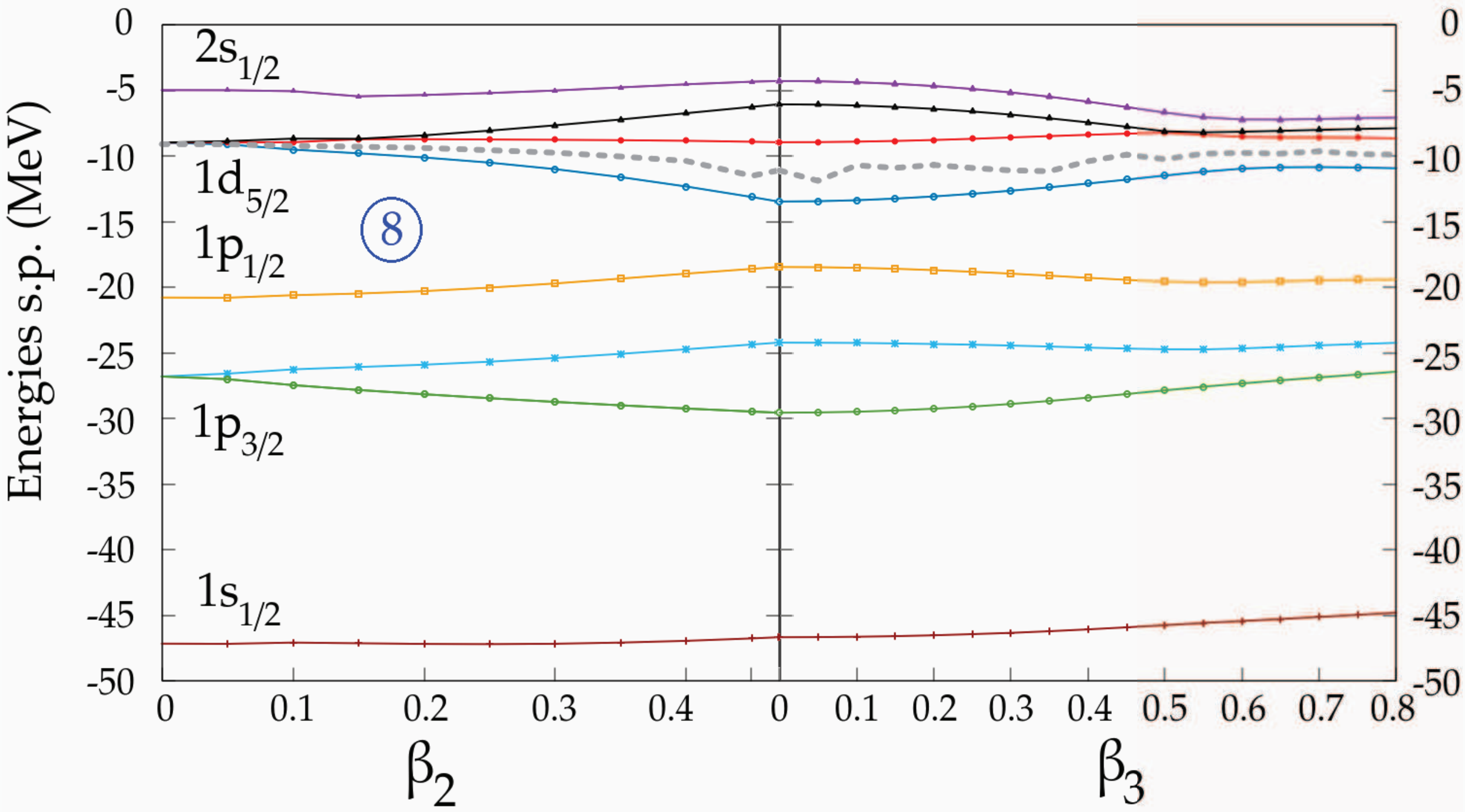

^{20}Ne: ^{16}O $+ \alpha$

Neon 20 structure

At single-particle energy level:

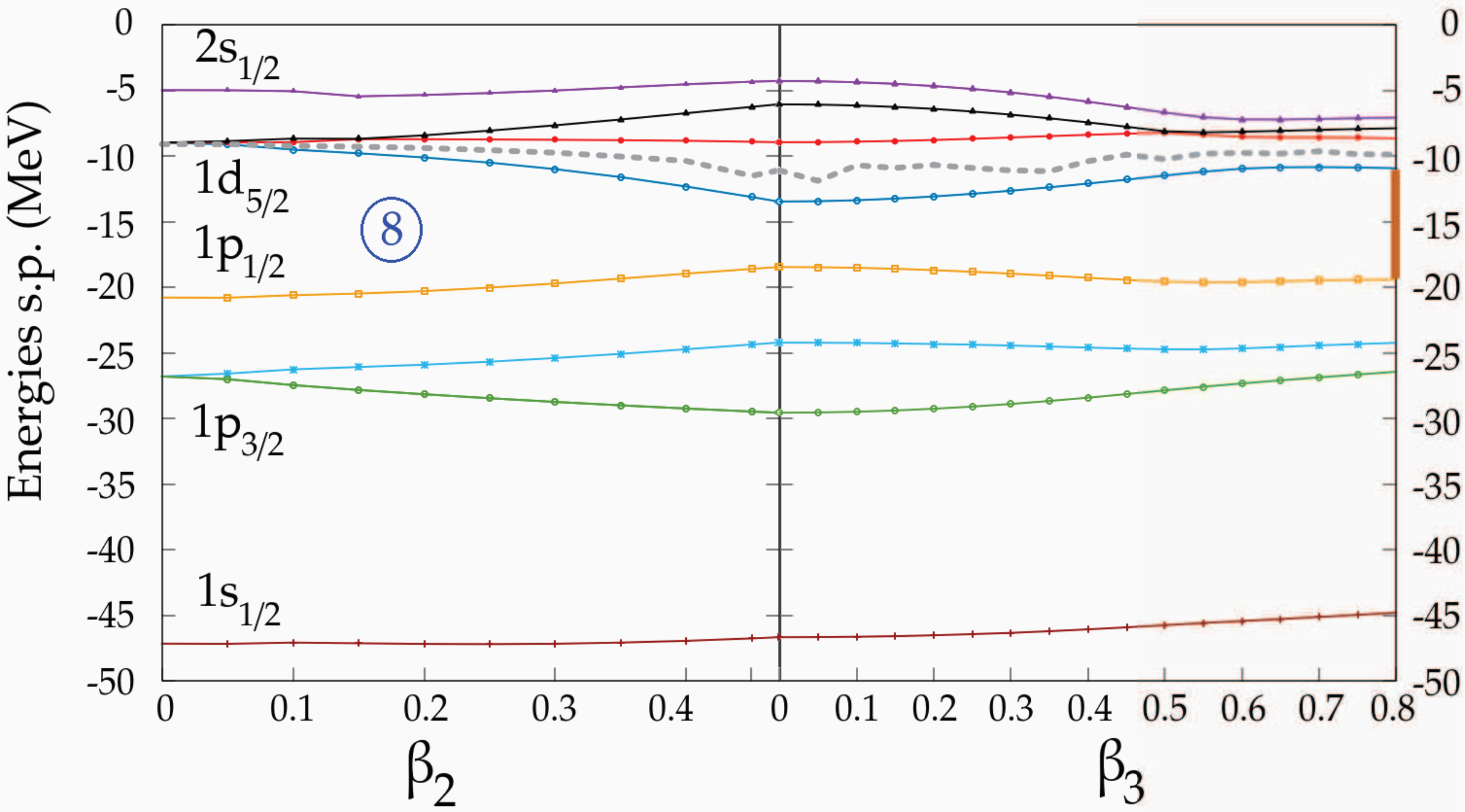

^{20}Ne: ^{16}O + α

Quartetting impact– ^{20}Ne

Energies:

Exp	RHB	RMF+QCM
160.6 MeV	157.9 MeV	161.3 MeV

Quartetting impact– ^{20}Ne

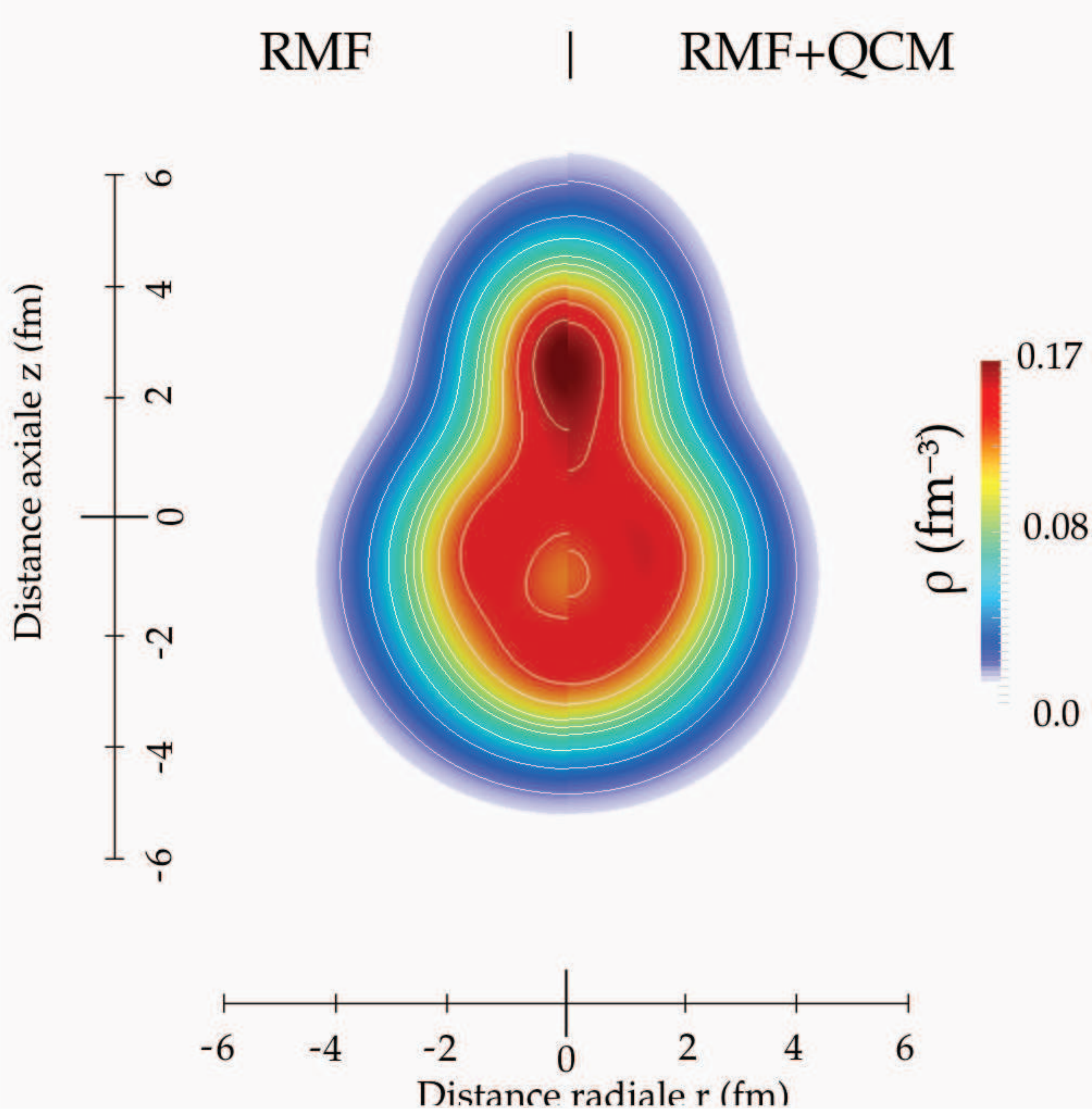

Quartetting impact– ^{20}Ne

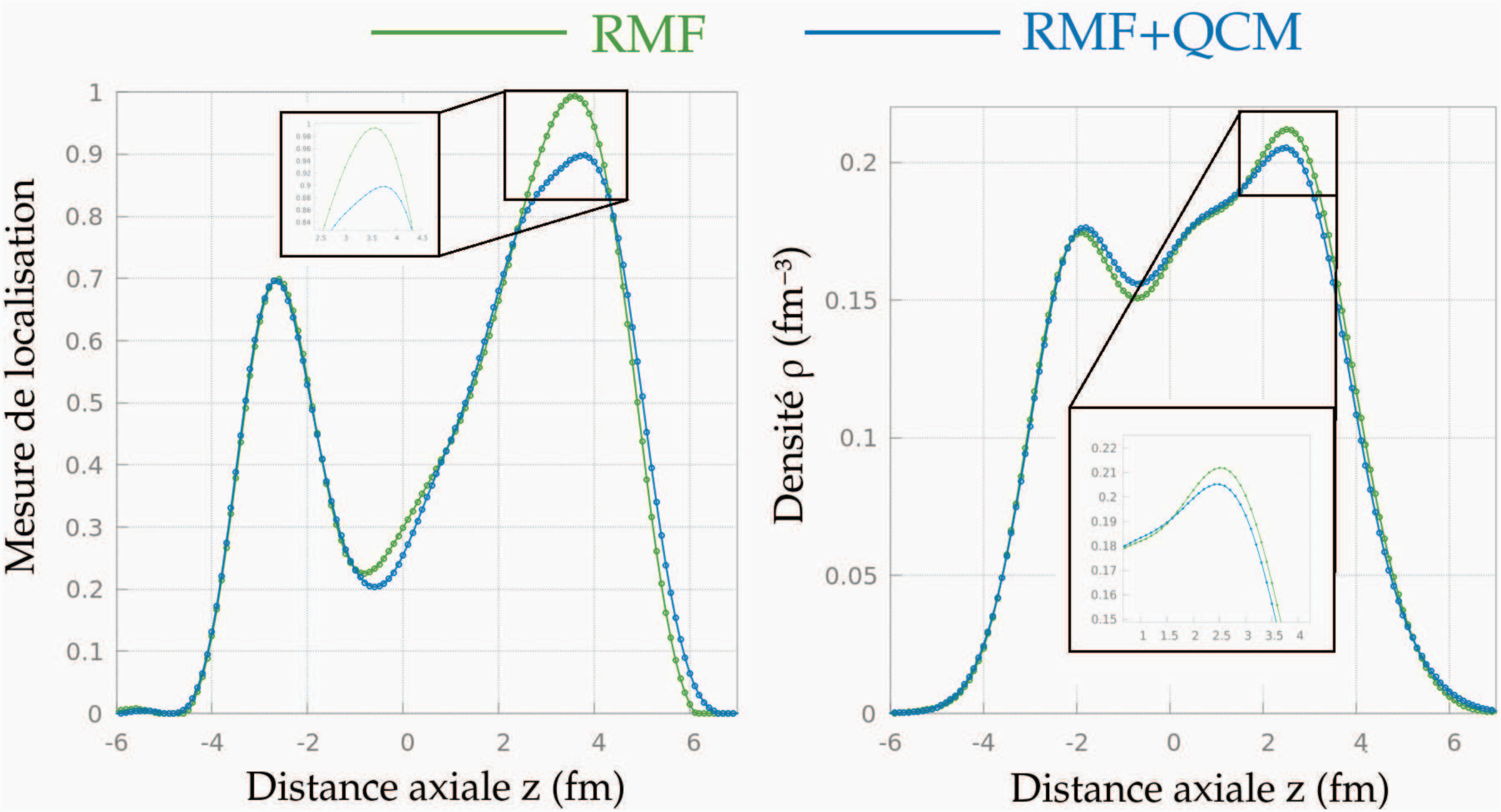

Pairing vs Quartetting

For the same correlation energy

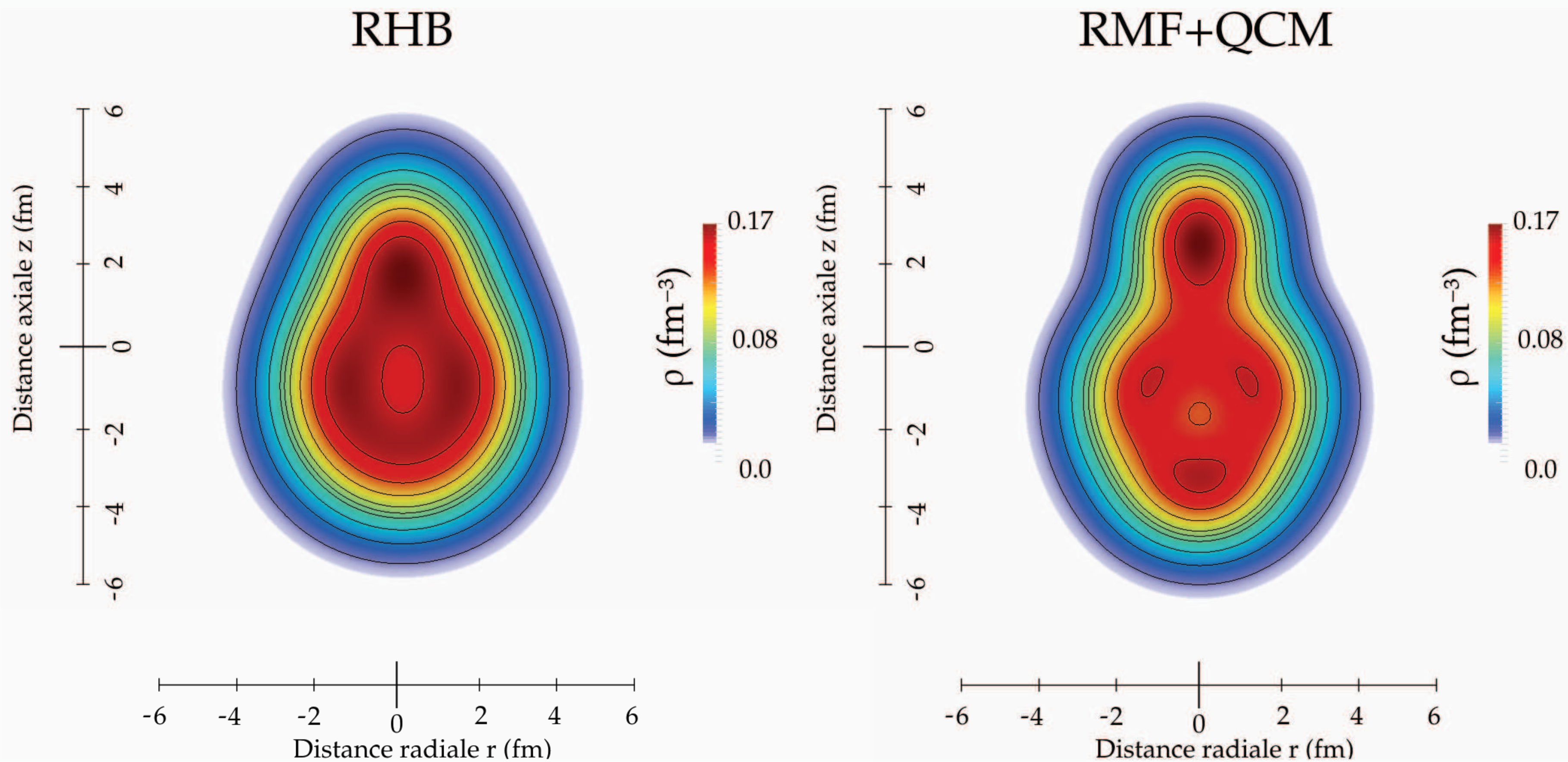

Superfluidities

Quartet localisation

Comparison of the local-part of the pairing tensor κ and of the $\mathcal{Q}$ operator

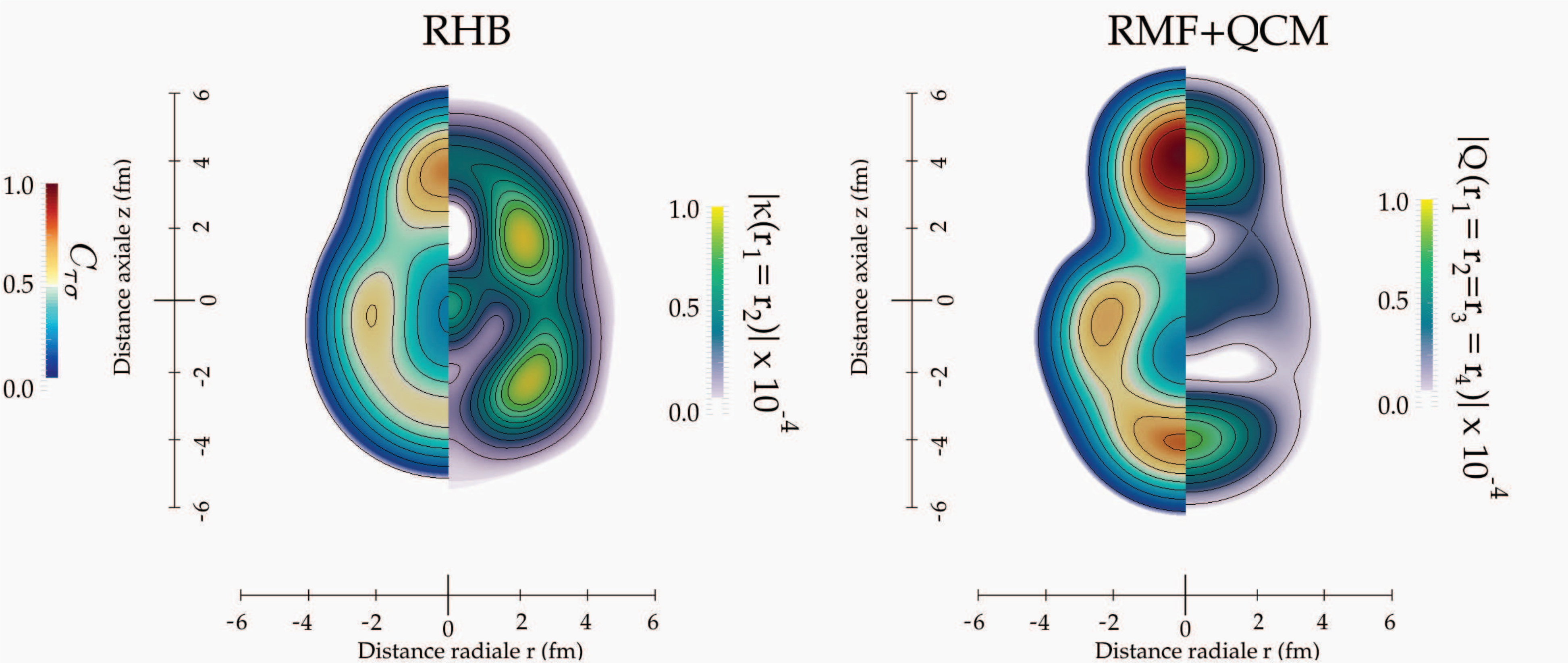

Localisation of the correlations

Contributions for each Isospin channel:

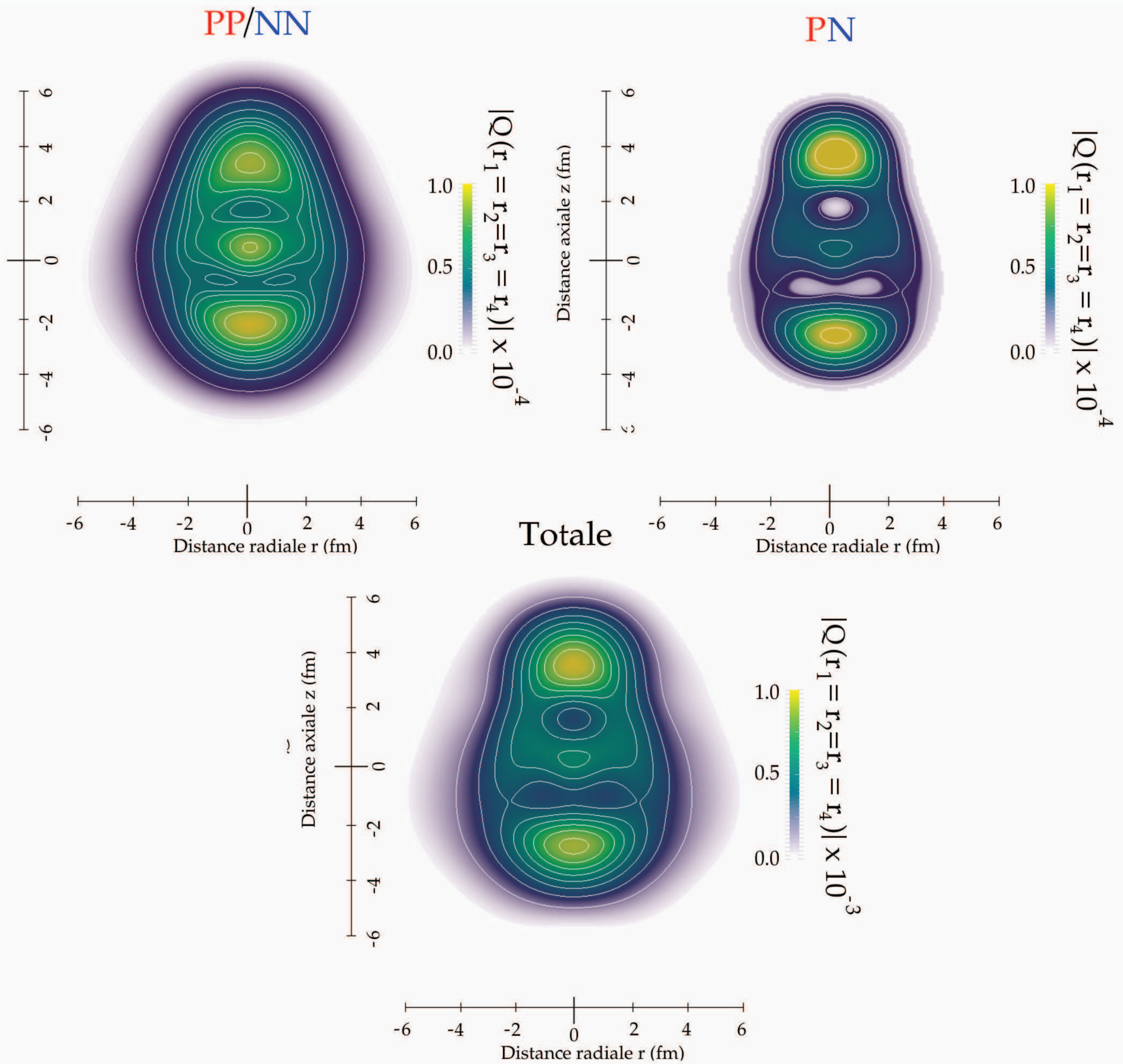

Superfluidities

Clusters and quartets

^{8}Be: $\alpha + \alpha$

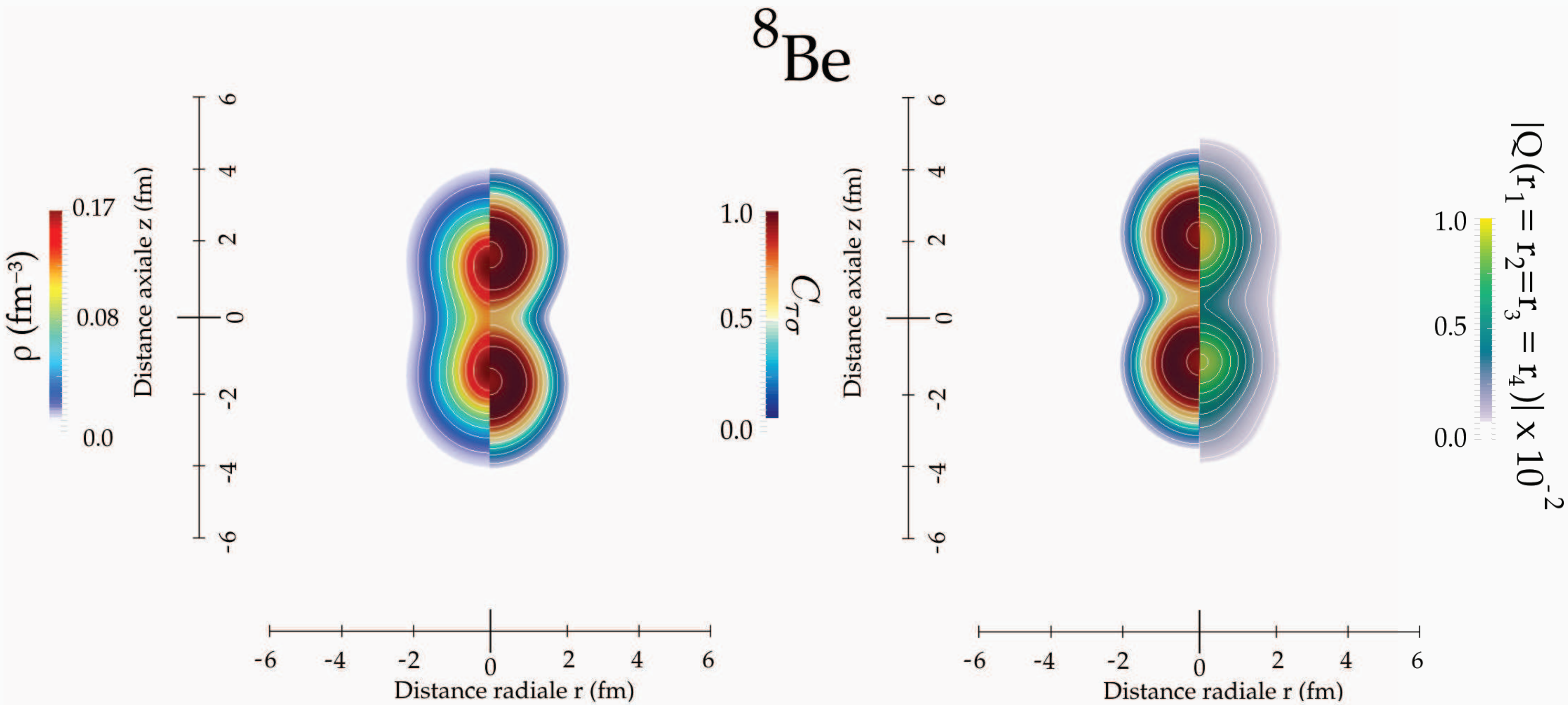

^{20}Ne: $^{16}O + \alpha$

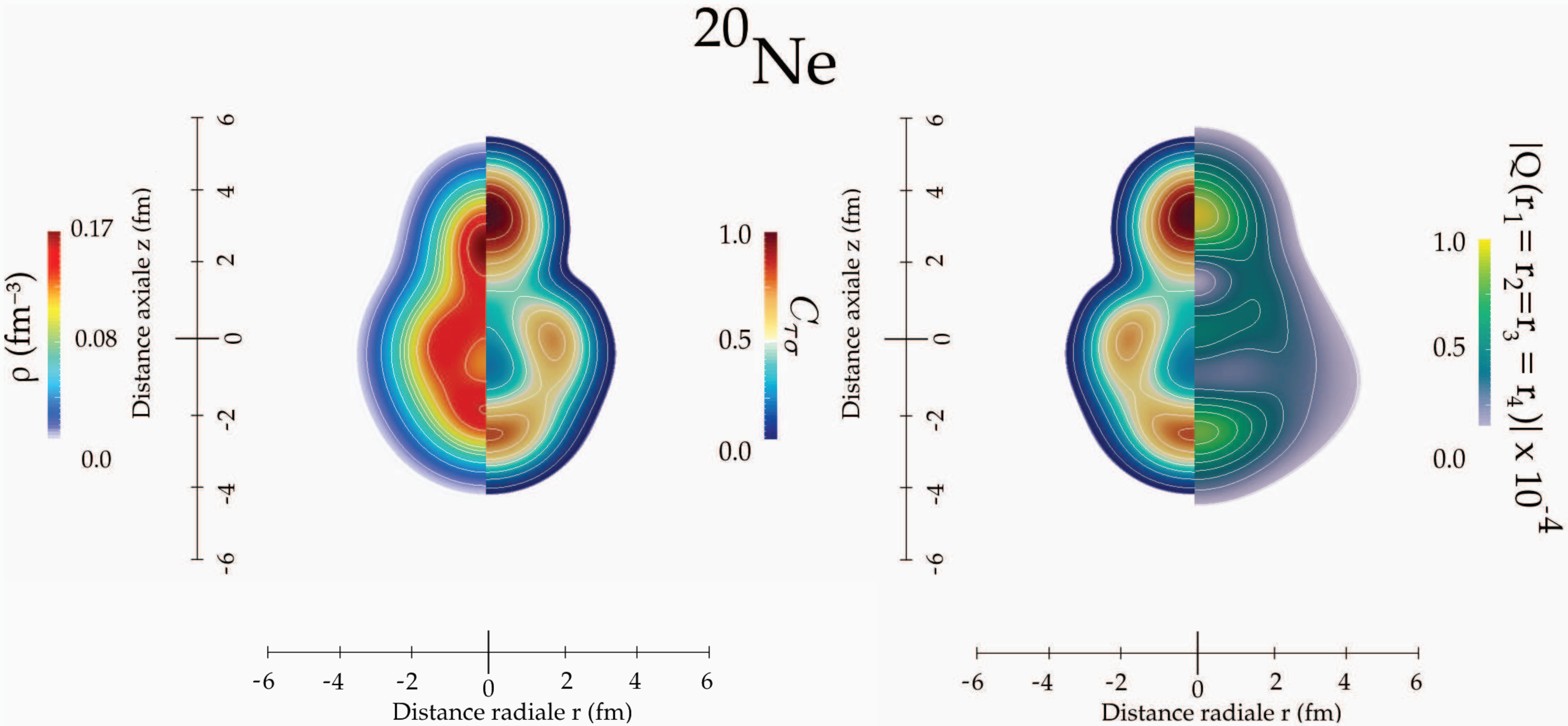

^{24}Mg: $^{16}O + \alpha + \alpha$

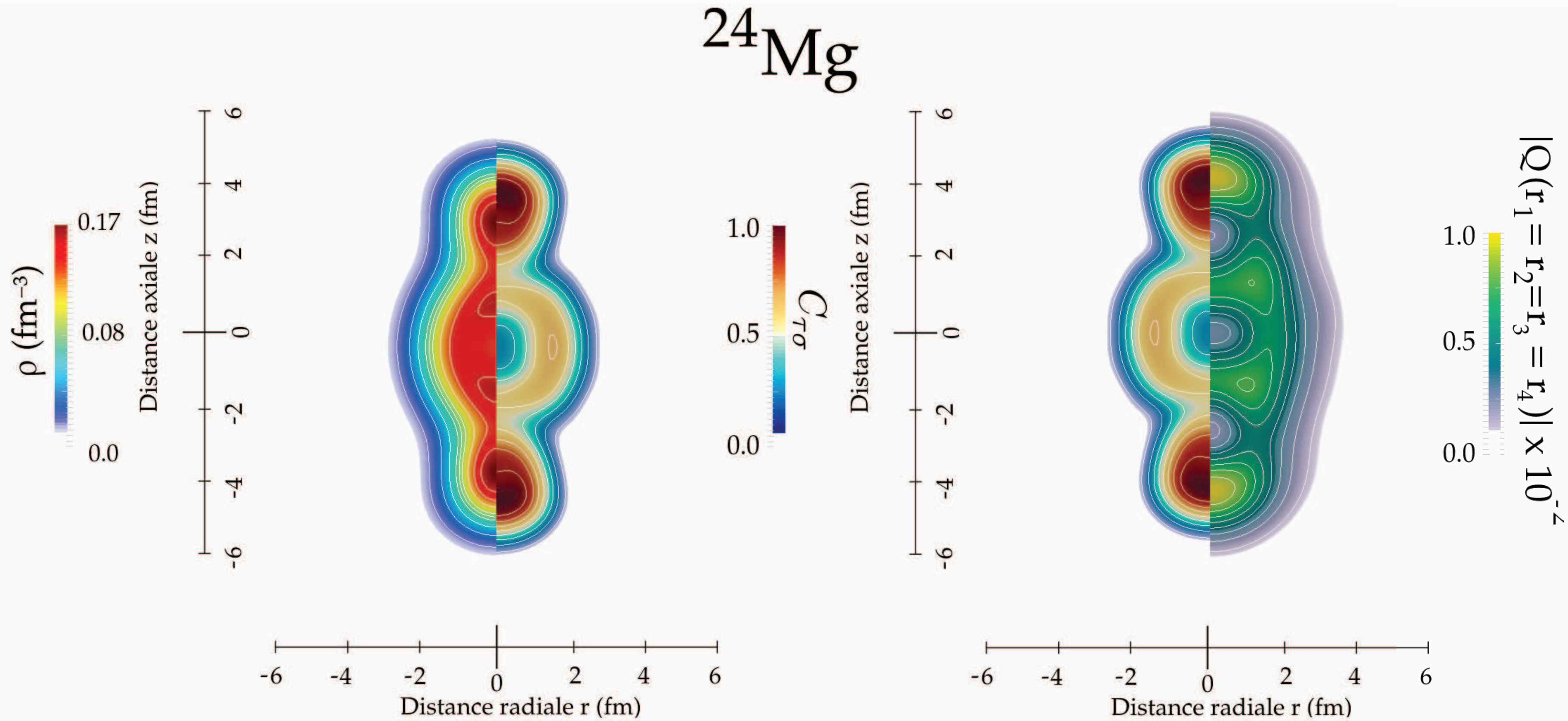

Conclusions

Conclusions

Principal results:

- Reduction of the pair extension at surface of nuclei
- Deeper understanding of cluster emergence
- Self-consistent RMF+QCM implementation
- Genetic algorithm optimization

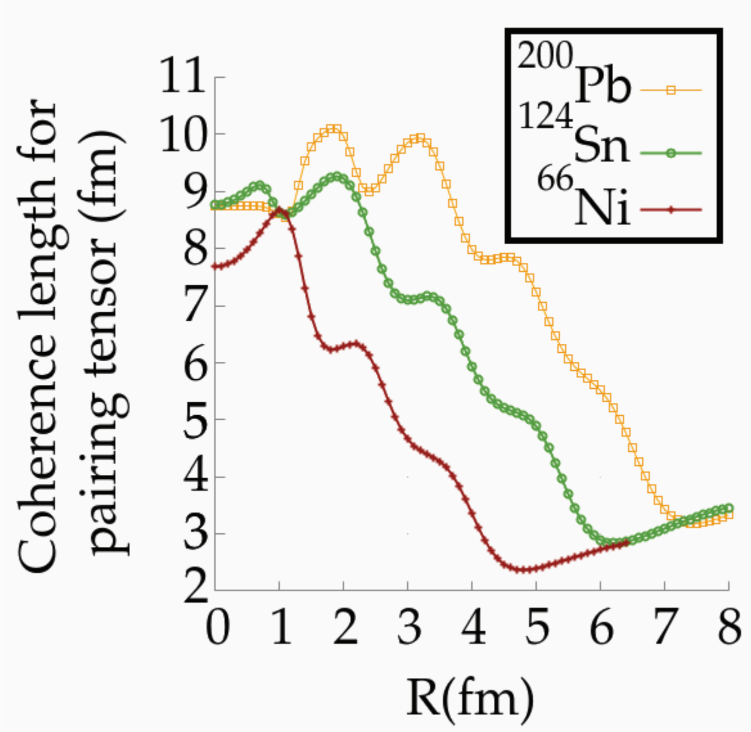

Conclusions

Principal results:

- Reduction of the pair extension at surface of nuclei
- Deeper understanding of cluster emergence
    - Localisation parameter
    - Interpretation as a QPT
- Self-consistent RMF+QCM implementation
- Genetic algorithm optimization

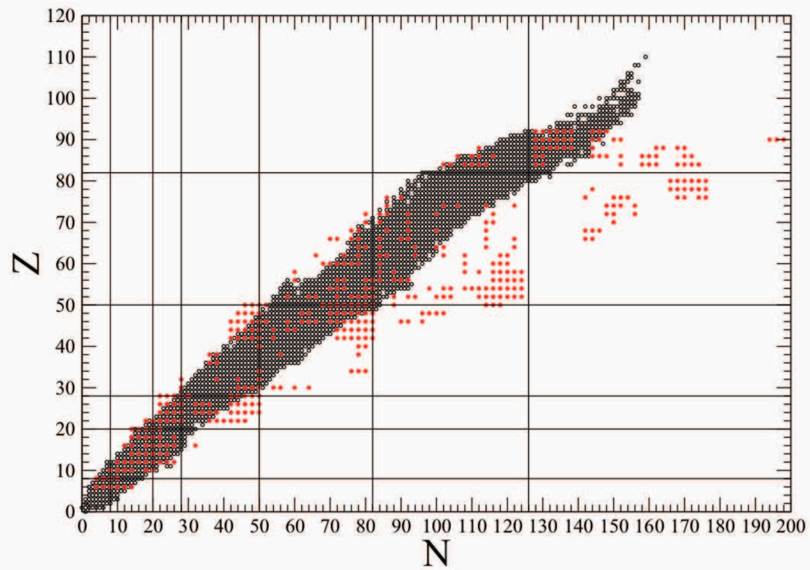

Conclusions

Principal results:

- Reduction of the pair extension at surface of nuclei
- Deeper understanding of cluster emergence
    - Localisation parameter
    - Interpretation as a QPT
- Self-consistent RMF+QCM implementation
- Genetic algorithm optimization

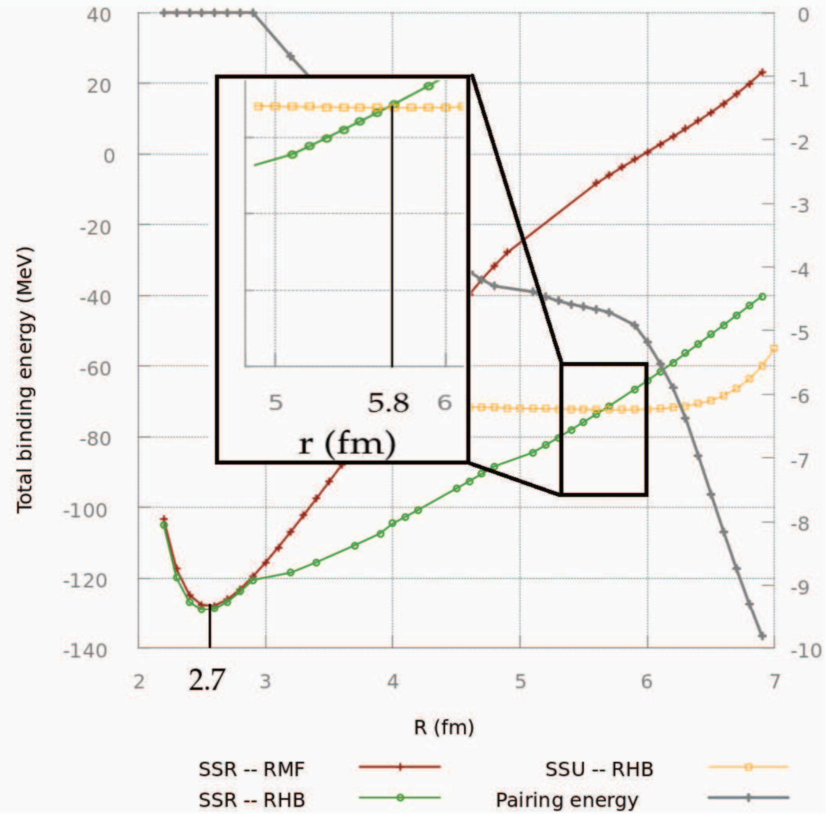

Conclusions

Principal results:

- Reduction of the pair extension at surface of nuclei
- Deeper understanding of cluster emergence
  - Localisation parameter
  - Interpretation as a QPT
- Self-consistent RMF+QCM implementation
- Genetic algorithm optimization

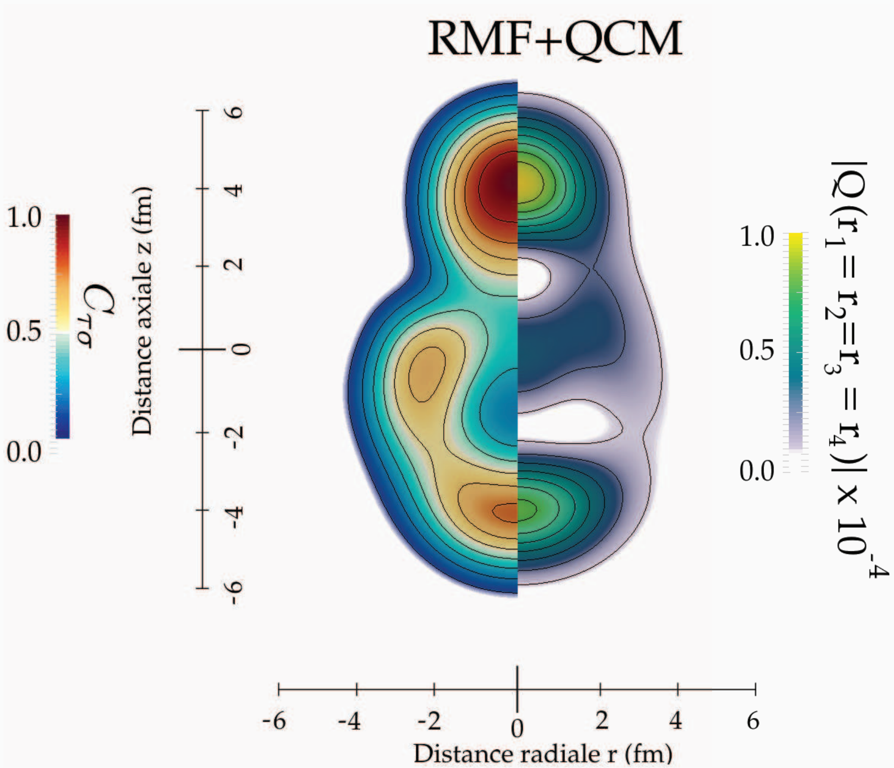

Conclusions

Principal results:

- Reduction of the pair extension at surface of nuclei
- Deeper understanding of cluster emergence
  - Localisation parameter
  - Interpretation as a QPT
- Self-consistent RMF+QCM implementation
- Genetic algorithm optimization

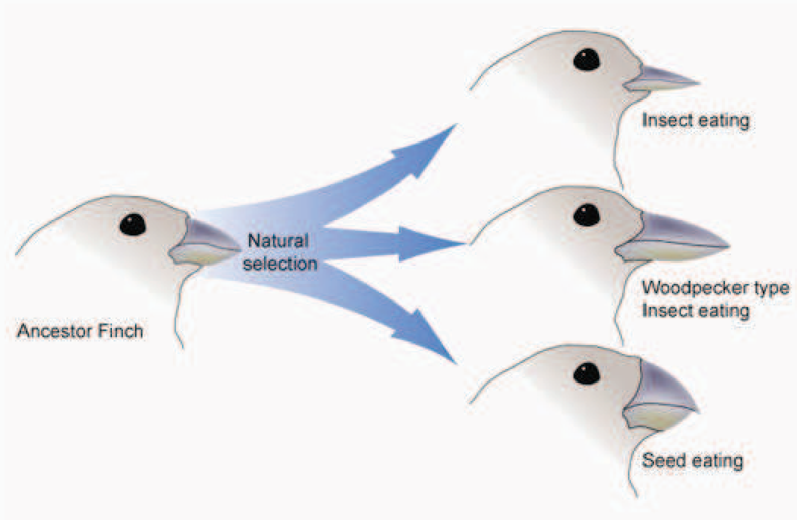

Perspectives

- ◇ Precise link between Quartet and α-cluster
  - Study of a Quartet coherence length
  - Systematic study of N=Z nuclei
- ◇ New type of genetic solver
  - Replace iterative methode (both MF and QCM)
  - Tackle more complex restoration (generalized GCM)
- ◇ Study other chanels of QCM (tetra-neutrons studies)
- ◇ Explore the impact of these new formalisms for description of α and cluster radioactivity

Thanks for your attention !

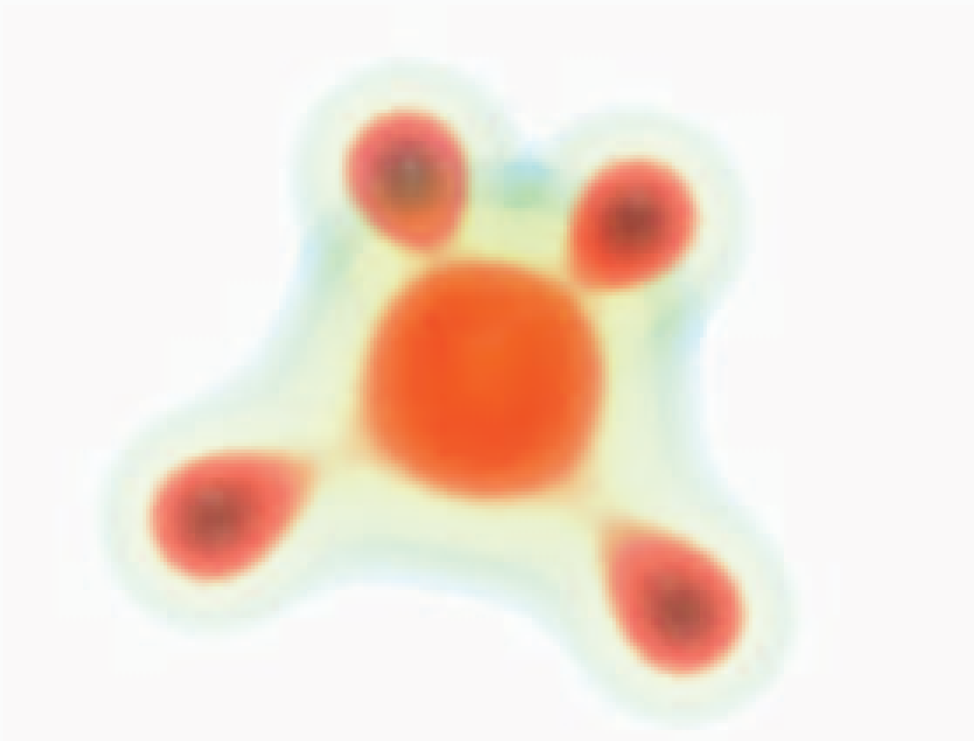

Théorie effective chirale

Les degrés de liberté, pour une χ-EFT: Nucléons et Pions.

$$\mathcal{L}_{\chi\text{-EFT}} = \mathcal{L}_{\pi} + \mathcal{L}_{\mathrm{NN}} + \mathcal{L}_{\mathrm{N}\pi}$$

1-pion

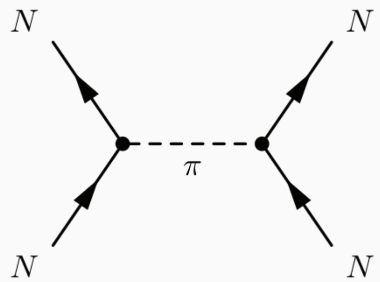

Théorie effective chirale

Les degrés de liberté, pour une χ-EFT: Nucléons et Pions.

$$\mathcal{L}_{\chi\text{-EFT}} = \mathcal{L}_{\pi} + \mathcal{L}_{\rm NN} + \mathcal{L}_{\rm N\pi}$$

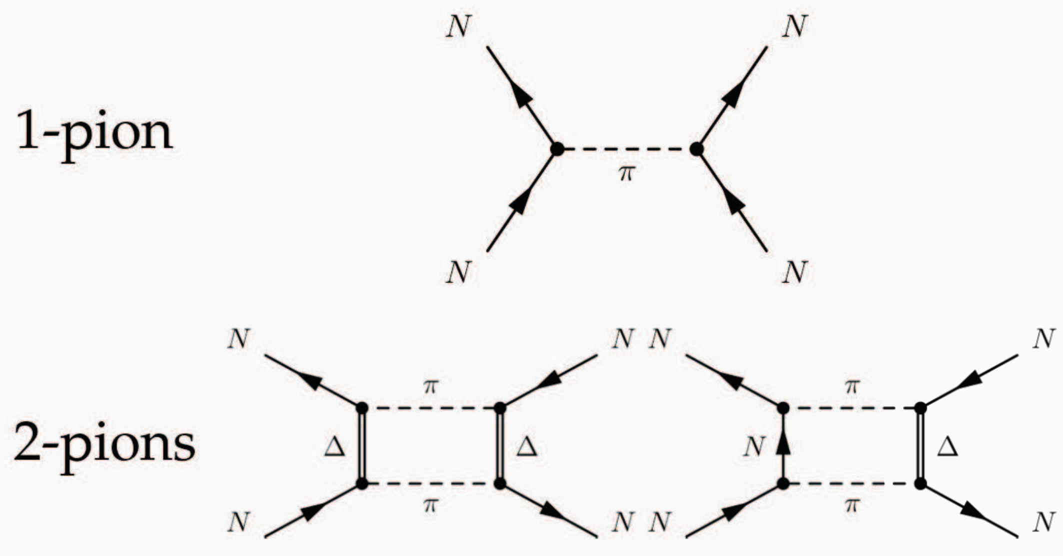

Théorie effective chirale

Les degrés de liberté, pour une χ-EFT: Nucléons et Pions.

$$\mathcal{L}_{\chi\text{-EFT}} = \mathcal{L}_{\pi} + \mathcal{L}_{\mathrm{NN}} + \mathcal{L}_{\mathrm{N}\pi}$$

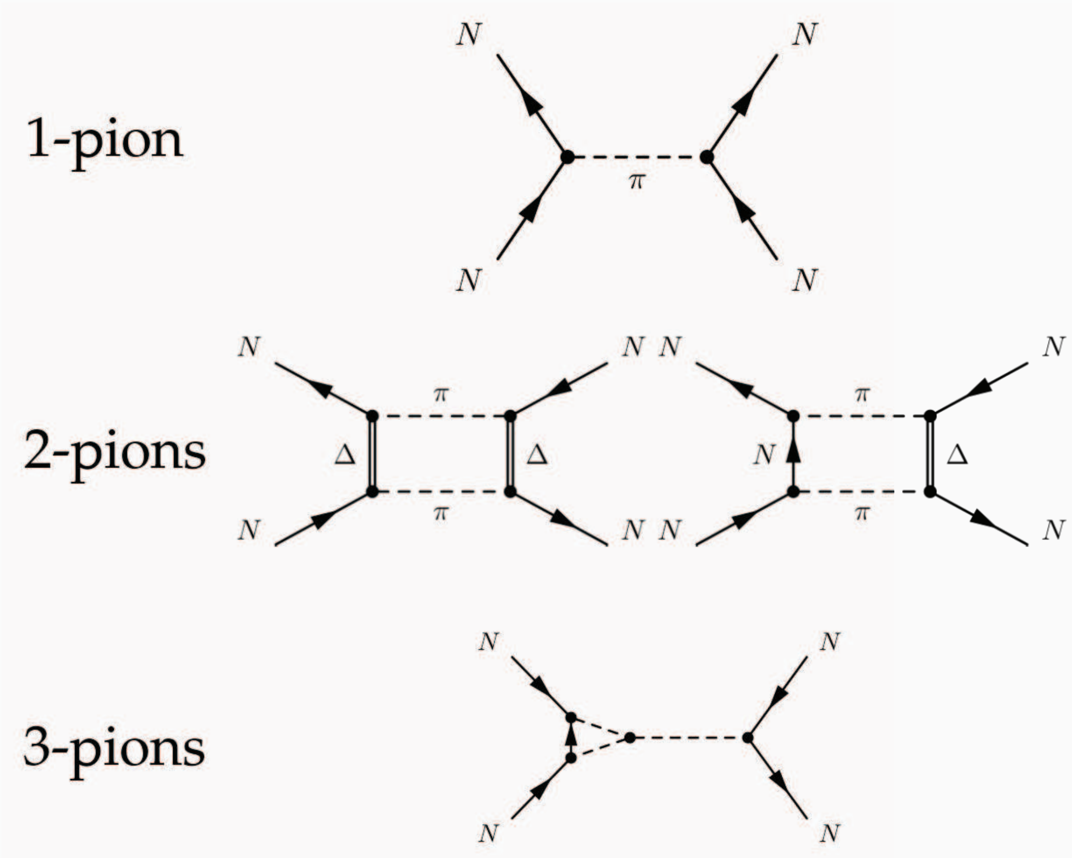

Théorie effective chirale

Les degrés de liberté, pour une χ-EFT: Nucléons et Pions.

$$\mathcal{L}_{\chi\text{-EFT}} = \mathcal{L}_{\pi} + \mathcal{L}_{\mathrm{NN}} + \mathcal{L}_{\mathrm{N}\pi}$$

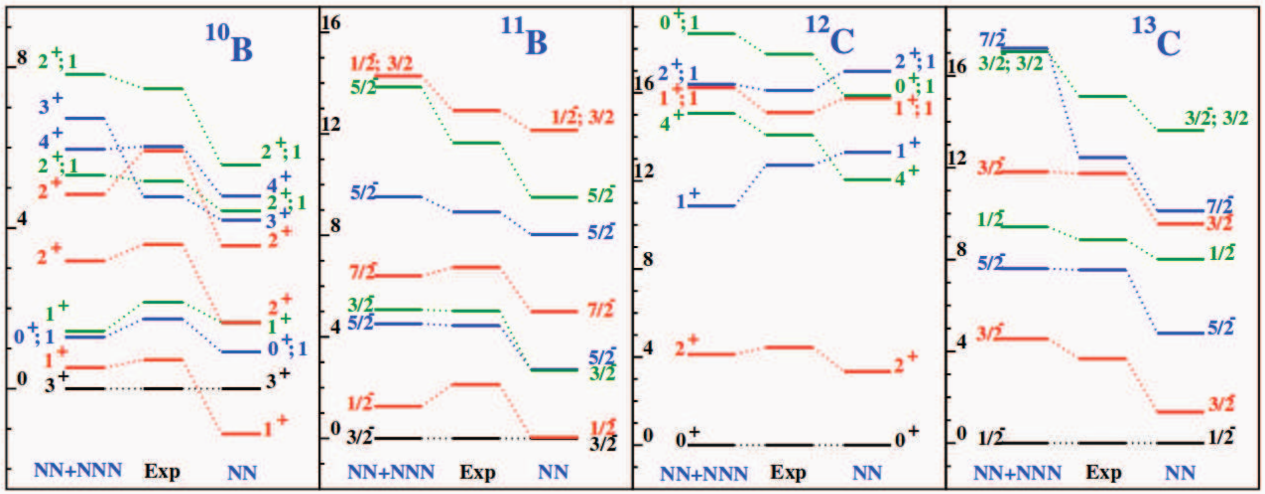

- Résultats remarquables dans la matière nucléaire
- Très complexe pour une étude systématique des noyaux

Théorie effective chirale

Les degrés de liberté, pour une χ-EFT: Nucléons et Pions.

$$\mathcal{L}_{\chi\text{-EFT}} = \mathcal{L}_{\pi} + \mathcal{L}_{\mathrm{NN}} + \mathcal{L}_{\mathrm{N}\pi}$$

- Résultats remarquables dans la matière nucléaire
- Très complexe pour une étude systématique des noyaux

Nouvelle approximation nécessaire

Density Functional Theory vs Energy Density Functional

Hohenberg-Kohn: Existence d'une fonctionnelle $F[\rho]$

$$E[\rho] = \langle \Psi | H^N | \Psi \rangle = F[\rho] + \int d\mathbf{r} V_{\text{ext}}(\mathbf{r}) \rho(\mathbf{r})$$

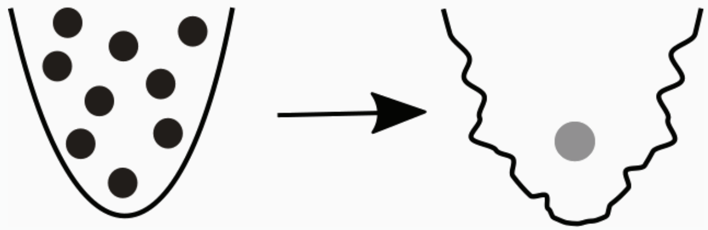

- Définition d'une classe d'universalité
- Correspondance exacte entre système en interaction et système auxiliaire
- Obtention de l'état fondamental par minimisation de $E[\rho]$

Density Functional Theory vs Energy Density Functional

Hohenberg-Kohn: Existence d'une fonctionnelle $F[\rho]$

$$E[\rho] = \langle \Psi | H^N | \Psi \rangle = F[\rho] + \int d\mathbf{r} V_{\text{ext}}(\mathbf{r}) \rho(\mathbf{r})$$

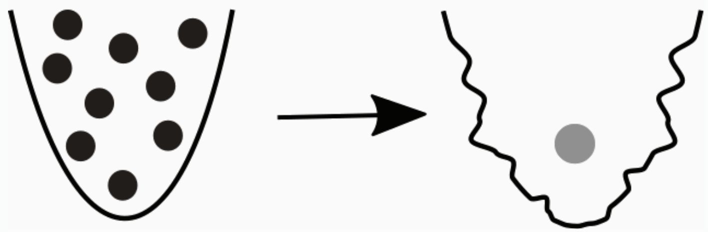

Toutefois:

- Pas d'indication sur la construction de $F[\rho]$
- Ne s'applique pas (directement) aux systèmes auto-liés

Problème à N-corps

On peut distinguer les résolutions:

1. Exactes
2. Ab-initio
3. EDF

Traitement explicite de la fonction d'onde totale

- $\hat{H}\Psi = E\Psi$
- Très efficace avec une interaction réaliste
- Excessivement complexe numériquement

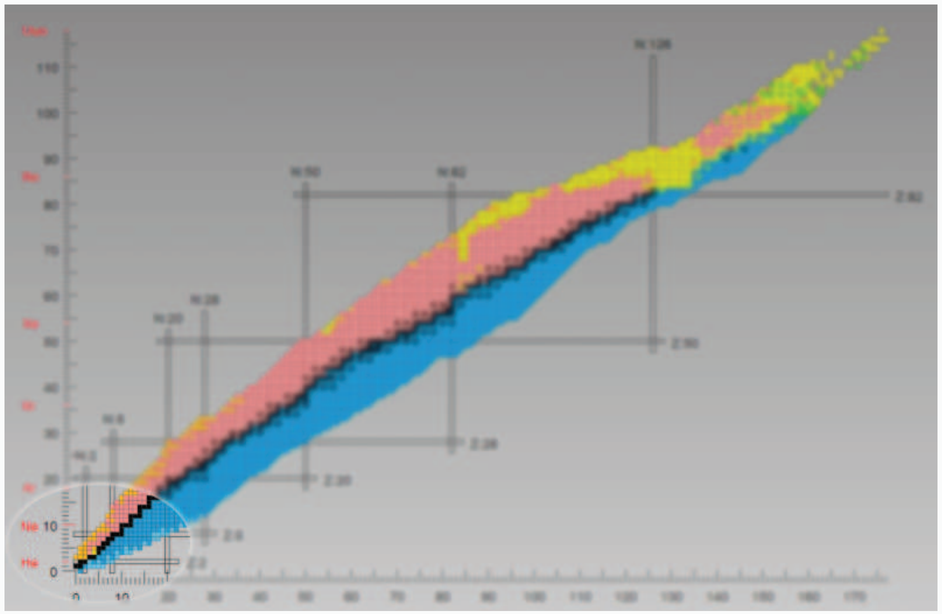

Problème à N-corps

On peut distinguer les résolutions:

1. Exactes
2. Ab-initio
3. EDF

Traitement explicite d'une troncation de la fonction d'onde

- $\Psi = \sum_I c_I \psi_I$
- Prédictive avec interaction phénoménologique
- Très lourd numériquement.

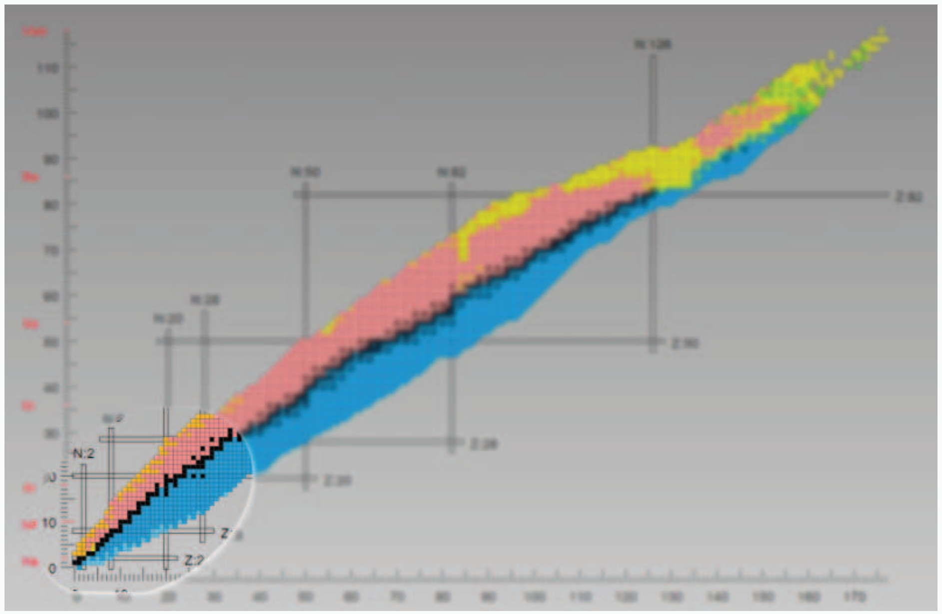

Problème à N-corps

On peut distinguer les résolutions:

1. Exactes
2. Ab-initio
3. EDF

Traitement de type champ-moyen

- $[\hat{H}, \hat{\rho}] = 0$
- Universel avec interaction phénoménologique
- Relativement simple numériquement

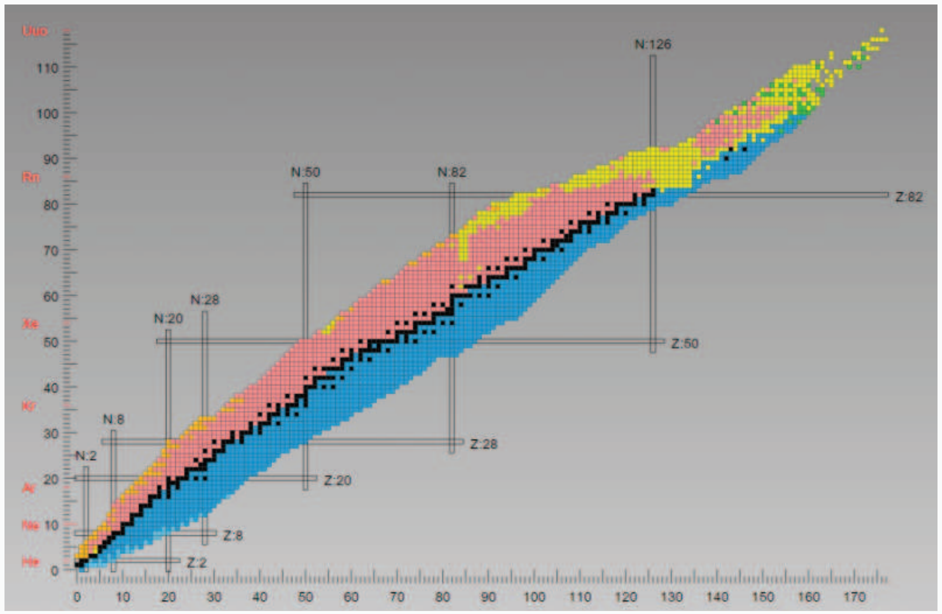

Déformations spatiales – Classification

Pour un état:

$$|\lambda\rangle = \sum_{nljm\tau} C^{\lambda}_{nljm\tau} |nljm\tau\rangle$$

Avec:

• n principal, • l azimuthal, • j angulaire, • m magnétique, • τ isospin

---

Et $\vec{J}$ l'opérateur moment cinétique total

$$[H, \vec{J}] = 0$$

$$|\lambda j_\lambda m_\lambda\rangle = \sum_{nl\tau} \mathcal{C}^{\lambda}_{nl\tau} |nlj_\lambda m_\lambda \tau\rangle$$

Système sphérique

Déformations spatiales – Classification

Pour un état:

$$|\lambda\rangle = \sum_{nljm\tau} C^{\lambda}_{nljm\tau} |nljm\tau\rangle$$

Avec:

• n principal, • l azimuthal, • j angulaire, • m magnétique, • τ isospin

---

$$[H, J_z] = 0$$

$$|\lambda m_\lambda\rangle = \sum_{l\in 2\mathbb{Z}} \sum_{nj\tau} C^{\lambda}_{nlj\tau} |nljm_\lambda\tau\rangle$$

Système axial

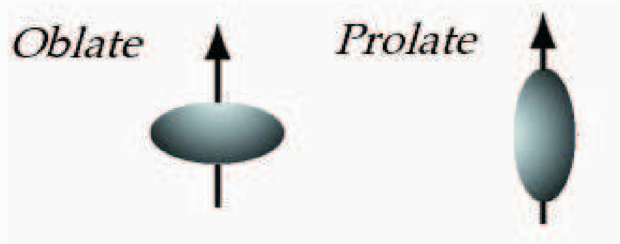

$$Q_{20} \propto \sum_{i}^{A} \left(2z_i^2 - x_i^2 - y_i^2\right)$$

Déformations spatiales – Classification

Pour un état:

$$|\lambda\rangle = \sum_{nljm\tau} C^{\lambda}_{nljm\tau} |nljm\tau\rangle$$

Avec:

• n principal, • l azimuthal, • j angulaire, • m magnétique, • τ isospin

---

$$[H, J_z] = 0$$

$$|\lambda m_\lambda\rangle = \sum_{l\in\mathbb{Z}} \sum_{nj\tau} C^{\lambda}_{nlj\tau} |nljm_\lambda\tau\rangle$$

Système octupolaire

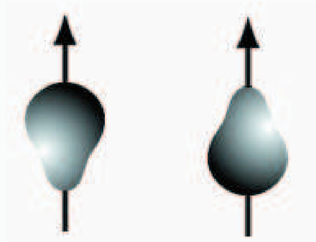

$$Q_{30} \propto \sum_{i}^{A} \left(z_i^3 - \frac{3}{2} z_i \left(x_i^2 + y_i^2 \right) \right)$$

Réalisation pratique – Paramètres de la base

Base des états propres de l'Oscillateur Harmonique

$$V_{OH}(r,z) = \frac{1}{2} M \left(\omega_r^2 r^2 + \omega_z z^2\right) \text{ ou } V_{OH}(x,y,z) = \frac{1}{2} M \left(\omega_x^2 x^2 + \omega_z^2 z^2 + \omega_z^2 z^2\right)$$

N_f: Nombre de couches

- Légers: 8
- Masses intermédiaires: 8-10
- Lourds: 14

$\hbar\omega$

Optimisation sur les première itérations

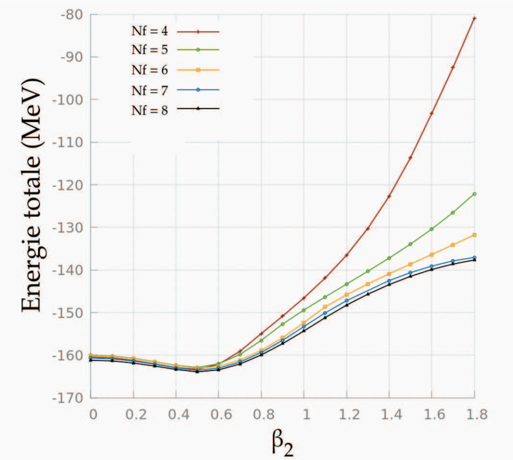

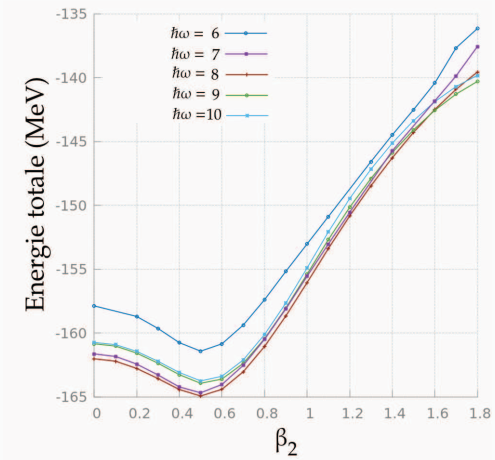

Obtenir un "vrai" minimum

Réalisation pratique – Paramètres de la base

Base des états propres de l'Oscillateur Harmonique

$V_{OH}(r,z) = \frac{1}{2}M\left(\omega_r^2 r^2 + \omega_z z^2\right)$ ou $V_{OH}(x,y,z) = \frac{1}{2}M\left(\omega_x^2 x^2 + \omega_z^2 z^2 + \omega_z^2 z^2\right)$

N_f: Nombre de couches

- Légers: 8
- Masses intermédiaires: 8-10
- Lourds: 14

$\hbar\omega$

Optimisation sur les première itérations

Avantages	Inconvénients
Expression aisée d'opérateurs	Mauvais traitement des *drip-lines*
Numériquement accessible	Peut induire une stabilité artificielle

Impact de $\hbar\omega$

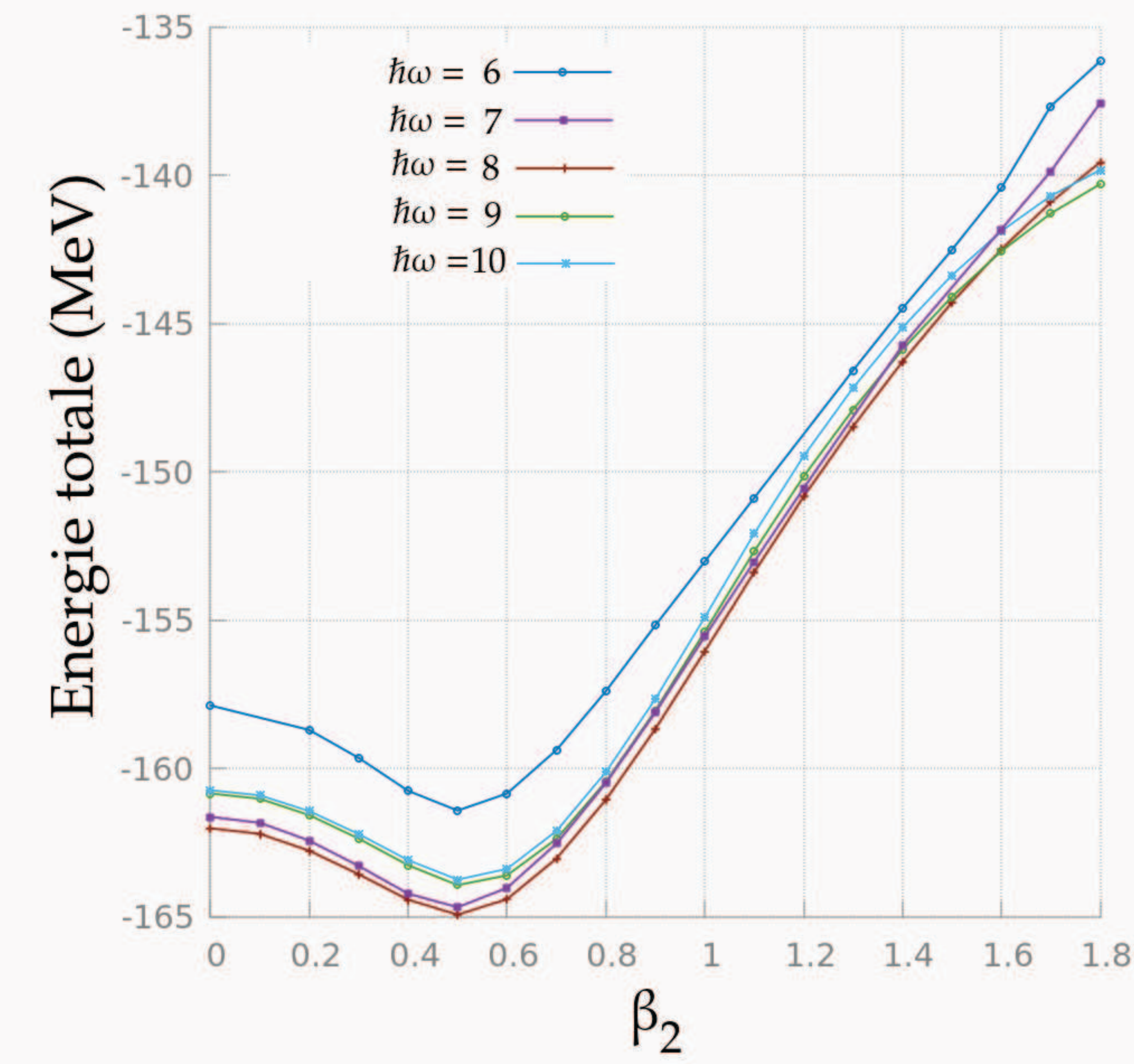

Impact du nombre de couches

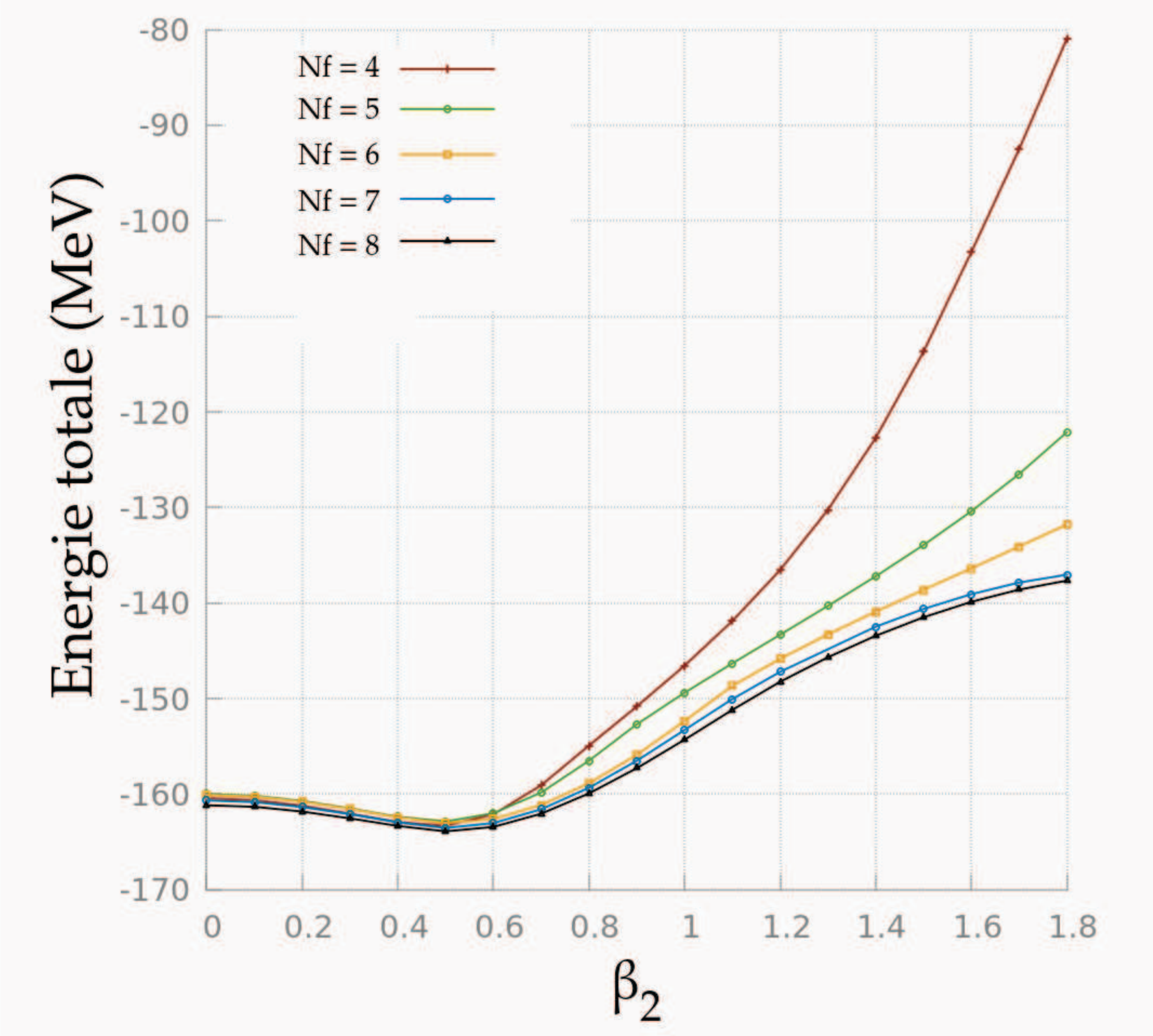

Appariement: Nécessité expérimentale

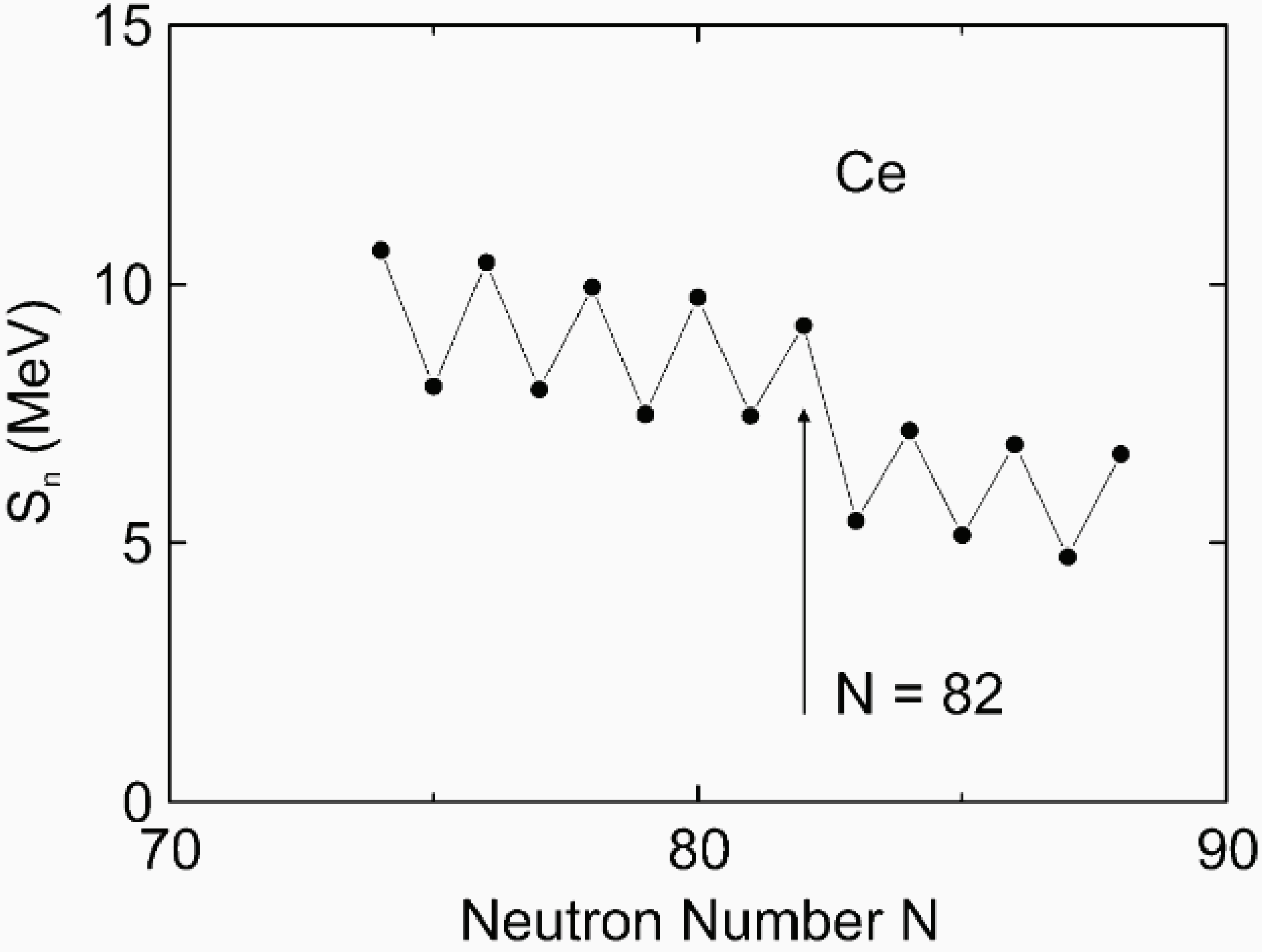

Appariement: Nécessité expérimentale

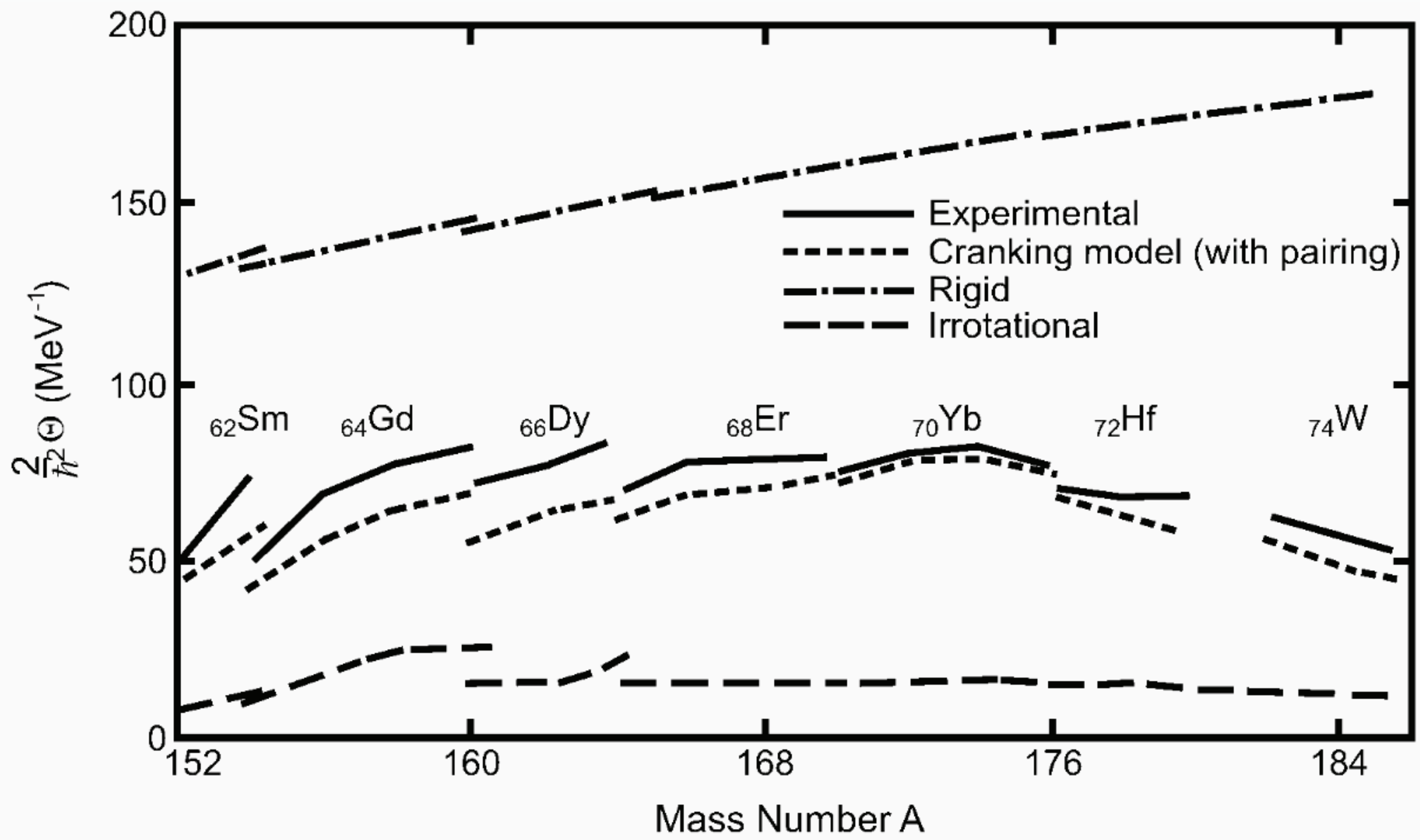

Réalisation pratique – Base d'oscillateur

Base d'oscillateur harmonique axialement déformé

$$V_{OH}(r,z) = \frac{1}{2}M\omega_r^2 r^2 + \frac{1}{2}M\omega_z z^2$$

$|\alpha\rangle = |n_z, n_r, \Lambda, m_s\rangle$ $\qquad$ $\Phi_\alpha(\mathbf{r}, s, \tau) = \psi_{n_r}^{\Lambda}(r)\psi_{n_z}(z)\frac{e^{i\Lambda\theta}}{\sqrt{2\pi}}\chi_\Sigma(s)\chi_T(\tau)$

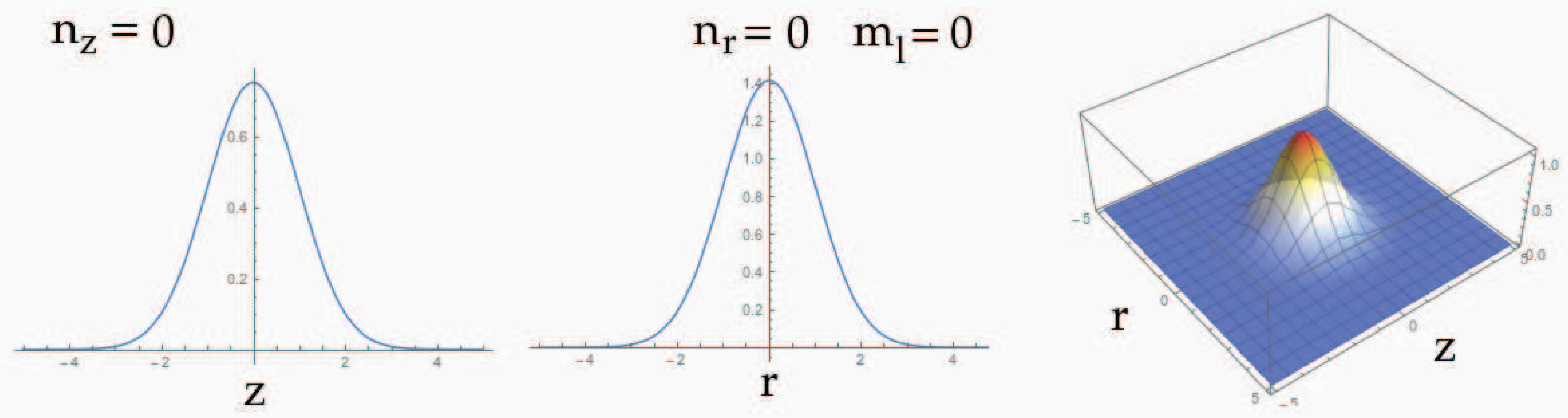

Réalisation pratique – Base d'oscillateur

Base d'oscillateur harmonique axialement déformé

$$V_{OH}(r,z) = \frac{1}{2}M\omega_r^2 r^2 + \frac{1}{2}M\omega_z z^2$$

$$|\alpha\rangle = |n_z, n_r, \Lambda, m_s\rangle \qquad \Phi_\alpha(\mathbf{r}, s, \tau) = \psi_{n_r}^{\Lambda}(r)\psi_{n_z}(z)\frac{e^{i\Lambda\theta}}{\sqrt{2\pi}}\chi_\Sigma(s)\chi_T(\tau)$$

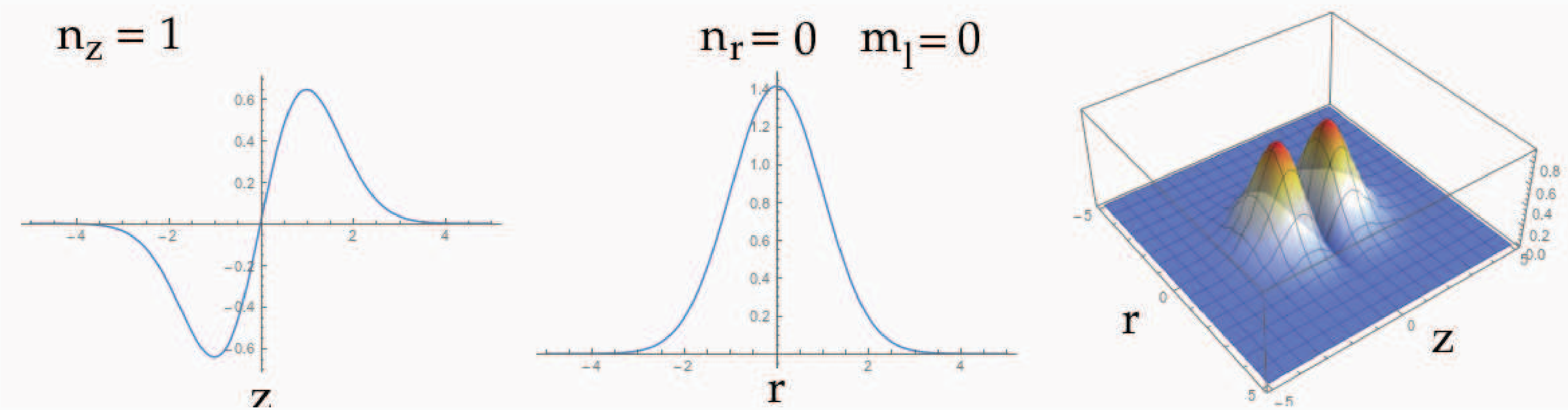

Réalisation pratique – Base d'oscillateur

Base d'oscillateur harmonique axialement déformé

$$V_{OH}(r,z) = \frac{1}{2}M\omega_r^2 r^2 + \frac{1}{2}M\omega_z z^2$$

$$|\alpha\rangle = |n_z, n_r, \Lambda, m_s\rangle \qquad \Phi_\alpha(\mathbf{r}, s, \tau) = \psi_{n_r}^{\Lambda}(r)\psi_{n_z}(z)\frac{e^{i\Lambda\theta}}{\sqrt{2\pi}}\chi_\Sigma(s)\chi_T(\tau)$$

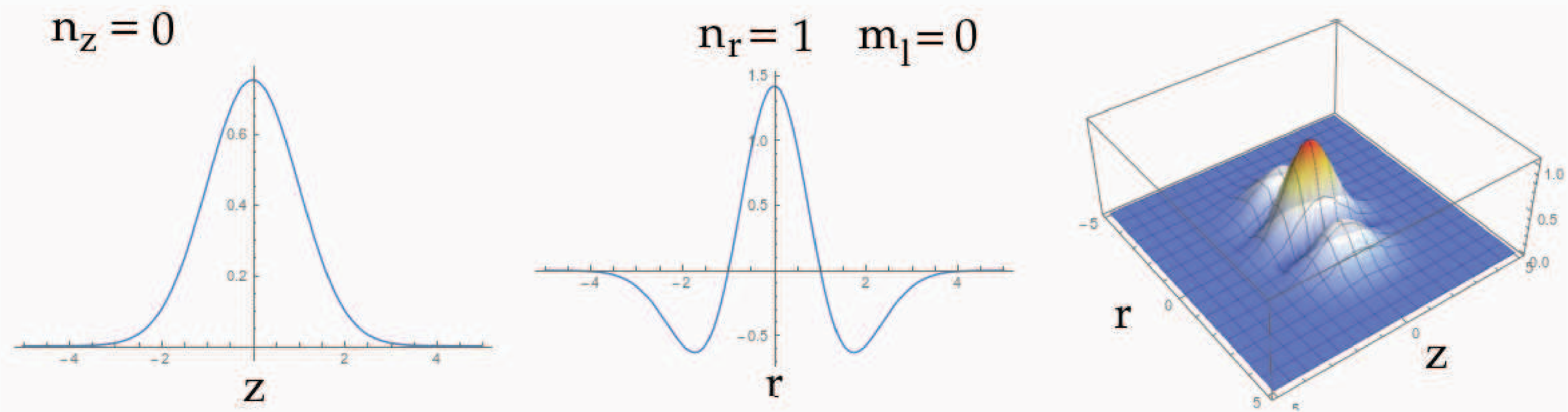

Réalisation pratique – Base d'oscillateur

Base d'oscillateur harmonique axialement déformé

$$V_{OH}(r,z) = \frac{1}{2}M\omega_r^2 r^2 + \frac{1}{2}M\omega_z z^2$$

$$|\alpha\rangle = |n_z, n_r, \Lambda, m_s\rangle \qquad \Phi_\alpha(\mathbf{r}, s, \tau) = \psi_{n_r}^{\Lambda}(r)\psi_{n_z}(z)\frac{e^{i\Lambda\theta}}{\sqrt{2\pi}}\chi_\Sigma(s)\chi_T(\tau)$$

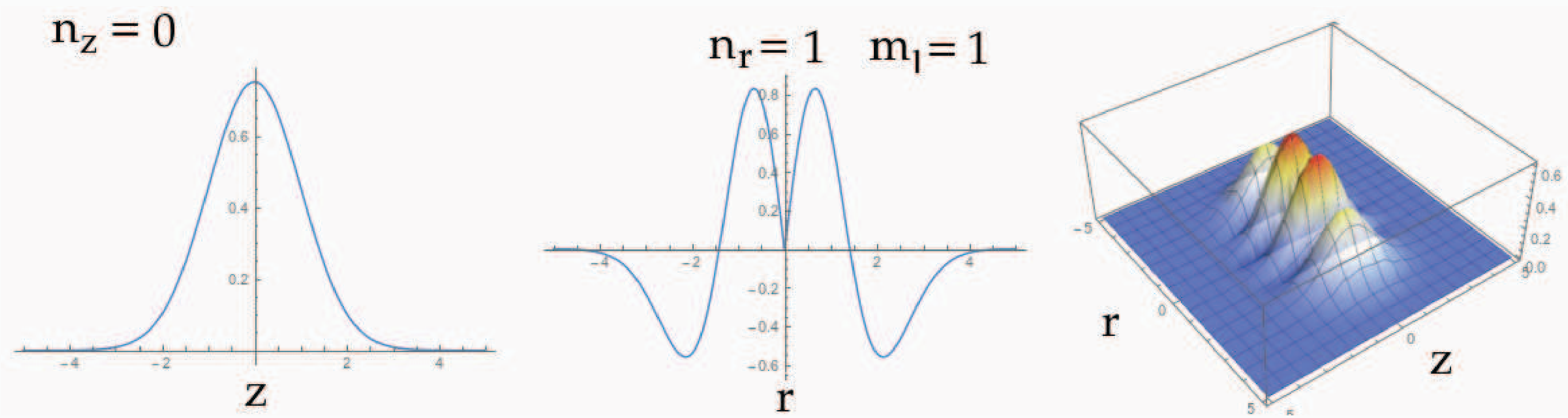

Déformations axiales – DD-ME2

Uranium 234

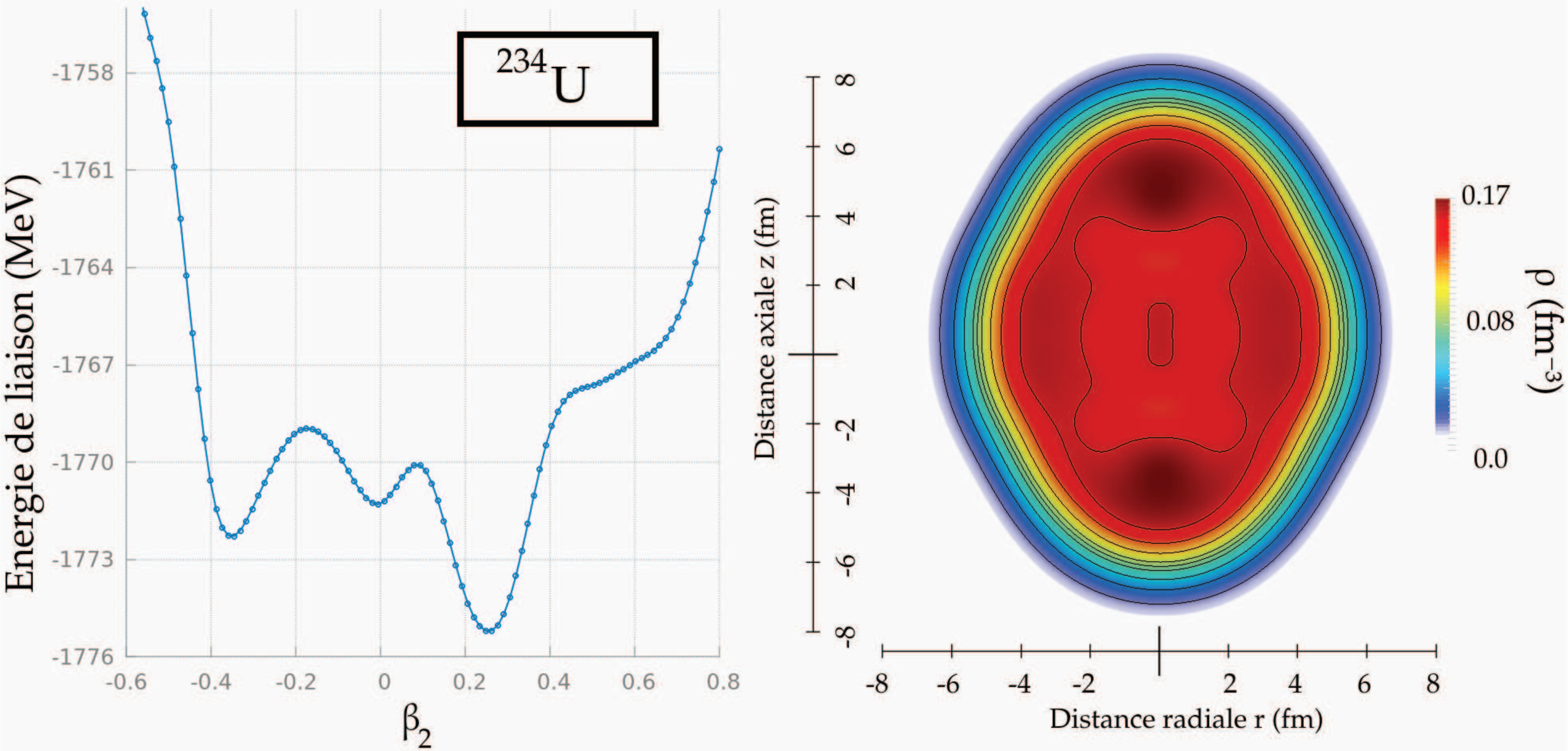

$E_{\text{Exp}} = -1778.0$ MeV

Déformations axiales – DD-ME2

Uranium 234

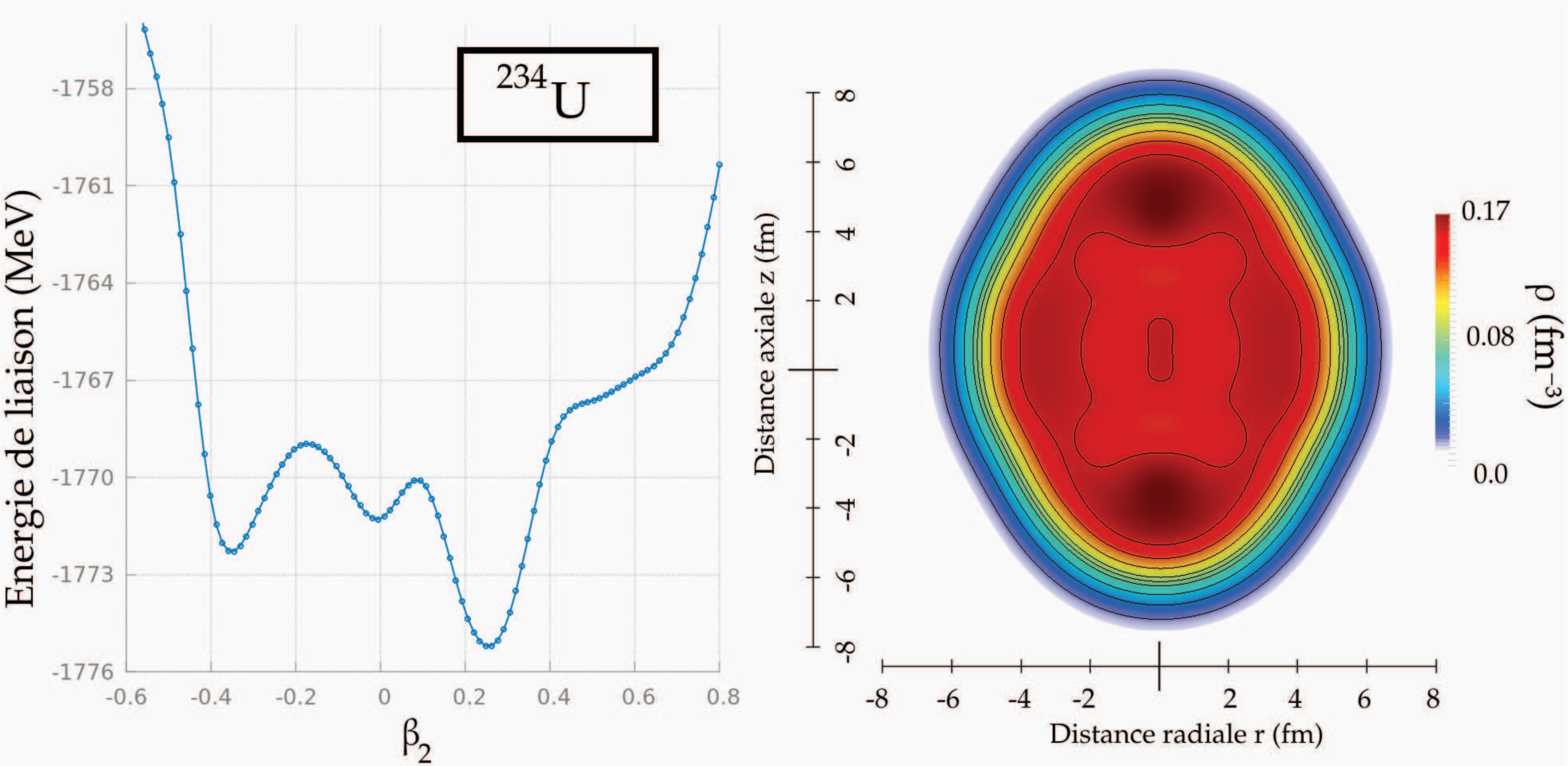

$E_{\text{Exp}} = -1778.0$ MeV $\qquad E_{\text{RMF}} = -1775.6$ MeV

Déformations octupolaires – DD-ME2

Radium 224

Déformation en poire: $\rho(r, z) \neq \rho(r, -z)$

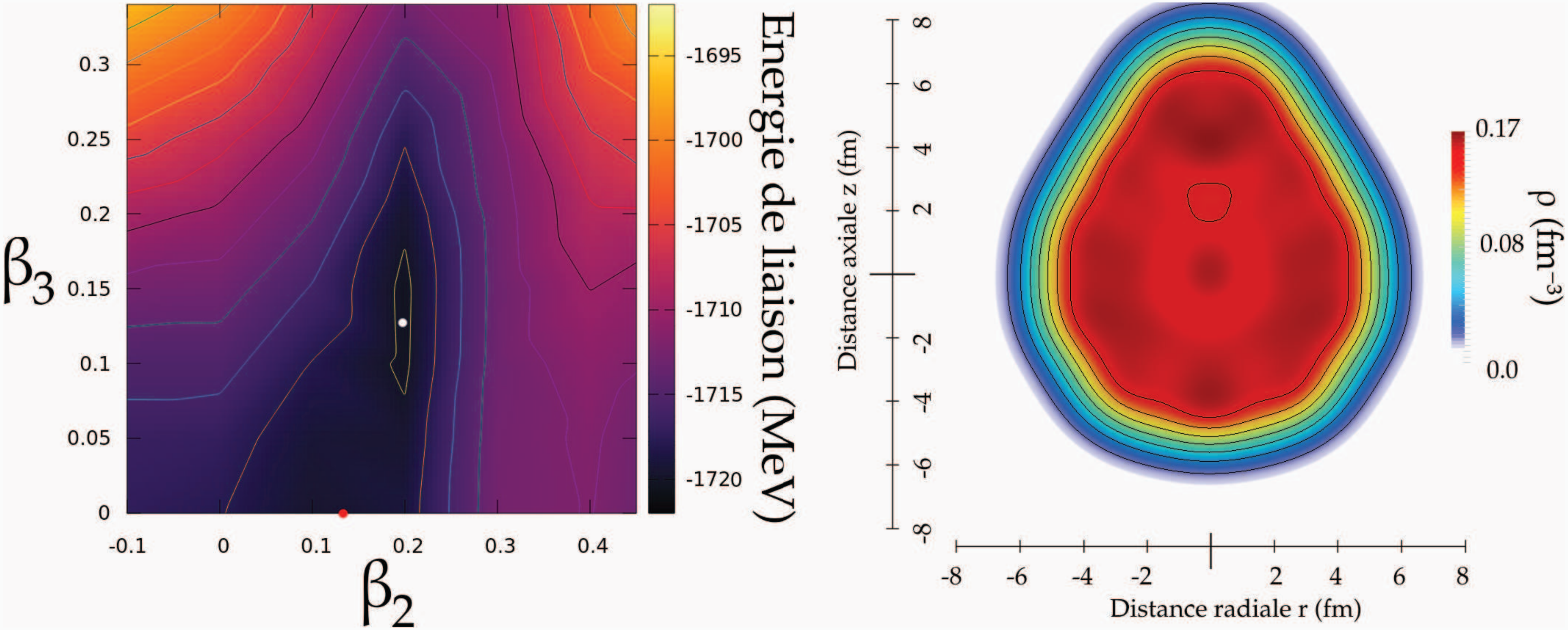

$E_{\text{Exp}} = -1720.3$ MeV $E_{\text{RMF}} = -1726.8$ MeV

Déformations triaxiales – DD-ME2

Platine 190

Base triaxiale: $V_{OH}^{3D} = \frac{1}{2} m \left(\omega_x^2 x^2 + \omega_y^2 y^2 + \omega_z^2 z^2 \right)$

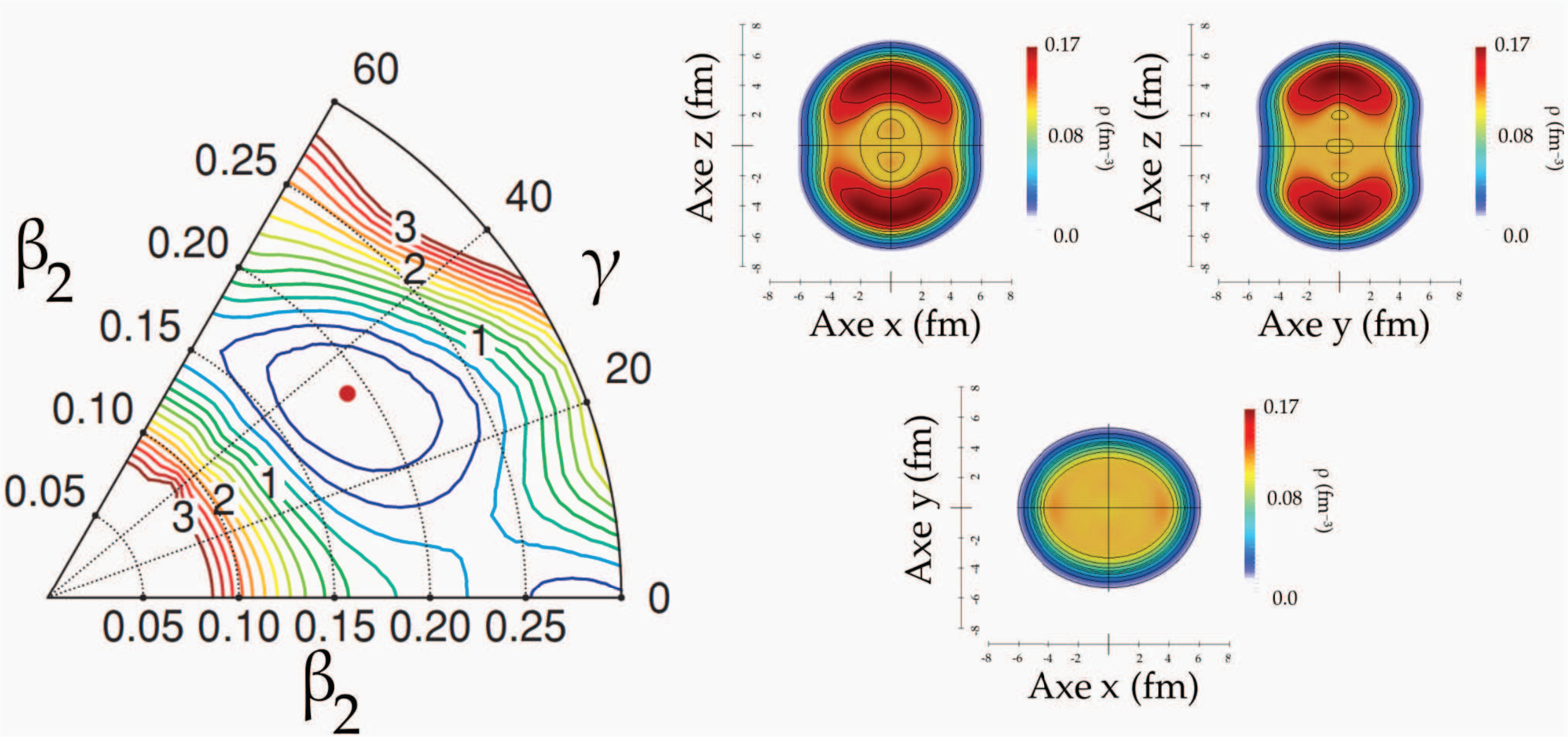

$E_{\text{Exp}} = -1509.9$ MeV

$E_{\text{RMF}} = -1521.6$ MeV

Déformations triaxiales – DD-ME2

Platine 190

Base triaxiale: $V_{OH}^{3D} = \frac{1}{2} m \left(\omega_x^2 x^2 + \omega_y^2 y^2 + \omega_z^2 z^2 \right)$

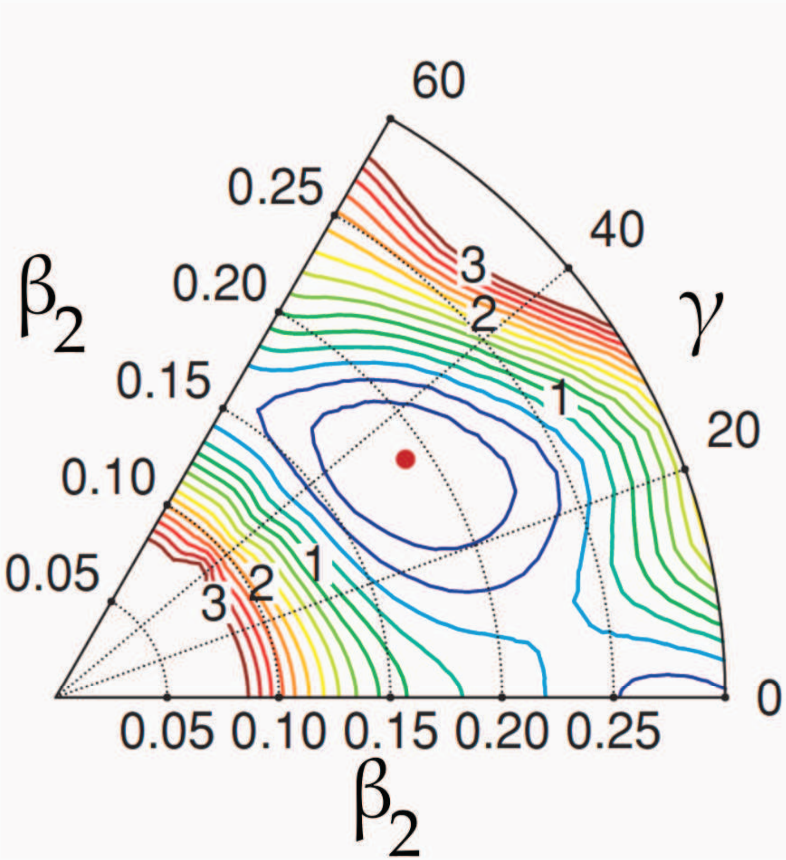

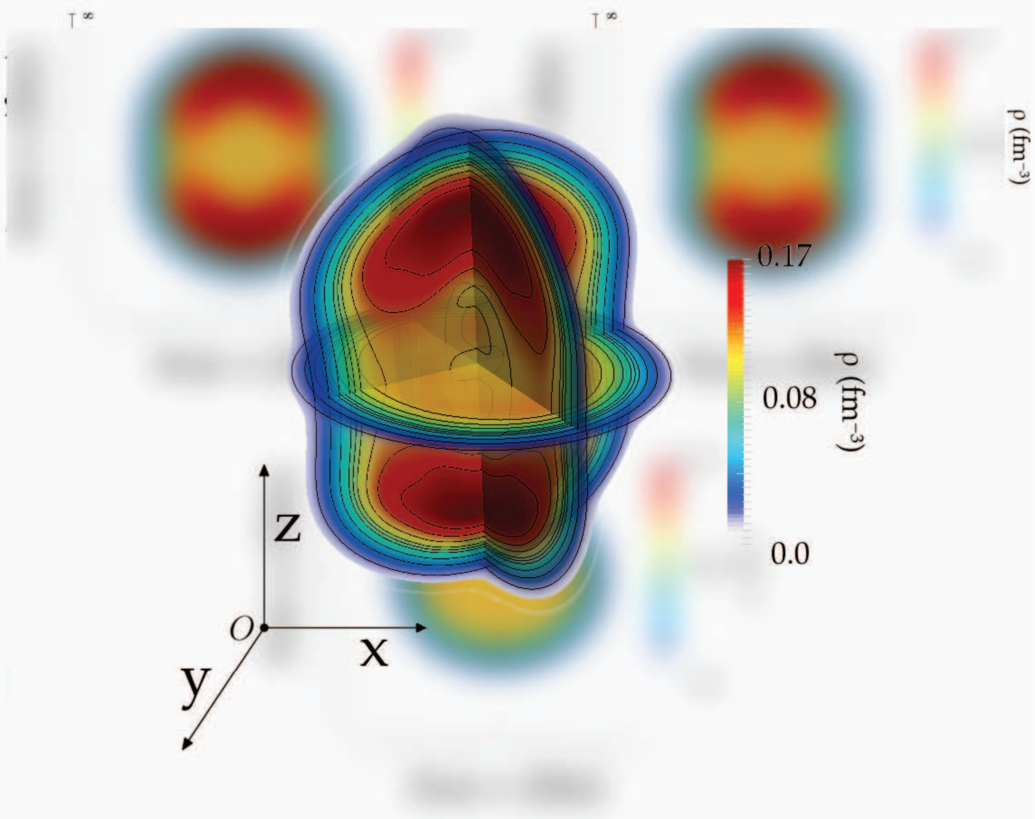

$E_{\mathrm{Exp}} = -1509.9$ MeV

$E_{\mathrm{RMF}} = -1521.6$ MeV

Dérivation α_{loc}

Pour des légers sphériques

$$\phi_{lm}(r) = \frac{r^l}{b^{3/2+l}} e^{-\frac{r^2}{2b^2}} Y_l^m(r) \tag{4}$$

Ou $b = \sqrt{\frac{\hbar}{m\omega_0}} = \sqrt{\frac{\hbar}{(2mV_0)^{1/4}}}$

Ainsi

$$\alpha_{\text{loc}} = \frac{\Delta r}{\bar{r}} \simeq \frac{b}{r_0} = \frac{\sqrt{\hbar R}}{(2mV_0)^{1/4}} \tag{5}$$

Ou $R = r_0 A^{1/3}$,

$$\alpha_{\text{loc}} = \frac{\sqrt{\hbar} A^{1/6}}{\left(2r_0^2 m V_0\right)^{1/4}} \tag{6}$$

Cluster et EDF classiques

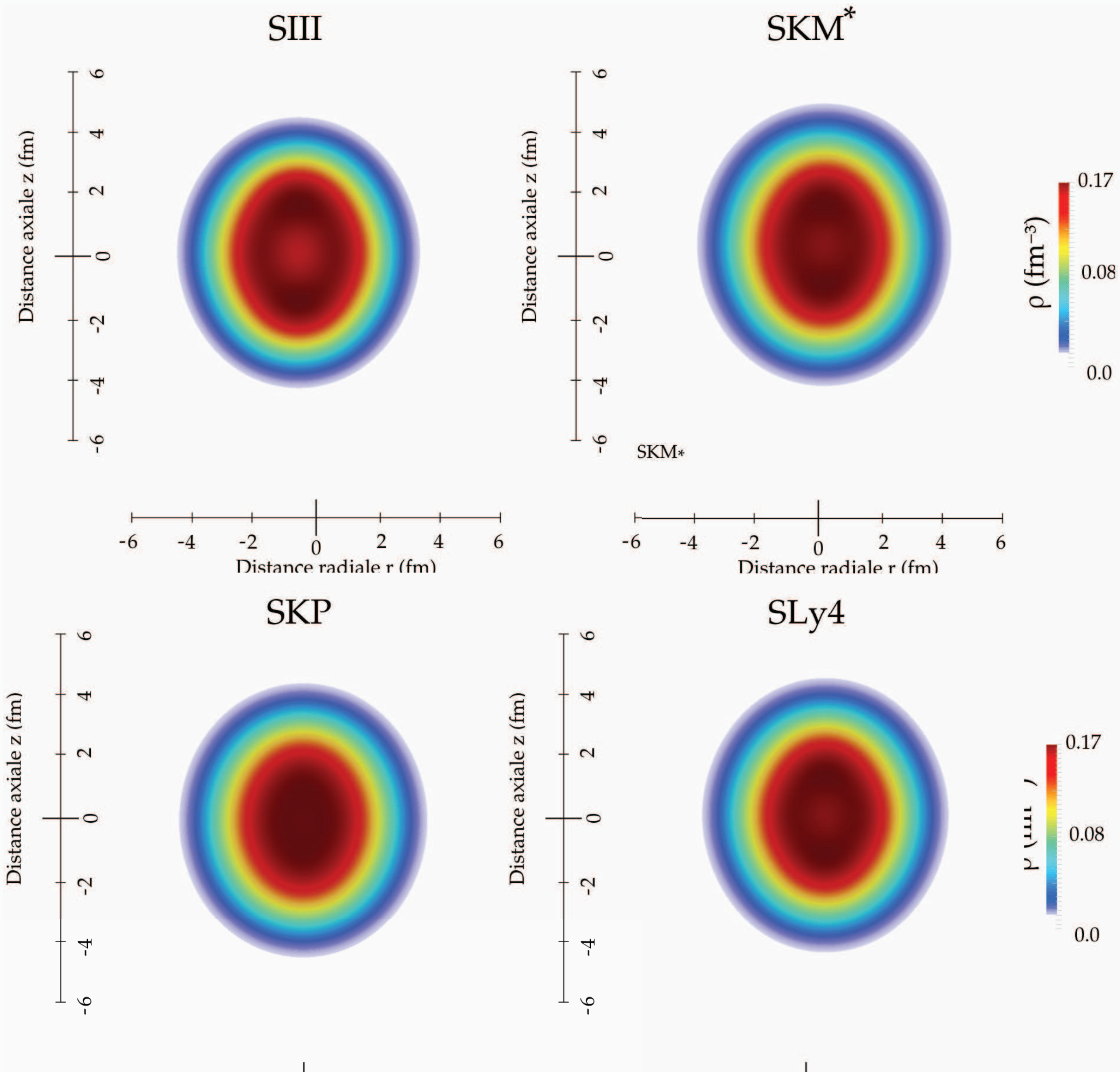

Modèles d'appariement – BCS

$$|\Psi_{\mathrm{BCS}}\rangle = \prod_{k>0}(u_k + v_k b^\dagger_{\bar{k}} b^\dagger_k)\,|0\rangle$$

- Paire de nucléons conjugués temporels
- u_k,v_k coefficients variationnels
- b_k créateur dans la base Hartree

Mais

$$\langle\Psi_{\mathrm{BCS}}|\hat{N}^2|\Psi_{\mathrm{BCS}}\rangle - N^2 = 4\sum u_k^2 v_k^2$$

- Superposition de paires de Cooper
- Ne conserve pas N

Aussi

$$\hat{H}' = \hat{H} - \mu N$$

Tenseur d'appariement – Longueur de cohérence

$$\xi(\mathbf{R}) = \left(\frac{\int \mathbf{r}^2 |\kappa(\mathbf{R},\mathbf{r})|^2 d\mathbf{r}}{\int |\kappa(\mathbf{R},\mathbf{r})|^2 d\mathbf{r}} \right)^2$$

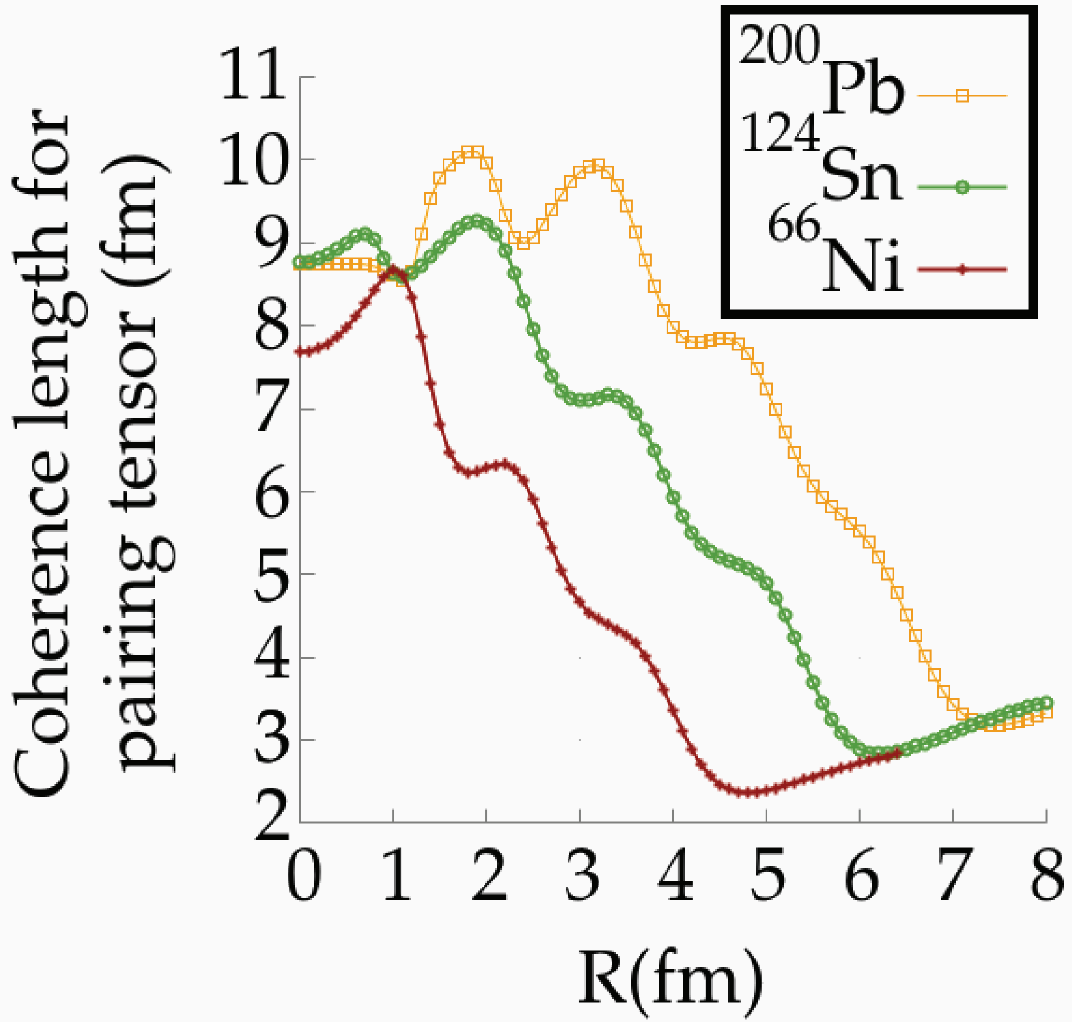

Tenseur d'appariement – Longueur de cohérence

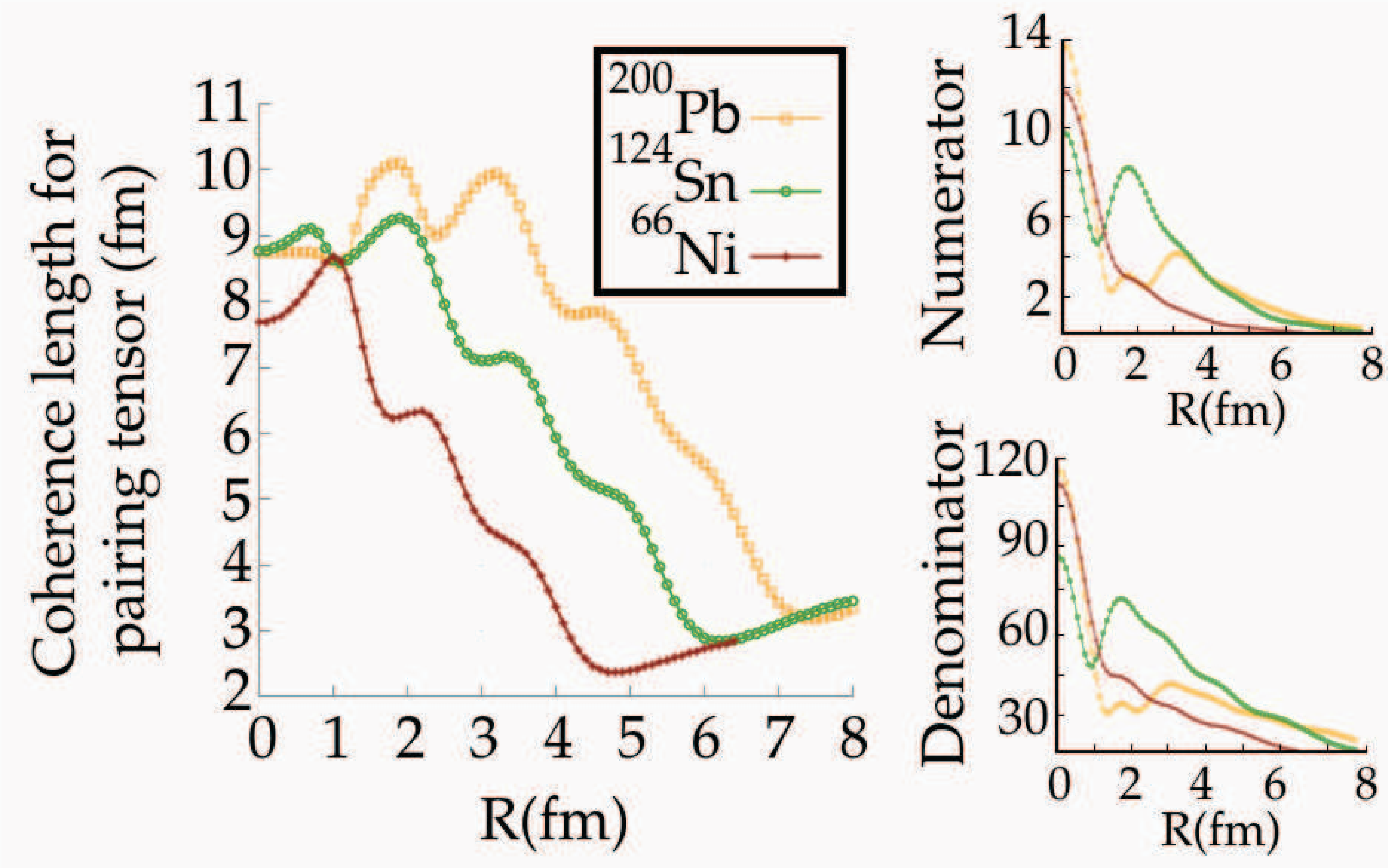

Types de corrélations

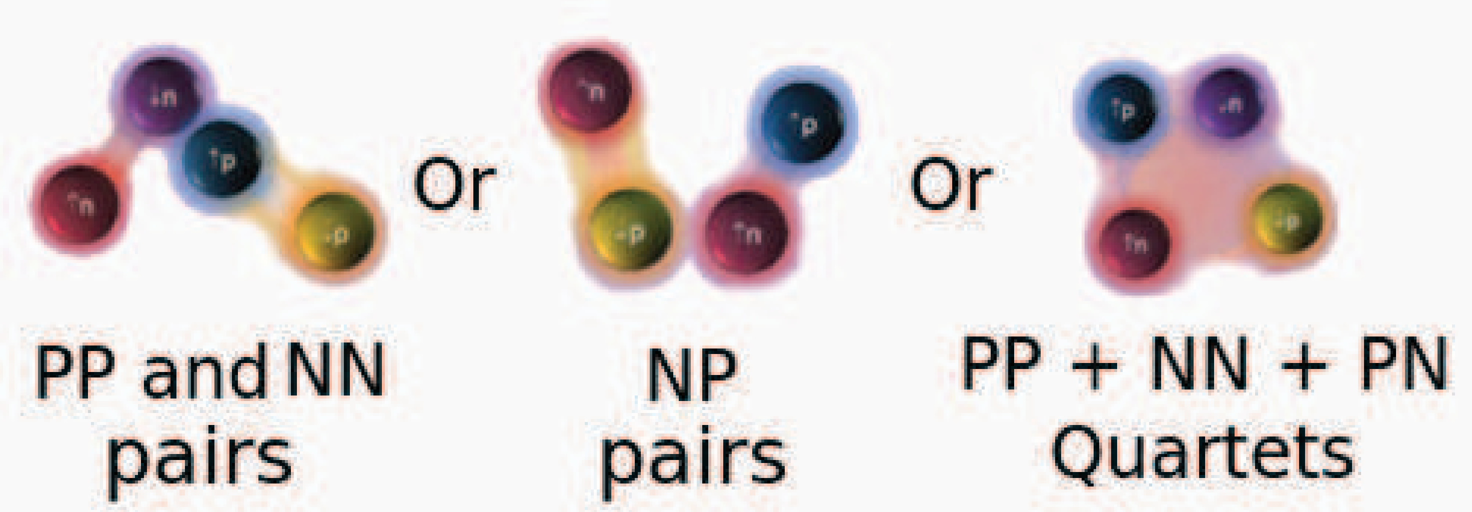

Par la suite:

- Appariement
  - BCS
  - HFB
  - Restauration de symétrie
- Quartteting

Récapitulatif

Développement formels:

- Appariement et théorie des graphes
- Extension spatiale d'objets corrélés
- Mesure et paramètres de localisations
- Théorie des graphes et MBPT

Développement numériques:

- Vectorisation et parallélisation
  - HFBTHO (CPC Rodriguez,Schunck,Lasseri et al (2017))
  - NL-RHB
- Optimisations génétiques
- Développement conjoint d'ADG (CPC Arthuis, Tichai, Duguet, Lasseri et al (2018))